JYU DISSERTATIONS 333

Jia Liu

Electrophysiological Brain Activity Fluctuations during a Long Period of Task Engagement

UNIVERSITY OF JYVÄSKYLÄ
FACULTY OF INFORMATION TECHNOLOGY

JYU DISSERTATIONS 333

Jia Liu

Electrophysiological Brain Activity Fluctuations during a Long Period of Task Engagement

Esitetään Jyväskylän yliopiston informaatioteknologian tiedekunnan suostumuksella
julkisesti tarkastettavaksi joulukuun 9. päivänä 2020 kello 9.

Academic dissertation to be publicly discussed, by permission of
the Faculty of Information Technology of the University of Jyväskylä,
on December 9, 2020 at 9 o'clock am.

JYVÄSKYLÄN YLIOPISTO
UNIVERSITY OF JYVÄSKYLÄ

JYVÄSKYLÄ 2020

Editors
Timo Männikkö
Faculty of Information Technology, University of Jyväskylä
Ville Korkiakangas
Open Science Centre, University of Jyväskylä

Cover picture by Jia Liu.

Permanent link to this publication: http://urn.fi/URN:ISBN:978-951-39-8457-1

ISBN 978-951-39-8457-1 (PDF)
URN:ISBN:978-951-39-8457-1
ISSN 2489-9003

ABSTRACT

Liu, Jia
Electrophysiological brain activity fluctuations during a long period of task engagement
Jyväskylä: University of Jyväskylä, 2020, 67 p. (+included articles)
(JYU Dissertations
ISSN 2489-9003; 333)
ISBN 978-951-39-8457-1 (PDF)

Humans generally fail to maintain their task performance during a long period of task involvement, leading to performance declines and mental fatigue increases. This phenomenon is called the time-on-task effect or vigilance decrement. It is still unclear whether the impairment of time-on-task is task-specific or not. Although some theoretical frameworks of vigilance decrement have been proposed in the literature, there is still no agreed framework generalizing to all fatigue-related findings. To address these questions, we conducted a selective visual attention task for 2 hours 20 minutes and provided monetary rewards in the early and late blocks. We also adopted the 80-minute sustained attention EEG dataset with motivation manipulation in the interval of 60-80 minutes. We explored the effects of time-on-task on selective attention and sustained attention, and investigated the modulations of motivation in these studies. We also examined the differences between vigilance and congruency. For data analysis methods, we applied the ERP, time-frequency analysis, automatic dynamic function connectivity detection approach, temporal PCA, and single-trial analysis, obtaining indicators of ERPs (e.g., N1, P2, N2, P300), ERSP (e.g., delta and theta bands), frequency-specific dynamic functional connectivity (fdFC) across different studies. Our results found that cognitive functions in selective attention were impaired by time-on-task and partially restored by motivation manipulation. Similarly, cognitive processes involved in sustained attention were degraded by vigilance decrement and partially and transiently improved by providing rewards. We also demonstrated different influences between vigilance and congruency in conflicting tasks. Overall, this dissertation elucidates the effects of prolonged task involvement on different types of attentional tasks and provides evidence for the theoretical framework of motivational control and energetical costs.

Keywords: mental fatigue, time-on-task, vigilance decrement, selective attention, sustained attention, congruency.

TIIVISTELMÄ (ABSTRACT IN FINNISH)

Liu, Jia
Elektrofysiologiset aivotoiminnan vaihtelut pitkän sitoutumisen aikana
Jyväskylä: University of Jyväskylä, 2020, 67 s. (+artikkelit)
(JYU Dissertations
ISSN 2489-9003; 333)
ISBN 978-951-39-8457-1 (PDF)

Ihmiset eivät yleensä pysty keskittymään kunnolla pitkien tehtävien suorittamiseen ja tämä johtaa suorituskyvyn heikkenemiseen ja henkisen väsymyksen lisääntymiseen. Tätä ilmiötä kutsutaan aikatehtävävaikutukseksi tai valppauden heikentymiseen. Edelleen on epäselvää, liittyykö tehtävän suorittamisen kesto heikentymiseen tehtäväkohtaisesti vai ei. Kirjallisuudessa on ehdotettu teoreettisia puitteita valppauden heikkenemiseen, mutta vielä ei ole sovittua kehystä, joka yleistää kaikki väsymykseen liittyvät havainnot. Näiden kysymysten ratkaisemiseksi tässä väitöskirjassa on toteutettu valikoivan visuaalisen tarkkailutehtävä ja analysoitu siihen osallistuvia henkilöitä. Tehtävässä seurattiin aikatehtävän vaikutuksia valikoivaan huomioon ja jatkuvaan tarkkailuun, ja lisäksi tutkittiin erilaisten motivaatiotekijöiden vaikutuksia. Tietojen analysoinnissa käytettiin ERP:tä, aikataajuusanalyysiä, automaattisen dynaamisen toimintoyhteyden havaitsemisen lähestymistapaa, ajallista PCA:ta ja yhden kokeen analyysiä. Työn tuloksista havaitaan, että selektiivisen tarkkaavaisuuden kognitiiviset toiminnot heikkenivät tehtävän suorittamisen aikana ja osittain palautuivat palkkioilla. Vastaavasti kognitiiviset prosessit, joihin liittyy jatkuva huomio, heikentyivät valppauden heikkenemisellä ja parantuivat osittain ja ohimenevästi tarjoamalla palkkioita. Työssä on näytetty myös erilaisia vaikutuksia valppauden ja yhdenmukaisuuden välillä ristiriitaisissa tehtävissä. Kokonaisuudessaan tämä väitöskirja selvittää pitkäaikaisten tehtävien osallistumisen vaikutuksia erityyppisiin tarkkaavaisuustehtäviin ja tarjoaa todisteita motivaation merkityksestä pitkäaikaisissa tehtävissä.

Avainsanat: henkinen uupumus, tehtävän aika, valppauden vähennys, valikoiva huomio, jatkuva huomio, yhdenmukaisuus.

Author

Jia Liu
Faculty of Information Technology
University of Jyväskylä
Finland

Supervisors

Tapani Ristaniemi
Faculty of Information Technology
University of Jyväskylä
Finland

Fengyu Cong
School of Biomedical Engineering
Dalian University of Technology
China

Zheng Chang
Faculty of Information Technology
University of Jyväskylä
Finland

Timo Hämäläinen
Faculty of Information Technology
University of Jyväskylä
Finland

Reviewers

Jing Jin
Department of Automation
East China University of Science and Technology
China

Zhong-ke Gao
School of Electrical and Information Engineering
Tianjin University
China

Opponent

Chin-Teng Lin
Faculty of Engineering and Information Technology,
University of Technology Sydney
Australia

ACKNOWLEDGEMENTS

I would like to express many thanks to many people who helped and supported me during my doctoral studies.

First of all, I would like to give my deepest gratitude to my supervisor Prof. Tapani Ristaniemi. I want to thank him for providing me the opportunity to study in Finland. I am also grateful for all his guidance, supports, and encouragement during my doctoral studies. I still remembered his guidance for my research and future plan. This research is to memorize his help for me and other co-authors.

I would like to give my deep gratitude to my supervisor Prof. Fengyu Cong for his dedicated support and guidance throughout my doctoral studies. You have provided a precious opportunity for us to study in Finland with support from the China Scholarship Council (No. 201606060227). You have also created an environment where I can learn a lot and feel confident to take up challenges from academics and life. I also appreciate the freedom you give me to work on the research topics I am really interested in. Your passion for work and thoughtful care for group members contribute to the unions of our research group.

I am also grateful to my supervisor Prof. Timo Hämäläinen for his help and supports at the last stage of my doctoral studies. He is patient with all my questions and gives me rapid responses and useful suggestions. His efficiency and responsibility inspire me a lot. I also appreciate his recommendation as references during my search for a postdoc position.

I would like to thank my supervisor Dr. Zheng Chang, who is a smart and energetic researcher. He is also like a big brother sharing his experiences with me and providing so many good suggestions. He and Dr. Nie Dan are always glad to help me with my research and life. I appreciate their help and support.

I must thank Associate Prof. Tiina Parviainen for her guidance and help during my doctoral studies. She is a researcher that strict in research and with a good scientific attitude, and I will be such a researcher in the future research career. I am also grateful for her trust in my doctoral research and further cooperation in the next MEG studies. Her passion for work and wide cooperation with researchers worldwide inspire me a lot. I am also would like to show thanks to Dr. Monto Simo for the training in MEG driving license.

I would like to give my gratitude to Prof. Hongjin Sun for his exhaustive guidance and constructive suggestions. To help me with the experiment design, he and his team members shared research-related materials and programming codes with me. He also helped me with the mobility grant application to obtain an opportunity to visit the Macmaster University. He is such a kind and wise person and I would like to talk with him when I am confused and frustrated.

Especially, special thanks to my reviewers: Prof. Jing Jin from East China University of Science and Technology in China and Prof. Zhong-ke Gao from Tianjin University in China, and opponent Prof. Chin-Teng Lin from the

University of Technology Sydney in Australia. Thanks them for their efforts and constructive comments.

Furthermore, many thanks to my co-authors: Dr. Chi Zhang, Dr. Yongjie Zhu, Yunmeng Liu for their useful advice, strong support, and good cooperation. I also want to thank all my colleagues in the Faculty of Information Technology and Department of Psychology at the University of Jyväskylä and the ASAP members of the Dalian University of Technology. Many thanks to all my friends for their company and help during my doctoral studies. Especially, thanks to Xueqiao Li, Dr. Weiyong Xu, Biying Wang, Dr. Ye Ren, Wenya Liu, Dr. Deqing Wang, Dr. Xiulin Wang, Lili Tian for their organization of parties on special days and festivals.

Finally, I am so grateful to my family for their unconditional support and understanding. I have been studied in abroad for four years and they have been always companying and encouraging me in my difficulties. During holidays back to China, they took me to enjoy so many delicious food and entertainment. The time staying with them is the most relax and happy moment. They give me all their love to make me be the one who I am. They are the origins of my happiness and I would always be standing by their side.

Jyväskylä, Finland
20.10.2020
Jia Liu

LIST OF ABBREVIATIONS

ACC	Anterior cingulate cortex
ALFF	Amplitudes of low-frequency fluctuation
ANOVA	Analysis of variance
ARAS	Ascending reticular activating system
ASL	Arterial spin labeling
BOLD	Blood oxygen level-dependent
CC	Clustering coefficient
CPL	Characteristic path length
CSP	Common spatial patterns
CWT	Continuous wavelet transform
DMN	Default mode network
DWPT	Discrete wavelet packet transform
ECG	Electrocardiogram
EEG	Electroencephalogram
EOG	Electrooculography
ERP	Event-related potential
ERSP	Event-related spectral perturbation
LPC	Late positive complex
FC	Functional connectivity
fdFC	Frequency-specific dynamic FC
fMRI	Functional magnetic resonance imaging
ICA	Independent component analysis
KSS	Karolinska Sleepiness Scale
MEG	Magnetoencephalography
MPCA	Multilinear principal components analysis
nP3	Novelty P3
PCA	Principal components analysis
PCC	Posterior cingulate cortex
PCs	Principal components
PSD	Power spectral density
PVT	Psychomotor vigilance test
RT	Response time
SNR	Signal-to-noise ratio
STFT	Short-time Fourier transform
SVM	Support vector machine
SW	Slow wave
TCA	Tensor component analysis
TFT	Time-frequency transformation
wPLI	Weight phase lag index

LIST OF FIGURES

LIST OF ORIGINAL PUBLICATIONS

I Liu, J., Zhang, C., Zhu, Y., Liu, Y., Sun, H., Ristaniemi, T., Cong, F. and Parviainen, T., 2020. Dissociable effects of reward on P300 and EEG spectra under conditions of high vs. low vigilance during a selective visual attention task. Frontiers in human neuroscience, 14, p.207. https://doi.org/10.3389/fnhum.2020.00207

II Liu, J., Zhu, Y., Sun, H., Ristaniemi, T. and Cong, F., 2020. Sustaining Attention for a Prolonged Duration Affects Dynamic Organizations of Frequency-Specific Functional Connectivity. Brain Topography, pp.1-16. https://doi.org/10.1007/s10548-020-00795-0

III Liu, J., Zhang, C., Zhu, Y., Ristaniemi, T., Parviainen, T. and Cong, F., 2020. Automated detection and localization system of myocardial infarction in single-beat ECG using Dual-Q TQWT and wavelet packet tensor decomposition. Computer Methods and Programs in Biomedicine, 184, p.105120. https://doi.org/10.1016/j.cmpb.2019.105120

IV Liu, J., Zhu, Y., Chang, Z., Hämäläinen, T. and Cong, F., 2020. Congruency and vigilance produce separable changes in the late positive complex during a Flanker task. (Submitted)

Taken into account the instruction given and comments made by the co-authors, the author of this thesis contributed to the original publications as follows: In article I, she designed the experiment, conducted the analysis, and wrote the manuscript; In article II, she adopted one public mental fatigue EEG dataset, and re-analyzed the data, conducted the analysis, and wrote the manuscript; In article III, she adopted one public ECG dataset, developed the single-beat automatic detection and localization system, conducted all these analyses, and wrote the manuscript; In article IV, she re-analyzed the EEG dataset collected from article I, re-analyzed the data, conducted the PCA and single-trial analysis, and wrote the manuscript.

CONTENTS

1 INTRODUCTION

Mental fatigue is a common feature in modern life and usually impairs our task performance. The impairment of mental fatigue is pronounced especially in industries such as transportation, aviation, manufacturing factories, health care, military, and many public services (S. K. L. Lal & Craig, 2001). Mental fatigue can lead to serious consequences in these industries, for example, driver fatigue is one of the crucial factors contributing to traffic accidents and medical staff fatigue is an important element resulting in medical accidents. In fact, mental fatigue is a complex process of our body and can be affected by many factors such as sleep duration, personality, mood, and working time. While there is a bulk of evidence for mental fatigue detection and mechanism analysis, the term fatigue still lacks an agreed definition, and little is known about its mechanism.

It has been known that a long period of task involvement in cognitive tasks impairs neurobehavioral performance. However, the deficits of specific cognitive functions remain to be established in different cognitive tasks. In general, mental fatigue impairs plenty of cognitive functions, for instance, attention resources, cognitive control, working memory, and motor movement or inhibition, et.al. The way how these cognitive functions are impacted by long durations of task engagement needs to be characterized.

To explore the effects of mental fatigue on cognitive tasks, behavioral measures (e.g., response time, accuracy, and the number of errors) are the earliest indices in the literature though behavioral performance is only the external manifestation of a cascade of cognitive functions. Advances in neuroimaging and electrophysiological techniques such as functional magnetic resonance imaging (fMRI) and electroencephalogram (EEG) have allowed for a deep understanding of specific cognitive functions. Especially, EEG is one of the most popular techniques for mental fatigue detection and mechanism analysis owing to its property of low costs, high temporal resolution, and portability. By utilizing EEG, researchers have detected many neuromakers for mental fatigue, consisting of oscillatory brain activity, event-related potential (ERP), functional connectivity (FC), and so on. Nevertheless, developing the effectiveness and robustness of

neuromakers in different cognitive tasks is still challenging in mental fatigue studies.

In this chapter, we first figure out the definition and theories of mental fatigue. We then summarize the effects of long-term duration of task engagement on different cognitive tasks and outline the neuromarkers commonly used in fatigue studies. Finally, we illustrate the aim of the present research.

1.1 Mechanisms of fatigue and theories of vigilance decrement

1.1.1 Concepts of mental fatigue

Fatigue is a ubiquitous and complex phenomenon, which involves many behavioral and psychological processes and is related to many factors such as sleep duration, prolonged task involvement, nutrition, health, and environment. As a result, there are many concepts used in fatigue-related research. According to different health conditions of individuals, fatigue can be defined as acute and chronic fatigue (Shen, Barbera, & Shapiro, 2006). Acute fatigue, mainly pointing to healthy individuals, is typically considered as a protective function of our bodies and brains. It is generally alleviated after a rest and exercise. In contrast, chronic fatigue usually occurs in disordered patients (e.g., cancer disease), and it is generally not recovered by using traditional restoration techniques. Regarding different emphases of fatigue on muscle and brain, fatigue is typically divided into physical (physiological) and mental (psychological) fatigue (Aaronson et al., 1999) although mental fatigue also affects physical performance reported in an earlier study (Marcora, Staiano, & Manning, 2009). Physical fatigue represents the decreased performance of muscular movement and power, therefore, it is also called muscular fatigue. For instance, in strenuous exercise, the chemical substances (e.g., sugar and phosphorous) are consumed to provide energy and decomposed into lactic acid and carbon dioxide leading to feelings of acidic for muscular tissue (Grandjean, 1979). On the contrary, mental fatigue is a feeling of tiredness and can be induced by a prolonged duration of mental or cognitive tasks. Mental fatigue is an accumulate process and accompanies reduced motivation and deteriorated task performance. Moreover, mental fatigue can be caused by many factors, among which the sleep-related factors and a long period of task involvement are the most important ones (May & Baldwin, 2009). Based on these two causal factors, mental fatigue is usually studied in sleep-related and task-related research (Dawson, Ian Noy, Härmä, Kerstedt, & Belenky, 2011). In the sleep-related studies, researchers have explored the effects of sleep deprivation and circadian rhythm on vigilant performance and found the impairments of them on vigilant attention (Lim & Dinges, 2008; Van Dongen, Maislin, Mullington, & Dinges, 2003). Among many synonymous terms (e.g., sleepiness, drowsiness, and wakefulness) of fatigue, “sleepiness” and “wakefulness” are typically interchanged with fatigue in the sleep-related studies. In the task-related studies, on the other hand, long task engagement

hours can lead to mental fatigue increases and performance deteriorations. According to the workload of task and environment, task-related fatigue has also been explored using the concepts of passive fatigue and active fatigue (Thiffault & Bergeron, 2003). Passive fatigue is usually resulted from a monotonous environment in the underload conditions, whereas active fatigue is mainly associated with the high density environment in the overload conditions. In fact, acute fatigue and mental fatigue aforementioned are the major origins of severe traffic and medical accidents. As reported in previous studies, task-related fatigue detection and countermeasure can effectively avoid the occurrence of traffic accidents (Lin et al., 2006; May & Baldwin, 2009).

Existing concepts of fatigue have been considered particularly following dualistic lines, but generalizing the concepts across conditions and tasks is still challenging. It is much difficult to define the type of fatigue because many factors overlap together. It is likely that mental fatigue emphasizes subjective feelings and common phenomena. The ambiguity and disagreement concepts of fatigue hinder the wide promotion of fatigue-related research, particularly in psychology and neuroscience fields. In essence, when humans engage in cognitive tasks for a long period of time, they will experience mental fatigue increases and motivation decreases to continue performing tasks along with more committed errors and diminished performance goals. This effect is defined as time-on-task effect or vigilance decrement in the fields of psychology and neuroscience (D R Davies; & Parasurman, 1982; Lim & Dinges, 2008; Mackworth, 1948; Reteig, van den Brink, Prinssen, Cohen, & Slagter, 2019; See, Howe, Warm, & Dember, 1995). In the present study, the terms "time-on-task" and "vigilance decrement" are used interchangeably with "mental fatigue", stating the neurobehavioral performance fluctuations affected by a long-term duration task involvement.

1.1.2 Theoretical frameworks of vigilance decrement

Theoretical frameworks explaining the mechanism of vigilance decrement have been widely studied in decades of research. Three theoretical frameworks of underload, overload, and motivational control have already prevailed. The underload theoretical framework argues that typical vigilance tasks are monotonous and simple enough without capturing attention, resulting in humans to disengage from the current task and fail to maintain task performance (Manly, Robertson, Galloway, & Hawkins, 1999). When humans shift their attention from the primary task, they are occupied by task-unrelated thoughts, and the mind-wandering occurs (Smallwood & Schooler, 2006). Additionally, the overload theoretical framework states that cognitive resources are limited and they are depleted during an extended period of task involvement (Helton & Warm, 2008). The monitoring of relevant information in external surroundings requires cognitive resources, and long-term monitoring and processing steadily exhaust the limited resources, causing task performance reductions. Furthermore, the theoretical framework of motivational control insists that vigilance decrement is the mental analysis of costs and benefits, and humans are in a

motivated state when they maintain their task performance (Kurzban, Duckworth, Kable, & Myers, 2013). When the costs outweigh the benefits during task performance, the level of vigilance decreases along with task performance declines.

Recent research has found that these three theoretical frameworks aforementioned still have limitations to explain all phenomena in daily life and experimental settings, and these frameworks are not mutually exclusive. Therefore, some synthesized theoretical frameworks are proposed based on these three frameworks. For example, the "resource-control" theory states that vigilance decrement cannot be explained by either overload or underload on its own, but should be described by a function of time-on-task (attention resources declines) combining theories of mind-wandering (Thomson, Besner, & Smilek, 2015). Alternatively, some researchers find that mind-wandering is closely related to motivation, suggesting that low motivated participants have more task-unrelated thoughts (Seli, Cheyne, Xu, Purdon, & Smilek, 2015). Moreover, vigilance decrement is also attributed to the framework of motivational control and energetical costs stating that humans will balance the rewards and costs and further consider their limited resources (Boksem & Tops, 2008).

Taken together, although many theoretical frameworks have been proposed in previous studies, the mechanisms of vigilance decrement still need to be established in an agreed theoretical framework.

1.1.3 Neurophysiological aspects of mental fatigue and vigilance

The reticular formation, located in the brainstem, is closely related to the degree of vigilance (Grandjean, 1979). The reticular formation comprises of the ascending reticular activating system (ARAS) and the descending tracts to the spinal cord (Jones, 2008). Specifically, the ARAS plays an important role in regulation of wakefulness or arousal levels and awake-sleep transactions. The ARAS includes some neural circuits linking the posterior midbrain and anterior pons to the cerebral cortex through different pathways that central to the thalamus and hypothalamus (Brudzynski, 2014). With the decrease of vigilance, the activation level of the reticular formation generally increases.

In addition, the limbic system has also been reported to associate with motivation, emotion, and level of vigilance (Grandjean, 1979). The limbic system located deep through the brain, which is above the brainstem and underneath the cerebral cortex. It contains the cingulate gyrus, parahippocampal gyrus, hippocampus, amygdala, hypothalamus, nucleus accumbens, et al. The level of vigilance is linked to the limbic system for circadian rhythms and motivation, and is also related to dopamine (Mistlberger & Mumby, 1992).

Apart from the activating reticular and limbic systems, the inhibiting system in the interbrain and medulla also has close relationships with vigilance or sleep-related functions (Grandjean, 1979). Besides, the autonomic nervous system controlling the activating and inhibiting functions has close links to the level of vigilance (Grandjean, 1979).

In the review of the synthesized theoretical frameworks combining motivational control and energetical costs (Boksem & Tops, 2008), researchers show that the neuropsychological brain structures involved in reward systems are intimately related to mental fatigue, consisting of the midbrain dopamine neurons, orbitofrontal cortex, basolateral amygdala, insula, anterior cingulate cortex (ACC), and nucleus accumbens. When humans deal with goal-directed tasks, they will evaluate the potential rewards and aversive results and adjust their task performance by complex interactions between these neural substructures in the reward system. The dopamine neurons in the ventral tegmental area project dopamine to the prefrontal cortex carrying information on reward value (Leon & Schultz, 1999). The expected appetitive and aversive value of actions is coded by the orbitofrontal cortex, basolateral amygdala, and insula. The reward coding information is transmitted to the ACC, in which the reward information is compared to the costs to perform tasks expecting to realize the least aversive and largest reward. The determined strategy is relayed to the behavioral output through the dopamine projections from ACC to nucleus accumbens. The ACC integrates the reward and costs information with the energetical resources to allow for optimal decision making and action outcomes.

1.2 Modulations of time-on-task on cognitive functions

A long-term task involvement leads to mental fatigue increases, causing deficits in a series of cognitive functions. Previous experimental studies using different cognitive tasks have demonstrated the effects of time-on-task on specific cognitive processes such as selective attention (Boksem, Meijman, & Lorist, 2005; Faber, Maurits, & Lorist, 2012), sustained attention (B.S.Oken, M.C.Salinsky, 2006; Reteig et al., 2019; Sun, Lim, Kwok, & Bezerianos, 2014), cognitive control (Lorist, Boksem, & Ridderinkhof, 2005), action monitoring or error detection (Boksem, Meijman, & Lorist, 2006; Lorist et al., 2005), decision making (Lorist, Klein, & Nieuwenhuis, 2000), working memory (Gergelyfi, Jacob, Olivier, & Zénon, 2015), and response execution and inhibition (Guo et al., 2018; Kato, Endo, & Kizuka, 2009; Möckel, Beste, & Wascher, 2015). Especially, the impairment of time-on-task on attention and cognitive control can lead to severe consequences in many fields of practical situations. What is more, attention plays a pivotal role during all perceptual and cognitive functions (Chun, Golomb, & Turk-Browne, 2011). Therefore, the deficits of attention and cognitive control should be emphasized during long lasting task engagement.

1.2.1 Effects of time-on-task on attention

Although attention is ubiquitous in our daily life, the colloquial and general understanding has hampered its development in scientific research. In essence, “attention”, in the field of psychology, has a broad range of meanings (Lim & Dinges, 2008). A large body of taxonomies has been proposed to separate

component parts of attention. As one of the earliest psychologists, William James states that "attention" is not a unitary process, and it includes independent attentional processes of voluntary and involuntary (James, 1890). These two attentional processes are probably equivalent to the classificatory processes, labeled in recent years, of top-down and bottom-up (Corbetta & Shulman, 2002; Sarter, Givens, & Bruno, 2001). The top-down processes embody the knowledge-driven mechanisms, which facilitates the contrast between signal and distractors and enhances the processing of task-relevant information (Sabine & Ungerleider, 2000). On the contrary, the bottom-up processes are driven by the sensory context and characteristics of stimulus (Sarter et al., 2001). It will be interesting to analyze the effects of time-on-task on these top-down and bottom-up processes to untangle more detailed information in attention. However, top-down and bottom-up processes are only conceptual principles instead of dichotomous constructs or anatomical system, and they are generally interact with each other to implement an optimization attentional performance (Egeth & Yantis, 1997; Sarter et al., 2001). At the level of neuropsychology, it is hard to dissociate the influences of time-on-task on these two attentional component processes owing to the difficulty of teasing apart these two processes.

From another point of view, "attention" has also been subcategorized into components of intensity and selective aspects (Posner & Boies, 1971; Sturm & Willmes, 2001). The intensity aspects contain the alertness and sustained attention, whereas the selective aspects include focussed and divided attention, namely selective attention. Comparable to the intensity aspects, the selective aspects are more complex including orienting and executive functions in addition to the alerting function (Fan, Mccandliss, Sommer, Raz, & Posner, 2002). Similarly, Parasuraman showed that, according to the different requirements of attentional resources, vigilance tasks could be fallen into two types of tasks representing successive and simultaneous discrimination tasks (Parasuraman, 1979). The successive tasks are required to contrast the current stimuli with a standard one maintained in working memory to separate the target from non-target stimuli. Instead the simultaneous tasks are instructed to distinguish the targets from non-targets based on the properties of stimuli not the memory of signal features (Parasuraman, 1979; Warm, Parasuraman, & Matthews, 2008). Obviously, the successive tasks are more complex than simultaneous tasks, which contains less working memory demanding. The successive and simultaneous tasks are likely corresponding to the selective and intensity aspects, respectively. Evidence has amassed from successive and simultaneous research that the impairment of vigilance or time-on-task presents a greater degree on successive tasks than simultaneous tasks might because of more working memory resource demanding in successive discrimination (Warm et al., 2008). Whether a long period time of task involvement elicits discrepancies between sustained and selective attention remains an interesting research topic. It should also be noted that sustaining attention to the current tasks is the precondition while carrying out more complex selective attention tasks, and thus the more

resources demanding tasks should also consider the attention lapses during task performance (Lim & Dinges, 2008).

1.2.2 Influences of time-on-task on cognitive control

Cognitive control, also called executive functions or executive control, contains a series of top-down cognitive functions. Cognitive control is necessary when humans dealing with the novel stimulus and when they resisting irrelevant temptations (Diamond, 2013). As opposed to the bottom-up cognitive functions, the cognitive control is effortful because it is resource consuming to respond to a novel stimulus rather than a familiar one. In general, cognitive control is comprised of three core components: inhibitory control—including interference control (cognitive inhibition and selective attention) and self-control (behavioral inhibition), working memory, and cognitive flexibility (also named as mental set shifting) (Lehto, Juujärvi, Kooistra, & Pulkkinen, 2003; Miyake et al., 2000). Furthermore, higher-order cognitive control also involves the processes of problem solving, reasoning, and decision making (Collins & Koechlin, 2012).

As one of the core cognitive control components, inhibitory control involves the control contents of attention, thoughts, and behavior. Inhibitory control of attention illustrates that humans selectively attend to the goal-directed stimuli and suppress the other stimuli. The process has also been termed as focused or selective attention, attentional control, attentional inhibition, as well as executive attention (Theeuwes, 1991). Interference control of thoughts and mental representations is also called cognitive inhibition (Diamond, 2013). This control process includes suppressing unwanted or extraneous thoughts/memories such as intentional forgetting (Anderson & Levy, 2009). The cognitive inhibition typically coheres with working memory instead of other inhibitory functions. Inhibitory control of behavior, also named as self-control, enables humans to resist temptations and impulsive actions. Previous studies have explored the time-on-task effect on these processes such as selective attention (Boksem et al., 2005; Faber et al., 2012) and cognitive control (Lorist et al., 2005).

The other aspect of core cognitive control components is working memory, which indicates the process of retaining information in the mind and working with the information (Anderson & Levy, 2009). Working memory is closely associated with other cognitive functions even seemingly unrelated things, and it integrates other functional elements together. Dissociating working memory and inhibitory control is an important question to learn the effects of other factors such as time-on-task on a specific function. Specifically, there are close relationships between working memory and inhibitory control, suggesting that they generally emerge simultaneously and interact with each other (Diamond, 2013). The solution to this question is that one function should be minimized or controlled instead of cancelling their interactions. In fact, working memory is not just a subcomponent of cognitive control, and it is broadly defined in the literature (Conway & Engle, 1994; Kane & Engle, 2000). In that way, the working memory is approximately synonymous with cognitive control. Although

working memory is a significant part in implement tasks, not many studies have focused on the effects of time-on-task on working memory (Gergelyfi et al., 2015).

The third component of cognitive control is cognitive flexibility, which is usually realized based on the two cognitive control components aforementioned (Diamond, 2013). This process enables humans to adjust their task performance according to changed task priorities and demands and to employ unexpected chances. The task-switching paradigms are ordinarily used for exploration of cognitive flexibly. For instance, the Wisconsin Card Sorting Task, where participants are asked to adjust their sorting specification based on the feedbacks and to switch the sorting criterions whenever new feedbacks emerge (Stuss et al., 2000). An earlier study has used a switching task to explore the effects of mental fatigue on planning and preparation (Lorist et al., 2000).

Taken together, these processes involved in cognitive tasks are essential for successful task performance in experimental settings and practical environment. Therefore, the effects of long-term task engagement on cognitive control should be studied and the improvement methods (e.g., training (Karbach & Kray, 2009) and practice (Erickson & Kramer, 2009)) for it still need to be addressed to reduce all modes of risks in practical tasks.

1.3 Indices of mental fatigue and vigilance decrement

From the past decades of research, abundant studies have emerged seeking to measure indices reflected in mental fatigue and level of vigilance. These indices involve behavioral performance, perceptual, psychological, electrophysiological, and biochemical measurements (S. K. L. Lal & Craig, 2001), obtained from different techniques such as self-reported questionnaires (e.g., Karolinska Sleepiness Scale, KSS (Åkerstedt & Gillberg, 1990)), behavioral measurements (e.g., accuracy and response time (RT)), electrophysiological and neuroimaging modalities (e.g., EEG, fMRI, electrooculography (EOG), electrocardiogram (ECG)), eye-tracking, and video images. In all categories of techniques, electrophysiological and neuroimaging modalities are more precise compared with other techniques because these techniques can directly record the neurophysiological activities of humans. In particular, owing to the advantage of high temporal resolution, low costs, potable and convenient, EEG is one of the most reliable techniques for mental fatigue studies. It is also promising to combine information from different techniques to search for reliable indices for mental fatigue.

1.3.1 Indicators from EEG

EEG is an electrophysiological technique used to record electrical activities that voltage fluctuations arising from ionic current within the neurons in the brain (Ernst Niedermeyer & Silva, 2005). EEG is usually non-invasive, and it records the electrical impulses with a small flat electrical conductor also named

electrodes attached to the scalp. EEG signals are rhythmic activities, which are differentiated into different bands according to frequency ranges. The frequency bands typically consist of delta (0.5–4 Hz), theta (4–7 Hz), alpha (8–13 Hz), beta, (14–31 Hz) and gamma (>32 Hz) (Klimesch, 1999). Some researcher also analyzed the frequency bands in sub-bands in terms of specific study, for example, a waking-sleeping transition study using alpha 1 (7.6–9.4 Hz), alpha 2 (9.6–11.4 Hz), and alpha 3 (11.6–13.4 Hz) (Tanaka, Hayashi, & Hori, 1997). Practical and experimental applications mainly focus on spectral content and ERP of EEG (Ernst Niedermeyer & Silva, 2005; Luck, 2005). Spectral content is applied for investigating brain rhythmic activities in the frequency domain, whereas ERP is used to explore the potential changes time-locked to an event in the time domain.

1.3.1.1 Spectral content

Delta band has been found associated with a long time task involvement and slow-wave sleep (Hobson & Pace-Schott, 2002; Saroj K.L. Lal & Craig, 2002). In particular, researchers have revealed an increase in delta band along with mental fatigue increases, and the delta oscillations generally occur in frontal and central brain regions (Saroj K.L. Lal & Craig, 2002; Santamaria & Chiappa, 1987). Converging evidence has shown that delta band have close linkages with brain reward system (Knyazev, 2012).

Similarly, theta band has also been reported related to drowsiness and sleep, and further linked to decline of information processing (S. K. L. Lal & Craig, 2001). The close relationships between increases of frontal and/or parietal theta oscillations and mental fatigue increases have been revealed in earlier studies (Saroj K.L. Lal & Craig, 2002; Trejo, Kubitz, Rosipal, Kochavi, & Montgomery, 2015). Theta band has also been pointed reflecting active cortical functioning and encoding of new information (Cavanagh & Frank, 2014; Klimesch, 1999).

In contrast to all frequency bands, alpha as well as theta oscillations are likely the most sensitive bands used for detecting fatigue, vigilance deteriorates or arousal levels (Åkerstedt & Gillberg, 1990; Trejo et al., 2015). Alpha activity, typically emerging from occipital cortex, increases evidently during eye closure and decreases during eye opening (Okogbaa, Shell, & Filipusic, 1994). Previous work has demonstrated that alpha band decreases during long-term task involvement, but the activations of alpha band are different, located at parietal (Trejo et al., 2015) and frontal brain regions (Saroj K.L. Lal & Craig, 2002), respectively. However, there are still some findings showing that alpha band increase during a long period of driving tasks or after shift work (Akerstedt, Kecklund, & Knutsson, 1991; Eoh, Chung, & Kim, 2005).

In terms of beta band, it has close association with arousal, alertness, and excitement (S. K. L. Lal & Craig, 2001). The increase of beta along with mental fatigue increase and shift work has been found in earlier research (Eoh et al., 2005; Saroj K.L. Lal & Craig, 2002). Especially, one study has found that beta activity is most useful indicator of vigilance decrement (Belyavin & Wright, 1987). Gamma band is seldom applied for fatigue-related studies.

In addition, a number of combining indicators have been investigated on the basis of four frequency bands aforementioned. For example, the indices of β/α and $(\alpha+\theta)/\beta$ have been used for drowsiness detection after sleep deprivation (Eoh et al., 2005). Other indices of θ/β, $(\alpha+\theta)/(\alpha+\beta)$, and θ/α have also been used in fatigue or level of alertness detection (Jagannathan et al., 2018; Jap, Lal, Fischer, & Bekiaris, 2009). Moreover, the indicator of alpha spindles, defined as short bursts in the alpha band, has also been used to assess the sleepiness of drivers after sleep-deprivation (Jap et al., 2009).

1.3.1.2 ERP

Although EEG has proved to be a useful technique in applications of scientific and clinics, its coarse measure of brain activity makes it difficult to estimate the highly specific cognitive and neural processes in the field of cognitive neuroscience (Luck, 2005). The EEG embodies the mixed up conglomeration from numerous neural activities, which means that brain response to a single event is not typically visible. Therefore, by means of a simple averaging approach, the neural responses mirroring specific cognitive functions can be extracted. These neural responses locked to a specific stimulus are corresponding to ERP. In contrast with EEG, ERP has a higher signal-to-noise ratio (SNR). In the research of fatigue or vigilance decrement during cognitive tasks, ERP might be an efficient approach to reveal the mechanisms underlying the effects of fatigue on specific neural processes or cognitive functions. Different component can be identified from ERP, and each ERP component is corresponding to specific cognitive function. By exploring whether ERP components are modulated by fatigue or not, researchers can infer which cognitive functions are impaired or enhanced by long period of task engagement.

In terms of P1 component, it usually occurs in the temporal window of 60–130 ms after stimulus-onset and at the lateral occipital brain regions (Luck, 2005). P1 has been reported in many attention-related studies, for example, an inseparable relationship between P1 and spatial attention (Luck & Vogel, 1998). Furthermore, previous work has detected attention-related P1 is not modulated by time-on-task (Boksem et al., 2005; Reteig et al., 2019), although an earlier study found its linkage with arousal states (Luck & Vogel, 1998).

P1 is followed by N1, which peaks around 100–200 ms stimulus-onset. The visual N1 is a useful index for discrimination process in focused attention (Luck & Vogel, 1998). In a sustained attention task for 60 minutes, no change of N1 was detected with time-on-task (Reteig et al., 2019). But in a visual-selective attention task during 3 hours, a decrease of N1 amplitude was found (Boksem et al., 2005). In fact, N1 is usually consisted of two subcomponents, with an earlier one peaks around 100–150 ms at anterior electrode sites and a later one peaks around 150–200 ms at posterior electrode sites, which might result in the fatigue-related fluctuations in different tasks.

P2 component, activated in anterior and central brain areas, is not usually reported in fatigue-related studies. But the links between auditory P2 and sleep has been summarized in a previous review work (Crowley & Colrain, 2004).

Compared to these ERP components listed above, N2 and P3 (or P300) components have been well acknowledged. N2 has many different subcomponents in this time range, for instance, N2a also called mismatch negative associating with deviant task-irrelevant stimuli especially the auditory modality, and N2b relating to deviant task-relevant processing (Luck, 2005). N2 is a negative wave emerged at frontal and central scalp topography, which reflects the neural processes of cognitive control and conflict processing (Borja-Cacho & Matthews, 2008; Kałamała, Szewczyk, Senderecka, & Wodniecka, 2018). The modulations of N2 by prolonged task engagement have been found in response selection during a Simon task (Möckel et al., 2015), in an action monitoring task (Boksem et al., 2006), and in response processes during a No-NoGo task (Kato et al., 2009).

There are some distinguishable ERP components in P3 time range. Especially, P3a and P3b are widely used in the literature, with P3a occurring in anterior electrode sites in an earlier time window and P3a occurring in posterior electrodes in the latter time window (Demiralp, Ademoglu, Comerchero, & Polich, 2001; Polich, 2007; Polich & Criado, 2006). Besides, other subcomponents such as novelty P3 (nP3) and slow wave (SW) have also been illustrated in previous studies (Barry et al., 2020; Linden, 2005; Polich, 2020). The effects of mental fatigue or sleep-deprivation on P3 (including latency and amplitude of P3, P3a, P3b) have been widely studied previous studies (Guo et al., 2018; Hopstaken, van der Linden, Bakker, & Kompier, 2015; Käthner, Wriessnegger, Müller-Putz, Kübler, & Halder, 2014; Kato et al., 2009). These properties of P3 might be one set of the most reliable indicators for mechanisms of mental fatigue and vigilance decrement.

1.3.2 Indicators from brain regions and functional connectivity

Comparable to traditional univariate approaches such as spectral analysis, in recent years, converging evidence has displayed that the multivariate FC may provide a new profile for dissociating mechanisms of mental fatigue. Recent studies have proven that mental fatigue is closely associated with the diverged reorganization of FC among different brain regions (Qi et al., 2019; Sun et al., 2014). In the laboratory experimental studies, the neural fluctuations during sustained attention have been widely used for exploration of time-on-task effect or vigilance decrement because of its validity and reliability. Both high spatial resolution fMRI and high temporal resolution EEG have been widely used to study the effects of vigilance.

By utilizing the arterial spin labeling (ASL) perfusion fMRI during 20 minutes psychomotor vigilance test (PVT), Lim and colleagues found the involvement of fronto-parietal attention network, sensorimotor regions as well as basal ganglia, and further detected a decrease of attention network with time-on-task (Lim et al., 2010). Based on these results above, Rao and his group blood oxygen level-dependent (BOLD) fMRI during a similar test for 20 minutes (Gui et al., 2015). They disclosed that the amplitudes of low-frequency fluctuation (ALFF) reduced in the default mode network (DMN) and increased in the

thalamus, and the anti-correlations between the right middle prefrontal brain areas and posterior cingulate cortex (PCC) reduced after a long period of task involvement.

The FC in specific frequency band using EEG has also been used for mental fatigue analysis. Sun et al. analyzed the graph theoretical indices from FC in the lower alpha band during a long period of PVT (Sun et al., 2014). By contrasting the FC maps between the first and last 5 minutes, he found that the weighted characteristic path length (CPL) increased in the last 5 minutes task performance and the asymmetrical pattern of FC changed in the fronto-parietal brain regions with mental fatigue increases. Georgios and colleagues compared the effect of mental fatigue on FC alterations using EEG between PVT and driving tasks (Dimitrakopoulos, Member, & Kakkos, 2018). They contrasted the CPL and clustering coefficient (CC) from the theta band; and found that the CPL increased following mental fatigue increases both in the vigilance and driving tasks, whereas the CC increased with prolonged task performance only in the driving task.

Although the brain networks and FC have been used in mental fatigue studies in recent decades, it is a promising approach to reveal the mechanisms underlying vigilance decrement, and an efficient prevention method for fatigue-related human errors in the practical application.

1.3.3 Indicators from other techniques

In addition to EEG and fMRI, other techniques (e.g., EOG, eye-tracking and ECG) can also provide promising indicators for fatigue and vigilance decrement. EOG and eye-tracking mainly assess the activity from eye movement, which is also an important sign of drowsiness (S. K. L. Lal & Craig, 2001), and its application in mental fatigue detection has been promoted in recent studies. The indicators extracted from eye movement involves the saccades, fixations, and blinks (Salvucci & Goldberg, 2000). Especially, indicators of the saccade velocity, duration of fixation, and blink interval and duration have been used in mental fatigue detection (Hirvonen et al., 2010; Schleicher, Galley, Briest, & Galley, 2008). The heart rate variability from ECG has also been reported reflecting the mental states of individuals during task performance (S. K. L. Lal & Craig, 2001). The indices of cardiac output has been successfully used in mental fatigue study (Marcora et al., 2009). Some other techniques such as galvanic skin responses, respiration rate, and systolic and diastolic blood pressure have also been used for fatigue detection. Some studies combing indicators from different types of techniques have also emerged in the literature (Eoh et al., 2005; Marcora et al., 2009; Papadelis et al., 2007).

1.4 Aim of this research

This research aims to explore the mechanism of mental fatigue or vigilance decrement during attentional cognitive tasks. To realize the purpose, we investigate the effects of prolonged task engagement on the selective attention tasks and sustained attention tasks, respectively; we also compare different neural responses modulated by vigilance (high vs. low vigilant states) and congruency conditions (congruent vs. incongruent conditions). In addition to traditional behavioral performance and ERP analysis, we also extend the analysis to event-related spectral perturbation (ERSP), dynamic FC, and single-trial classification. Especially, the principal components analysis (PCA) is used for separating ERP components, and the tensor component analysis (TCA) is applied to extract task-related dynamic FC. Based on these objectives, I have been working on four articles. The aim of each specific article is listed below.

For *Article* I, we explore the effect of vigilance decrement on selective visual attention and the modulations of motivation on it in different vigilant states by using behavioral measurements, ERP, and ERSP.

For *Article* II, we investigate the influences of vigilance decrement and motivation on sustained attention through extracting task-related FC using the TCA pipeline, which is composed of weight phase lag index (wPLI) and TCA.

For *Article* III, we develop a single-beat automatic detection and localization system used to detect different heart diseases. This automatic detection system at the level of single-trial is used in A*rticle* IV.

For *Article* IV, we contrast the discrepancies between vigilance and congruency using temporal PCA and single-trial analysis. The developed single-trial detection method in A*rticle* III is used in this article to obtain the single-trial classification results from high vs. low vigilance and congruent vs. incongruent conditions.

2 METHODS

Apart from the conventional behavioral performance (e.g., accuracy, RT, and the number of omitted responses or omissions) and ERP measurements, the temporal PCA for ERP separation, ERSP, dynamic FC analysis assisting with TCA, and single-trial analysis have also been applied in our research. Although ERP has been well-established in the field of neuropsychology, ERP components usually overlap together making it difficult to identify the constituent components. PCA has been identified as an efficient tool to separate specific ERP components (Dien, 2012). To supplement the limited information in time-domain time- and phase-locked ERP, we apply the ERSP that providing two-dimensional information including time and frequency domain. Both ERP and ERSP are univariate approaches, and the FC analysis is a multivariate approach that can provide neural information from whole brain regions. Taking advantage of the high temporal resolution and frequency information of EEG, the frequency-specific dynamic FC is extracted using the TCA pipeline to illustrate the effects of mental fatigue. We focus on not only averaged responses but also single-trial analysis to understand the real-time neural fluctuations because the brain acts in a way of real-time cognitive processing instead of an average one (Stokes & Spaak, 2016).

In summary, in contrast to conventional analysis, these sophisticated approaches make it feasible to explore some new findings and to provide more evidence for mechanisms of mental fatigue. This chapter briefly describes these approaches and their applications.

2.1 PCA for ERP separation

ERP reflects the electrophysiological activities from neural generators and these activities sum up and volume conduct to cortical electrodes (Rose & Woolsey, 1949). Therefore, the associations between ERP and underlying neural activities are not really known and different neural activities mixing together forming

overlapping ERP components. To solve this problem, PCA has been applied to identify a sequence of ERP components, separate specific ERP components for inferential testing, and improve the localized information for ERP sources (Dien, 2010, 2012). When applying the PCA to ERP, we usually conceptualize the ERP waveforms as an ordered sequence of electrical potentials. According to different ordering domains such as the channels (spatial) or the time (temporal), the PCA can be categorized into spatial PCA and temporal PCA, respectively (Kayser & Tenke, 2003). Compared with the spatial PCA, temporal PCA is better at charactering the topography information but worse at charactering the temporal information (Dien, 1998, 2010). Previous studies have found that temporal PCA commonly performs better than spatial PCA in the ERP separation analysis (Dien, 1998, 2012). Thereupon the temporal PCA has been widely used in ERP separation analysis (Barry et al., 2020; Bowers, Buzzell, Bernat, Fox, & Barker, 2018; Dien, Spencer, & Donchin, 2003).

For the temporal PCA approach, a group of ERP waveforms (also called the cases, determined by multiplying the scalp electrodes, experimental conditions, and participants), with each waveform containing some discrete time points (also called the variables, determined by the sampling rate and the segmented epochs) are decomposed into a linear combination of principal component coefficients (named as factor loadings) and the corresponding weights (named as factor scores) (Kayser & Tenke, 2003). The factor loadings represent the invariant loading patterns or component waveforms with respect to the cases, and the factor scores represent the contribution of each case. To obtain a reliable PCA decomposition, it is typically recommended the number of cases is larger than that of variables, and the ratio of cases to variables is suggested to larger than 5 (Gorsuch, 1983). However, one work by Guadagnoli challenged the rules for producing stable solutions but proposed that component saturation, absolute sample size, the number of variables per component (to a less degree) were critical factors in determining stability (Guadagnoli & Velicer, 1988).

In addition to the input variables, the type of association matrix, the manner of factors rotation, and the criterion for the principal components (PCs) to be extracted should also be considered for the application of temporal PCA (Picton et al., 2000). In terms of the association matrix, the correlation, cross-products, and covariance matrix are generally used, with different types of matrix resulting in serious implications for PCA results. Although Kayser shows the best performance of the unrestricted, unstandardized covariance-based PCA (Kayser & Tenke, 2003), there are still some arguments on which type of association matrix should be used in the practical application.

The manner of factors rotation simplifies the interpretation of the extracted components (Picton et al., 2000). The rotation includes the Varimax, Promax, Informax, Oblimin, and so on (Dien, 2010). Especially, the Varimax rotation has been widely used in ERP studies because it maximizes the loading variance, minimizes component overlap, and retains the orthogonality of component factors (Kayser & Tenke, 2003; Picton et al., 2000). However, some studies argue that the Informax is most suitable for spatial PCA and the Promax rotation is

most effective for temporal PCA (Dien, Khoe, & Mangun, 2007). Compared to the Varimax rotation, the Promax rotation adds relaxations to the orthogonal of factors considering that the PCs have some correlations between each other owing to the volume condition (Dien, 2012; Dien et al., 2007). Other rotations such as Oblimin is not usually used in ERP analysis.

The ERP waveforms are generally decomposed into an infinite number of PCs, and the maximum number of PC is determined by the minimum number of cases and variables. These PCs explain the percentage of the variance in the data, for instance, the first PC explains the largest percentage of the variance. Evidence from Fava and Velicer has verified that under-extraction and over-extraction of the true number of components can induce decreased and unstable factors, and thus produce inaccurate results (Fava & Velicer, 1992, 1996). The proposals for the number of PCs extracted have been widely used. For example, a scree plot proposed by Cattell displaying the eigenvalues of PCs in a line plot (Cattell, 1966); Kaiser suggested that only the first PC accounting for the average variance of the original variables could be used for PCA solutions (Kaiser, 1960); Some researchers also recommended that the properties of ERP (e.g., temporal and topological information) and the prior knowledge of the paradigm should be considered to select the PCs of interest (Kayser & Tenke, 2003; Spencer, Dien, & Donchin, 2001).

2.2 Time-frequency analysis

As we introduced in section 1.3.1, the spectral content is an important indicator of mental fatigue; therefore, taking into consideration of spectral information in cognitive tasks enables us to obtain comprehensive understandings. It has been widely accepted that cortical rhythmic activity includes on-going or spontaneous, evoked, and induced oscillations, and they mirror different neural processes (David, Kilner, & Friston, 2006). The oscillatory activities in situations of rest, naturalistic stimulus, and sensory event stimulus are different. For the brain responses to sensory or cognitive stimulus, these exist all three types of cortical oscillatory activities.

The pre-stimulus spontaneous oscillations affect the post-stimulus ERP including the amplitude and latency (Herrmann, Rach, Vosskuhl, & Strüber, 2014). The post-stimulus oscillatory activities are usually analyzed using evoked, induced oscillations, and the summation of them. The evoked oscillations are time- and phase-locked to the stimulus but the induced ones are only time-locked. The summation of evoked and induced power is the total power or ERSP. Operationally, the ERSP is obtained by applying time-frequency transformation (TFT) to each trial and then averaging the power across trials; the evoked power is estimated by first averaging the waveforms across trials and then conducting the TFT; the induced power is indirectly calculated by subtracting the evoked responses and background components from the total power (David et al., 2006).

TFT is a signal processing method used for the representation of the signals simultaneously in the time and frequency domain. Fourier transform is the basis of time-frequency analysis and transforms the time series into the spectrum based on the assumption that the input signals are stationary. The short-time Fourier transform (STFT), a basic TFT approach, is an extension of the Fourier transform through extracting brief segments of data using time windows, to address the limitations of stationarity assumption. There are many types of time windows used for STFT, consisting of Hamming, Hann, and Gaussian (Cohen, 2014). Nevertheless, the selection of time window length is a trade-off process, indicating that a longer time window causes low temporal resolution, and a short time window induces low spatial resolution.

A more sophisticated approach of wavelet transform (Chui, 1992; Daubechies, 1990) has been proposed considering the temporally localized changes, the limitations of time windows, and the computational complexity. The continuous wavelet transform (CWT) is used for TFT, providing representation of signals by varying the translation and scale parameters continuously (Phillies, 1996). To realize the CWT, the input signal is convolved by the function of the mother wavelet, which is similar to the time window function in the STFT, and the transformation is calculated for different segments of data in the field of time (translation factor b) and frequency (dilatation factor a) (Quotb, Bornat, & Renaud, 2011). The CWT can be described as:

$$\mathrm{CWT}_{\psi_{a,b}}\{x(t)\} = \int_{-\infty}^{+\infty} x(t) \bullet \psi_{a,b}(t)dt \quad (1)$$

$$\psi_{a,b}(t) = \frac{1}{\sqrt[2]{a}}\psi(t - \frac{a}{b}) \quad (2)$$

where $x(t)$ is the time series, $\psi_{a,b}(t)$ represents the mother wavelet, and $\psi(t)$ is a wave-like oscillation or window function with an amplitude begins at zero. The $\psi(t)$ can be defined by scaling filter, scaling function, and wavelet function. For the wavelet function, the Morlet and Meyer wavelets are widely used in previous studies (Daubechies, 1990; Jagannathan et al., 2018). By utilizing the a, b, and $\psi(t)$, the CWT realizes the multiresolution analysis.

2.3 Functional connectivity analysis

In the area of cognitive neuroscience, how the human brain network develops, functions, and supports cognition is an increasingly important topic (Sporns, 2010). Functional networks work at multiple spatial and temporal scales (Varela, Lachaux, Rodriguez, & Martinerie, 2001) . From the most intuitive point of view, FC is referred to as a statistical interdependency between recorded neuroimaging signals at spatially separate brain areas. For fMRI studies, FC usually refers to the correlation of BOLD signals. However, the definition of FC is quite broader for EEG and magnetoencephalography (MEG). The rich spatio-temporal natures of EEG and MEG data enable FC to be estimated in many different ways

(Schölvinck, Leopold, Brookes, & Khader, 2013). Many studies have shown that oscillatory synchronization might be a key mechanism by which neural populations transmit information and form larger networks (Fries, 2005; Fries & Str, 2015; Salinas & Sejnowski, 2001). Engel and colleagues reviewed the literature of functional connectivity, in which two types of intrinsic coupling modes were suggested (Engel, Gerloff, Hilgetag, & Nolte, 2013). One of them is the envelope-based coupling that measures the relation of power between pairs of signals. Another is the phase-based coupling that assesses the synchronization of the signals based on the phase. These two types of coupling metrics focus on different aspects of EEG signals and tend to reveal different parts of the broader functional connection diagram (Schölvinck et al., 2013). Amplitude-based methods tend to be more similar to the long-range connections measured in fMRI signals relative to the phase-based connectivity (Brookes et al., 2011; Tewarie et al., 2016), which is probably proven by invasive recordings where amplitude correlation appears to be longer range than correlations of the raw time series (Leopold, Murayama, & Logothetis, 2003). However, this does not mean that phase-based methods are useless in the analysis of electrophysiological FC since they have been successfully applied for a variety of electrophysiological studies (Gross et al., 2001; Hillebrand, Barnes, Bosboom, Berendse, & Stam, 2012; Kujala et al., 2007). Recent studies have shown the advantages of multi-metric analysis (combining amplitude and phase connectivity measurements), in which the combination of simultaneous phase and amplitude assessment could be better to predict the network patterns measured in fMRI than either amplitude or phase methods individually (Tewarie et al., 2016). In the current thesis, we use the phase-based methods to assess the FC in cognitive tasks.

2.3.1 Dynamic functional connectivity analysis

Although a great number of previous studies have well described the spatial signatures of neural connectivity (Bastos & Schoffelen, 2016; O'Neill et al., 2018), most of them have not considered the temporal structure of the data, for instance, when and how the amplitude of connections between spatially separate regions or electrodes fluctuates across the experimental stimuli. A dominant mechanism is that the neuronal communication between regions across the whole brain supports the functions of human cognition, and such communication is assumed to be coordinated by neural oscillations at certain frequencies (i.e., communication through coherence) (Fries, 2005; Fries & Str, 2015). Since such modulation of neural oscillations is very rapid (Bola & Sabel, 2015), it thus accompanies that connectivity should also vary quickly, especially in response to sensory and cognitive events. It would be crucial for characterizing the dynamic FC to allow us to clarify the essence of how the functional network supports cognitive operations. For instance, the time-locked neural response in classical experiments generally lasts on the scale of hundreds of milliseconds to a few seconds. The formation of these stimuli-related responses is important for recognizing them as top-down or bottom-up, or as the feedforward or feedback process (O'Neill et al., 2018). Static FC analysis has been commonly used to

examine the communication of brain areas during a specific cognitive process (Liddle et al., 2016; Peled et al., 2001). However, compared to dynamic connectivity measures, such static analysis is not time-resolved or frequency-resolved and cannot untangle the route of information processing in the human brain. Thence, a dynamic connectivity technique could provide a deep insight to the integration of information processing in the brain. Thus, we here exploit excellent temporal resolution and good spatial coverage of EEG for measuring neuronal oscillations and directly assessing rapid changes in neuronal coherence, which is the core of brain dynamic communication.

2.3.2 Identification of repeated patterns of connectivity

When examining dynamic FC, it is common to assess connectivity between all pairs of brain regions within lots of time windows. This requires an automatic approach to assist the analysis of large data due to the estimates of massive connectivity matrices. In the last decade, lots of approaches have been developed to extract features from massive connectivity matrices to find interpretable and functionally meaningful network patterns. Many of those approaches rely on the assumption that functional connectivity is expressed in repeating or recurrent temporal or spatial patterns (O'Neill et al., 2018). These automatic identification approaches includes K-means clustering (Hassan et al., 2015), matrix decomposition (e.g., PCA and ICA) (O'Neill et al., 2017), Tensor decomposition (Zhu et al., 2020) , and hidden Markov models (Vidaurre et al., 2018).

Amongst these approaches, tensor decomposition, a high order extension of matrix decomposition, can be used to reduce dimensions of multi-way data (e.g. from spectral, spatial and temporal modes of data) and extract low-dimensional, interacted descriptors. For example, in a previous EEG study, three tensor modes repressents the time, frequency, and electrodes (Mørup, Hansen, Herrmann, Parnas, & Arnfred, 2006). In the neurophysiological measures, the different modes can correspond to the neuron, time, and trials (Williams et al., 2018). Here for studying connectivity, tensor component analysis (TCA) has been increasingly used to a variety of connectivity data structures (Escudero, Acar, Fernández, & Bro, 2015; Mahyari & Aviyente, 2014; Ozdemir, Bernat, & Aviyente, 2017; Pester, Ligges, Leistritz, Witte, & Schiecke, 2015). Such technique has recently been used to M/EEG data and to derive the frequency-specific network dynamics during repeated task (Zhu et al., 2020) and naturalistic stimuli (Zhu, Liu, Mathiak, Ristaniemi, & Cong, 2019). In these cases, TCA was applied to atlas-based M/EEG data over connections, time, and frequency to derive separate components with low-dimensional features, corresponding to a pattern of FC with rapidly temporal dynamics and specific spectal mode.

2.4 Single-trial analysis

When implementing a cognitive task, our brain requires constant involvement and real-time perception, processing, and response (Stokes & Spaak, 2016). These real-time cognitive processes can also be modulated by many external and internal factors such as the practice (Clark, Gregory Appelbaum, van den Berg, Mitroff, & Woldorff, 2015), lapses of attention (Adam, Mance, Fukuda, & Vogel, 2015), and mental fatigue (Gergelyfi et al., 2015), resulting in the fluctuation changes of cognitive processes. Instead of analyzing the brain responses in an average manner, the single-trial analysis operates in a single trial level and provides new sights for understanding the neural dynamics and neural basis of task performance.

With the development of the brain-computer interface, single-trial analysis has been an important branch in the field of neuroscience. The single-trial analysis usually includes three parts, namely the feature extraction, feature selection, and pattern recognition (Chaudhary, Birbaumer, & Ramos-Murguialday, 2016; Wolpaw et al., 2000). The key to precisely perform the single-trial analysis is extracting reliable and efficient indices from low SNR single-trial signals, which are corrupted by artifacts and background oscillatory activities. Before conducting these three parts, the single-trial data are usually preprocessed to improve the SNR by utilizing the band-pass and spatial filters. The temporal filter based on wavelet transform has been proven to enhance the performance of the single-trial analysis (Hu et al., 2011; Jia, Peng, & Hu, 2015). Different spatial filters have also been verified as efficient approaches to improve the SNR, for example, the common average reference and the Laplacian methods (McFarland, McCane, David, & Wolpaw, 1997), the data-driven and unsupervised approaches of independent component analysis (ICA) (Stewart, Nuthmann, & Sanguinetti, 2014). In particular, the data-driven and supervised approach of common spatial patterns (CSP) plays an important part in spatial filters and is widely used in the literature (Ramoser, Müller-Gerking, & Pfurtscheller, 2000). Apart from the single temporal or spatial filter application, both of them can be applied to the single-trial analysis to improve the SNR to a great degree (Hu et al., 2011).

After the procedure of preprocessing, features are extracted from the single-trial data. There are many types of features, among which the typical features are from the time and frequency domain. The features in the time domain mainly include the ERP amplitude and latency, the maximum, minimum, mean, and median values, the variance, the skewness, and the parameters of Hjorth (Blankertz, Lemm, Treder, Haufe, & Müller, 2011; Liu, Zhang, Ristaniemi, & Cong, 2019). The features in the frequency domain involves the frequency band energy, the power ratio of different frequency bands, the power spectral density (PSD), the peak frequency and peak value of PSD (Zhou, Gan, & Sepulveda, 2008), and the event-related synchronization and desynchronization(Jia et al., 2015). Some other complex features have also been applied in the single-trial analysis, such as nonlinear features (e.g., fractal dimension), autoregressive models,

entropy indices (e.g., approximate entropy and sample entropy) (Zhang, Wang, & Fu, 2014), and high-order spectrum (Zhou et al., 2008). In recent years, functional connectivity from different brain regions has emerged as an efficient feature (Krusienski, McFarland, & Wolpaw, 2012). In addition to the features in the format of vector, the features in a format of tensor combing discrete wavelet packet transform (DWPT) and multilinear principal components analysis (MPCA) has been used in the single-trial analysis(He, Tan, & Xing, 2019; Liu et al., 2020). In the practical application, many types of features are generally used together to achieve good performance but also induce the high dimensionality impairing the classification performance.

The feature selection or dimensionality reduction procedure is applied to select a set of representative features and reduce the dimensionality of the feature space, solving the problem of curse-of-dimensionality and saving the processing and storage of the data (F. Lotte et al., 2018). A total of three types of feature selection approaches have been determined representing the filter, wrapper, and embedded methods (Fabien Lotte, Congedo, Lécuyer, Lamarche, & Arnaldi, 2007). The filter method measures the relationship between features and target class regardless of the classifier to be applied. The linear complexity of the filter approach is associated with the number of features, and the filter method can lead to redundant features (McFarland et al., 1997). The wrapper and embedded methods take into consideration of the classifier, but at a cost of longer computation time. The wrapper method separates the features from the classifier, whereas the embedded method integrates the feature selection and the evaluation. Many feature selection methods have been proposed attributed into these three types, such as the maximal mutual information (filter method) (Ang, Chin, Wang, Guan, & Zhang, 2012), linear regression for knowledge extraction (wrapper method) (Liang & Bougrain, 2012), and the stepwise linear discriminant analysis (embedded method) (Krusienski et al., 2006). Based on a public BCI competition dataset, researchers have tested many feature selection methods and finally verified a good performance of three methods, namely the correlation-based feature selection, information gain, and 1R ranking (F. Lotte et al., 2018).

The low-dimensional and representative features obtained from the feature selection procedure are input into classifiers to recognize specific mental state or subject groups. Conventional classification methods are generally subcategorized into five main families of classifiers including the linear classifiers (e.g., linear discriminant analysis), non-linear Bayesian classifiers (e.g., hidden Markov models), neural network (e.g., multi-layer perceptron), nearest neighbour classifiers (e.g., k-nearest neighbour algorithm), and combination classifiers (consisting of boosting, stacking, and voting combinations) (F. Lotte et al., 2018; Fabien Lotte et al., 2007). Although conventional methods have made great progress for single-trial analysis, the single-trial classification still faces many challenges such as the low SNR of single-trial data, non-stationarity of data across trials, tasks, or participants, a limited number of samples for training (Ahn & Jun, 2015; B. F. Lotte, 2015). In recent years, the adaptive classifiers have been

proposed which aims to cope with the non-stationary properties in single-trial classification. The adaptive classifiers achieve a good performance and more advanced adaptive classifiers have been developed in the practical application (F. Lotte et al., 2018; Shenoy, Krauledat, Blankertz, Rao, & Müller, 2006). Advances in deep learning also allow for its application in single-trial classification because deep learning can learn the features and classifiers directly and achieve a good performance. It has been widely used in single-trial analysis but mostly offline because of the long training time and computational complexity of deep learning networks (F. Lotte et al., 2018; Yin & Zhang, 2017; Yin, Zhao, Wang, Yang, & Zhang, 2017).

3 SUMMARIES OF STUDIES

3.1 Study 1: The dissociable effects of motivation on a selective visual attention task in different vigilance states

I. **Liu, J.**, Zhang, C., Zhu, Y., Liu, Y., Sun, H., Ristaniemi, T., Cong, F. and Parviainen, T., 2020. Dissociable effects of reward on P300 and EEG spectra under conditions of high vs. low vigilance during a selective visual attention task. Frontiers in human neuroscience, 14, p.207.

Motivation

Prolonged task engagement leads to behavioral performance deteriorates and mental fatigue increases. However, the mechanism of this phenomenon is still unknown. Previous studies have proposed many theoretical frameworks of mental fatigue or vigilance decrement, for example, the underload, overload, motivational control, and combinations of every two of them. Although great efforts into this mechanism, there is still no agreed conclusion on the theoretical framework.

We experience selective attention in daily life and in some critical situations. As pointed in Robert's study (Robert & Duncan, 1995), to successfully implement a selective attention task, humans need to filter out task-irrelevant stimuli and employ limited resources to process the task-relevant stimuli. The attentional process fluctuations after a long period of selective visual attention task involvement remain to be explored.

In this study, we conduct a selective visual attention task (Flanker task) for 2 hours 20 minutes and provide monetary rewards in the high and low vigilance states. We aim to explore the effects of mental fatigue on selective visual attention and the influences of motivation on it in the high vs. low vigilance states.

Methods

Twenty healthy participants (12 females, aged 21.9 ± 2.4 years) from the university population were recruited to perform a version of Eriksen Flanker task (Eriksen & Eriksen, 1974) for 2 hours 20 min without rest. In the Flanker task, participants responded the central letter M or N with their right or left finger and ignored the flankers around the central letter. The paradigm of the task and the experimental procedure are shown in Figure 1. During the formal experiment, participants conducted the task for seven blocks (20 min/block), each block containing 400 trials, a total of 2800 trials. The monetary reward was set in blocks 2 and 6. The 64-channel EEG data and behavioral data were recorded during the whole task performance.

The EEG data were preprocessed following procedures of filter, visual inspection, removing direct current, removing spikes using wavelet threshold method (Zhang et al., 2018), re-reference, and removing ICA artifact components (Himberg & Hyvärinen, 2003). Next, we extracted the behavioral measurements (e.g., accuracy, RT, and omissions) from seven blocks and electrophysiological measurements of ERP (e.g., P300 amplitude and latency) and ERSP (e.g., delta and theta bands) from blocks 1, 2, 5, 6 or NRHV, RHV, NRLV, RLV. We conducted 2×2 (vigilance states×motivation states) repeated-measures analysis of variances (ANOVAs) to explore the effects of vigilance decrement on bahavioral and electrophysiological measurements in the no-reward and reward conditions, and the impacts of motivation on them in the high and low vigilance states.

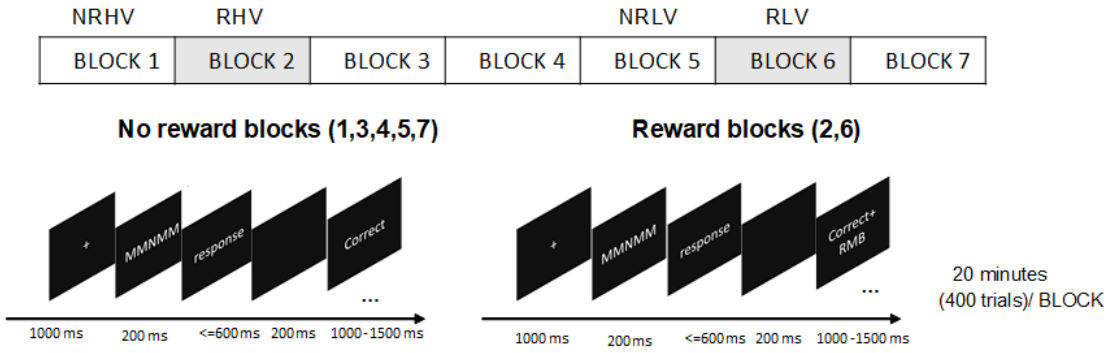

FIGURE 1 The overview of the experimental procedure and the illustration of one trial structure in the Flanker task.

Results

We found that accuracy decreased, RT and omissions increased after a long period of task performance indicating participants' mental fatigue increases and vigilance decrement. The influence of vigilance decrement and motivation on P300 is depicted in Figure 2. For the P300 amplitude, there was a main effect of reward state and an interaction effect between reward state and vigilance state; the P300 amplitude declined following vigilance decrement only in the no-

reward condition not in the reward condition, and it was improved by motivation only in the low vigilance state not in the high vigilance state. For the P300 latency, there was a main effect of vigilance state and an interaction effect between two factors; the P300 latency more lagged with mental fatigue increases in both the no-reward and reward conditions, but it was not modulated by motivation either in the low or in the high vigilance states. As shown in Figure 3, The ERSP results found that the delta band power degraded with the decrement of vigilance in the no-reward condition but not in the reward condition, and the improvement of motivation on the delta was only observed in the low vigilance state but not in the high vigilance state; the theta band power declined with vigilance decrement in both no-reward ad reward conditions, and no modulation of motivation on the theta was found in any vigilance state.

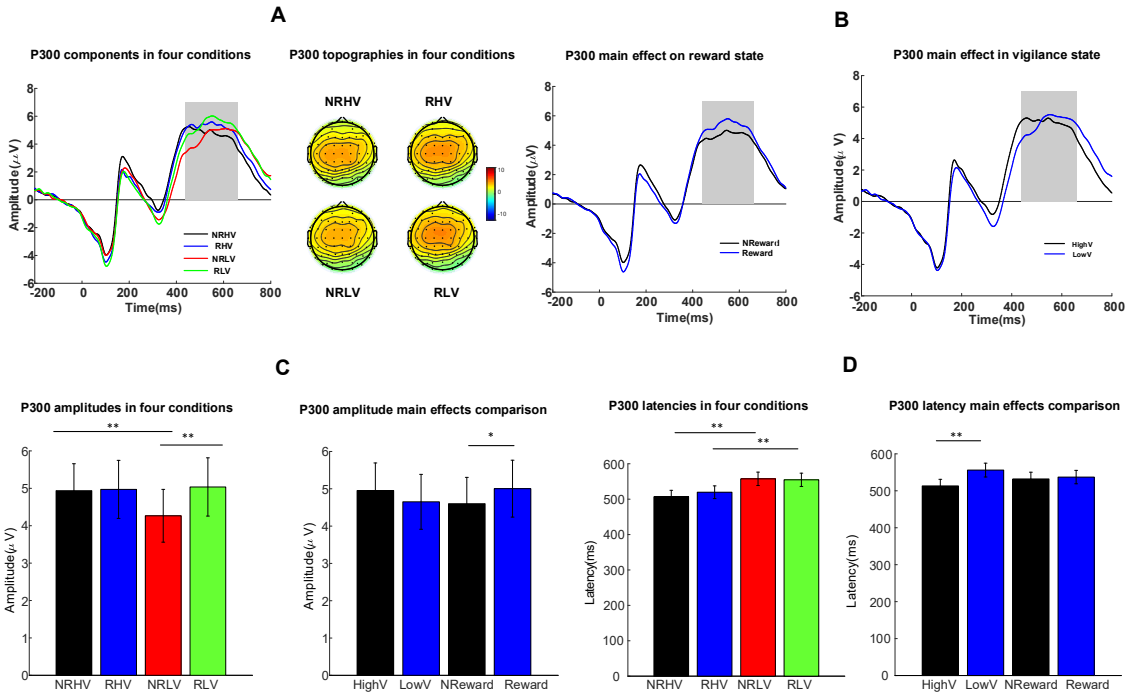

FIGURE 2 The P300 waveforms and topographies in four conditions (A), and a significant main effect of reward state on P300 amplitude and a significant main effect of vigilance state on P300 latency (B). The bars shows the changes of P300 amplitude (C) and latency (D) affected by four conditions and two main factors. The four conditions include no-reward high vigilance (NRHV), reward high vigilance (RHV), no-reward low vigilance (NRLV), and reward low vigilance (RLV). The two main factors represent reward state: no-reward (NReward) and reward (Reward) and vigilance state: high vigilance (HighV) and low vigilance (LowV).

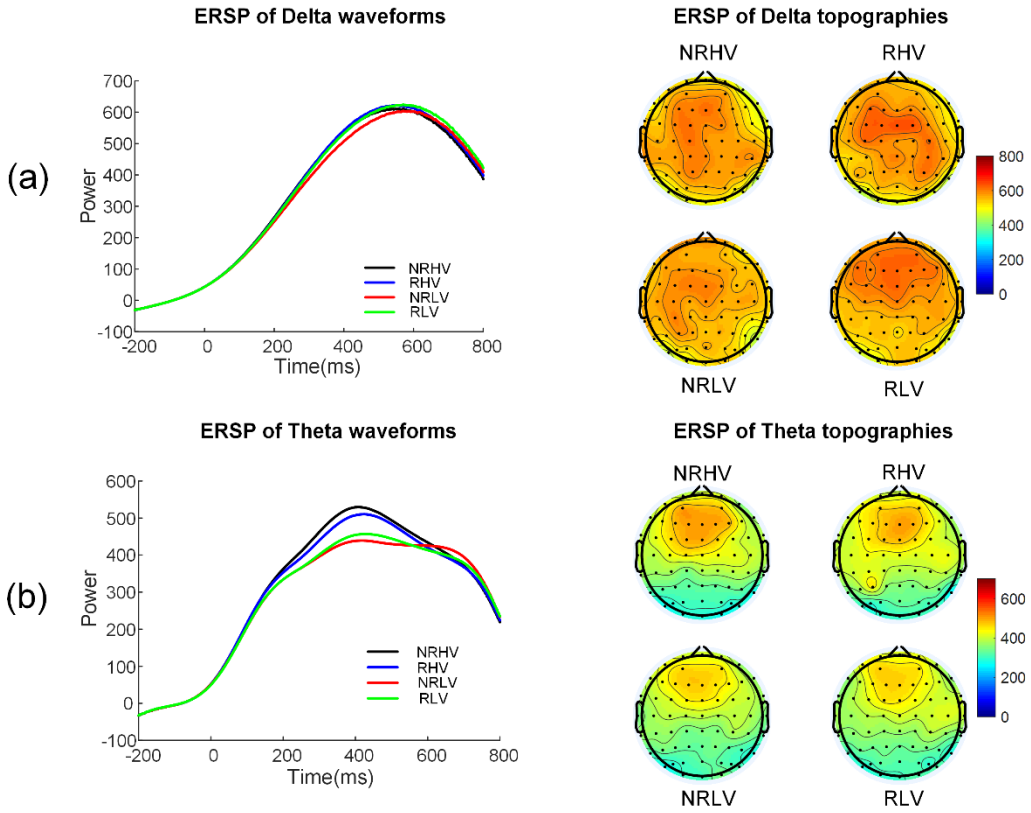

FIGURE 3 The spectral waveforms and corresponding topographies of delta band (a) and theta band (b) modulated by four conditions.

3.2 Study 2: Sustaining attention for a prolonged time affects dynamic functional connectivity

II. **Liu, J.**, Zhu, Y., Sun, H., Ristaniemi, T. and Cong, F., 2020. Sustaining Attention for a Prolonged Duration Affects Dynamic Organizations of Frequency-Specific Functional Connectivity. Brain Topography, pp.1-16.

Motivation

When sustaining attention for a long duration, humans generally failed to maintain task performance. To successfully conduct a sustained attention task, humans should employ a series of fundamental cognitive functions. It is still unknown which fundamental processes and how these processes are affected by prolonged task engagement. As reported in previous studies, the ability to perform a cognitive task is supported by dynamic brain networks in specific frequency bands (Hillebrand et al., 2012; Kujala et al., 2007; O'Neill et al., 2018). Therefore, we aim to explore the fluctuations of frequency-specific dynamic FC (fdFC) affected by vigilance decrement. To realize the extraction of sustained-attention modulated fdFC, we employ an automatic approach to characterize the

spectral, temporal, and spatial features from EEG data during a sustained attention task.

Methods

We adopted a public 64-channel EEG dataset (Reteig et al., 2019) recorded during 80 min sustained attention task without rest. The EEG data were obtained from twenty-one participants (eleven females, aged 21.6±3.4 years). In the last 20 min, participants were provided with rewards for motivation. Figure 4 shows the experimental procedure and the trial structure. After preprocessing, the segmented epochs were binned into three conditions including the correct rejections, hits, and misses. We analyzed the trials in eight 10 minutes blocks in the correct rejections condition, and in the four 20 minutes blocks in the hits and misses conditions. We also considered the number of trials across blocks in each condition.

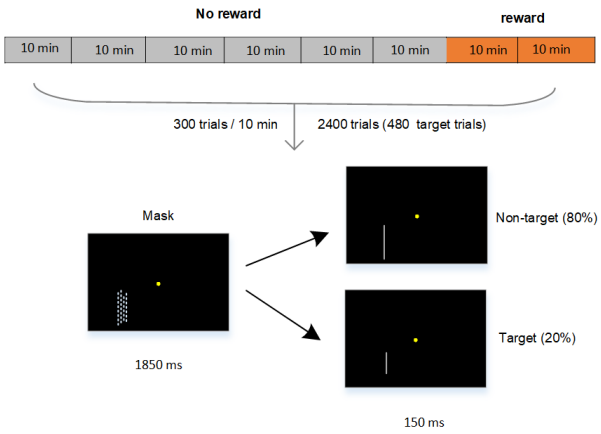

FIGURE 4 Outline of experimental procedure and structure of one trial in a sustained attention task.

To obtain spectral, temporal, and spatial signatures of electrophysiological frequency-specific dynamic FC, we proposed the analysis pipeline comprised of wPLI and TCA, and applied the pipeline (Figure 5) to characterize the repeating fdFC in the three conditions of the sustained attention task. The task-modulated fdFCs were selected using prior knowledge and the association with behaviral measurements (e.g., RT, accuracy or ACC, and hit rate or Hit). The effects of time-on-task (6 or 3 blocks) and motivation on these fdFCs were statistically analyzed using one-way ANOVA and pair-wise comparisons, and these results were corrected by false discover rate (FDR) (Y Benjamini & Yekutieli, 2001; Yoav Benjamini & Yekutieli, 2005).

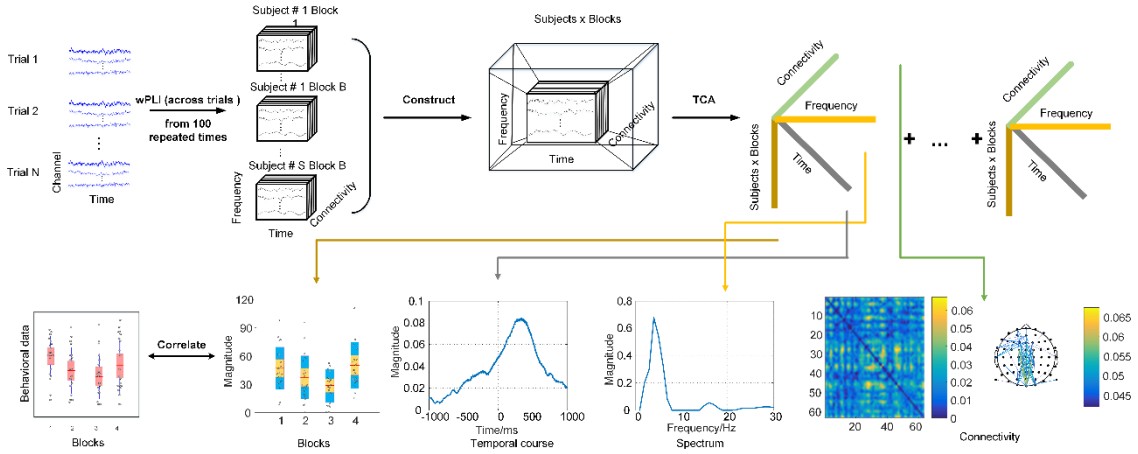

FIGURE 5 The analysis pipeline comprised of balancing trial number, wPLI tenor formation, applying TCA, and selection of task-related fdFC.

Results

As shown in Figure 6, in the correct rejections condition, we obtained four types of task-modulated fdFCs, in the temporal order of the pre-stimulus alpha right-lateralized parieto-occipital FC (I), the post-stimulus theta fronto-parieto-occipital FC (II), delta fronto-parieto-occipital FC (III), and beta right and left sensorimotor FCs (IV and V). Using the same criterion, in the hits condition, three types of fdFCs were extracted similar to these in the correct rejection condition, but without the beta right/left sensorimotor FCs. In the misses condition, only these two fdFCs in the alpha and theta bands were detected. These fdFCs occurred in different conditions with different fundamental fdFCs involvement. All fdFCs were impaired by prolonged task involvement but they are modulated differently by rewards. These fdFCs, apart from the beta left network, were restored by motivation. The restoration by motivation on the beta right network was transient.

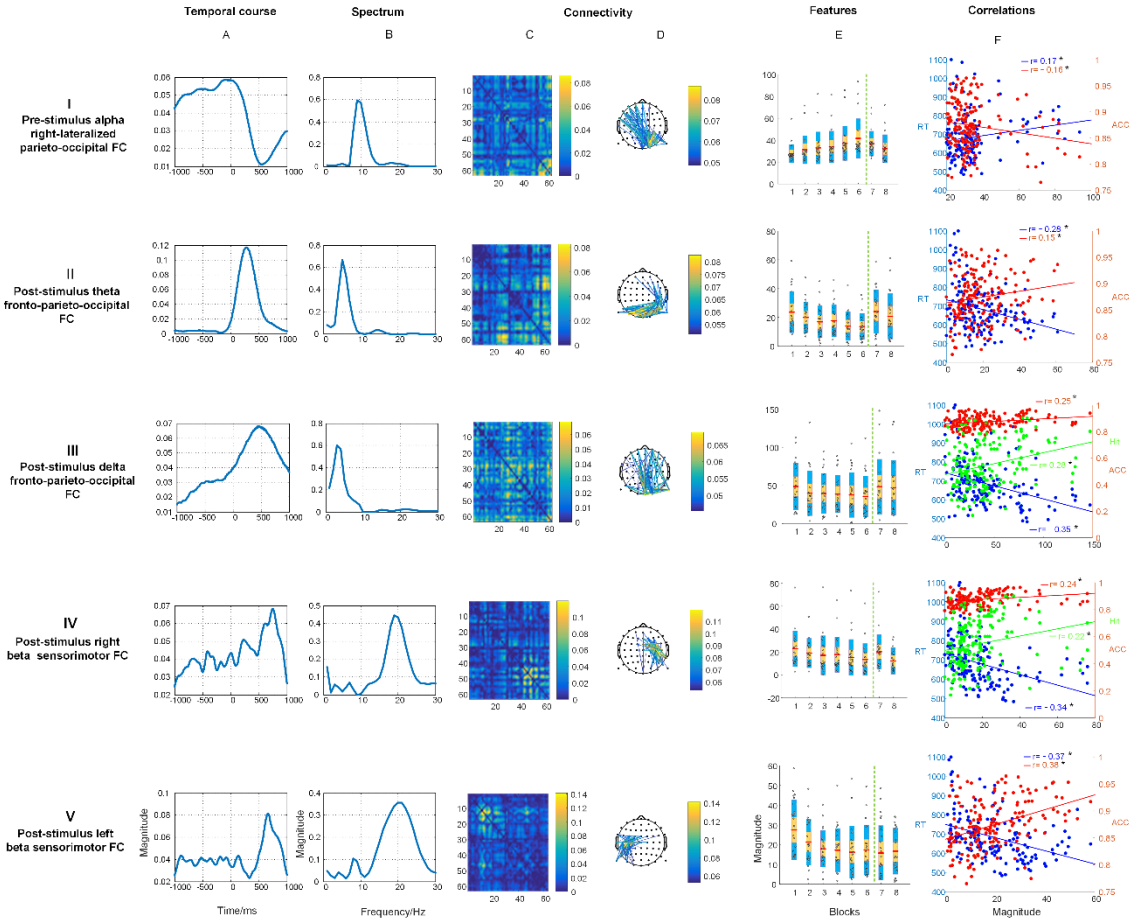

FIGURE 6 Five TCA components extracted from a sustained attention task in the correct rejections condition. Each row indicates one TCA component, consisting of six columns: the temporal course (A), spectrum (B), connectivity in the format of matrix (C) and 2-D visualization (D), and features (E). These components are correlated with behavioral measurements (e.g., RT, ACC, and Hit).

3.3 Study 3: The separable modulations of vigilance and congruency in a conflict task

III. **Liu, J.**, Zhang, C., Zhu, Y., Ristaniemi, T., Parviainen, T. and Cong, F., 2020. Automated detection and localization system of myocardial infarction in single-beat ECG using Dual-Q TQWT and wavelet packet tensor decomposition. Computer Methods and Programs in Biomedicine, 184, p.105120.

IV. **Liu, J.**, Zhu, Y., Chang, Z., Hämäläinen, T. and Cong, F., 2020. Congruency and vigilance produce separable changes in the late positive complex during a Flanker task.

Motivation

In a conflict task, humans usually need longer RT to process the incongruent stimuli than the congruent stimuli. Similarly, humans generally have slower responses in the low vigilance state than the high vigilance state. There is still an argument whether neural responses in conflict processing origins from true conflict processing or longer RT (Grinband et al., 2011; McKay, van den Berg, & Woldorff, 2017). Based on these questions, the purpose of the study is to reveal the neural differences between congruency (congruent vs. incongruent) and vigilance (high vs. low vigilant), and also to explore whether the neural fluctuations between incongruent vs. congruent are related to true conflict processing or not.

To address these questions, we adopted the same dataset as *Article* I. Instead of focusing on the vigilance state and motivation state, this study emphasizes the differences between congruency and vigilance. To identify more detailed information in a Flanker task, we apply the temporal PCA in addition to conventional ERP analysis. Considering the neural fluctuations across trials and blocks, we also try to explore the neural activity at the single-trial level. The single-beat automatic detection system developed in *Article* III was used in *Article* IV to obtain the single-trial classification results in different vigilant and congruent conditions. In the automatic detection system, the features containing spectral, temporal, and spatial information were extracted using DWPT, and high-dimensional features were dimensionality reduced using MPCA.

Methods

In this study, the same EEG dataset as study 1 obtained from twenty healthy participants (12 females, aged 21.9±2.4 years) during performing a version of Eriksen Flanker task were re-analyzed. According to the RT titration process (McKay et al., 2017), we examined the robust behavioral effect in the congruency state (RT is longer in the incongruent than congruent condition) and vigilance state (RT is longer in the low vigilant than the high vigilant state) for each participant. After this process, the averaged ERPs from channels, participants, and conditions were decomposed using temporal PCA to extract separate ERP in four conditions (e.g., high vigilance congruency or HVCon, high vigilance incongruency or HVIncon, low vigilance congruency or LVCon, low vigilance incongruency or LVIncon).

Additionally, we also explored the discrepancies of single-trial responses in the congruency and vigilance using the feature extraction and classification approaches. According to the flowchart in Figure 7, we applied the DWPT to extract multidimensional features and reconstructed the features in the temporal domain, and then we used the MPCA for feature reduction. The effectiveness of the combination of DWPT and MPCA for feature extraction and selection has been successfully applied in single-beat ECG analysis in *Article* III. The representative features were classified using the support vector machine (SVM).

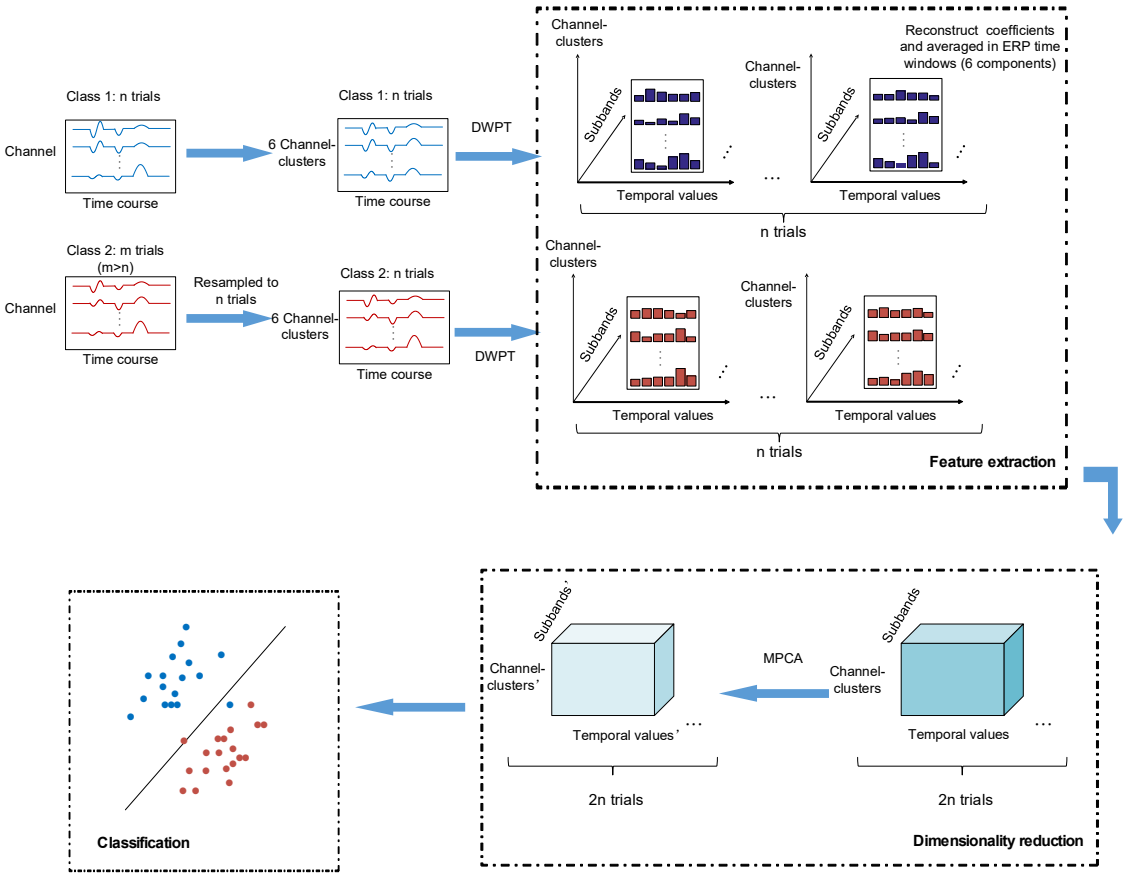

FIGURE 7 The flowchart of single-trial analysis for binary classification. DWPT are used to extract features from balanced trials in two conditions. These features are dimensionality reduced using MPCA and then input into SVM classifier.

Results

By utilizing the temporal PCA, we extracted six ERP components, accounting for the variance of 94.74%, as illustrated in Figure 8. These six components were identified in the temporal order of N1, P2, N2, and three LPC components, namely the P3a, P3b, and positive slow wave (SW). Statistical results revealed that there was a main effect of congruency on P3a and P3b; there was a main effect of vigilance on P2, P3a, and SW. No main effect was found in N1 and N2. No interaction was found in any of these extracted components.

For the single-trial analysis, we conducted four binary classifications: HVCon vs. HVIncon, LVCon vs. LVIncon, HVCon vs. LVCon, HVIncon vs. LVIncon to reveal the differences between congruent vs. incongruent and high vs. low vigilant. By using the framework in Figure 8, we achieved the accuracies of 61.93%, 61.44%, 72.57%, and 75.12% for these four classifications, respectively. The classification performance of vigilance was better than that of congruency. There was no difference in congruency contrast between high and low vigilance states. However, the vigilance contrast in the incongruent condition was better than that in the congruent condition.

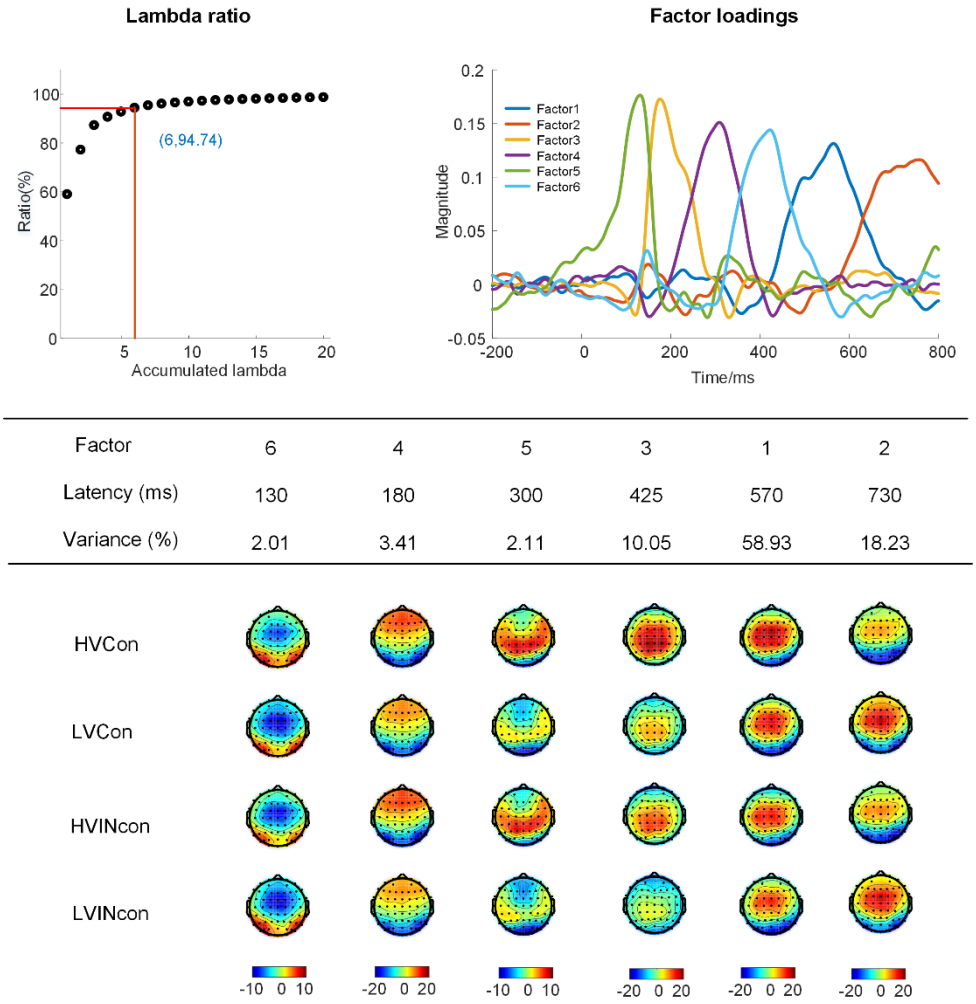

Factor	6	4	5	3	1	2
Latency (ms)	130	180	300	425	570	730
Variance (%)	2.01	3.41	2.11	10.05	58.93	18.23

FIGURE 8 The results of temporal PCA, including the lambda ratio, factor loadings, factor information, and factor scores

4 DISCUSSION

The dissertation investigated the fluctuations of brain activity in attentional cognitive tasks after a long period of time, examined the theoretical frameworks of mental fatigue or vigilance decrement, and also explored the neural differences between vigilance and congruency. This dissertation consisted of four articles to explore three studies, including study 1: the effects of vigilance decrement on selective visual attention (*Article* I), study 2: the influences of decrease of vigilance on sustained attention (*Article* II), and study 3: the differences of underlying functions between vigilance and congruency (*Article* III and IV). Specially, *Article* I conducted a version of Eriksen Flanker task (Eriksen & Eriksen, 1974) for 2 hours 20 minutes and provided monetary reward in intervals of 20-40 and 100-120 minutes. By analyzing the amplitude and latency of P300 and the delta and theta bands from ERSP, this article found that these electrophysiological measurements impaired by vigilance decrement only in the non-motivation state but not in the motivation state; the P300 amplitude and delta band were improved by motivation but only in the low vigilant state, whereas the P300 latency and theta band were not modulated by motivation either in the low and high vigilant state. *Article* II analyzed the EEG data from 80 minutes (the last 20 minutes provided with rewards) sustained attention task (MacLean et al., 2009; Reteig et al., 2019) by extracting dynamic FC patterns. This article detected four types of fdFCs—pre-stimulus alpha FC, post-stimulus theta FC, post-stimulus delta FC, and post-stimulus right and left FCs—corresponding to different fundamental functions, and found that these fdFCs were impaired by vigilance decrement but were differently modulated by motivation. *Article* IV revealed the differences between vigilance and congruency using temporal PCA and single-trial analysis (developed in *Article* III), and demonstrated that there were differences between vigilance and congruency, especially in the late positive complex (LPC). Overall, the prolonged task engagement impaired the neural functions involved in both selective attention and sustained attention, and the motivation played an important role in cognitive processes in the fatigue state.

4.1 Impacts of vigilance decrement on cognitive functions

As mentioned in the Introduction, "attention" can be divided into successive and selective attentional aspects (Posner & Boies, 1971; Sturm & Willmes, 2001), and the effects of vigilance decrement on two aspects may be different showing that the successive tasks are more sensitive to time-on-task (Warm et al., 2008). *Articles* I and IV investigated respectively the effects of prolonged task engagement on selective attention and conflict processing, and *Article* II explored the impacts of time-on-task on sustained attention.

In *Article* I, we conducted a Flanker task for a long time and analyzed the effects of vigilance decrement on selective attention. The electrophysiological indicators from ERP (e.g., P300 amplitude and latency) and ERSP (e.g., the delta and theta bands) were used to explore the neural activities modulated by mental fatigue. The P300 amplitude has been reported as an index of attentional capacity (Polich, 2007) and P300 latency has been identified as an indicator of the timing of stimulus evaluation and information processing in visual tasks (Käthner et al., 2014; Polich & Kok, 1995; Verleger, 1997). In this article, P300 amplitude and latency were impaired by vigilance decrement. These impairments suggest that prolonged task involvement degrades attentional capacity and deteriorates the cognitive process of stimulus evaluation or information processing. Furthermore, the delta and theta bands were also weakened by prolonged task engagement. The involvement of delta and frontal theta bands have also been found in visual attention tasks, indicating that the delta band is associated with attention allocation (Keller, Payne, & Sekuler, 2017) and frontal theta is related to internal processing (Harmony et al., 1996). The changes of delta and theta bands are likely interpreted that mental fatigue impairs the neural functions of attention allocation and internal stimulus processing.

In *Article* II, we adopted a sustained attention EEG dataset recorded for 80 minutes to examine the influences of vigilance decrement on sustained attention. In fact, successfully performing a sustained attention task requires a series of cognitive processes such as attentional preparation, attention stability, working memory, and responses (Clark et al., 2015; Reteig et al., 2019; Rosenberg et al., 2016; Slagter, Prinssen, Reteig, & Mazaheri, 2016). The indicators of ERP (e.g., P1/N1), theta oscillations, and pre-stimulus alpha power were reported in the original paper, and only the theta oscillations were sensible to time-on-task and motivation (Reteig et al., 2019). In the present article, taking advantage of the high temporal resolution of EEG, we applied the indicators of fdFC based on the hypothesis that whole brain regions interact at a rapid temporal scale through specific frequency band (Fries & Str, 2015; O'Neill et al., 2017; Seli et al., 2015). The dynamic FCs were computed using the wPLI (Vinck, Oostenveld, Van Wingerden, Battaglia, & Pennartz, 2011), which was robustness for the noise and volume conduction. We then applied the TCA rather than matrix decomposition to extract the repeating fdFC patterns, without stacking and concatenating data together (Zhu et al., 2019, 2020). Based on prior knowledge of cognitive processes

and close relationships with behavioral data, we identified four types of fdFCs in the temporal order of the pre-stimulus alpha right-lateralized parieto-occipital FC, post-stimulus theta fronto-parieto-occipital FC, post-stimulus delta fronto-parieto-occipital FC, and post-stimulus right and left sensorimotor FCs. These four types of fdFCs are likely corresponding to the cognitive processes of attentional preparatory, attentional stability, working memory, and response inhibition. This article found that vigilance decrement impaired all of these fdFCs. When checking the neural activities corresponding to these FC in a specific frequency band, these findings may indicate that the decrease of vigilance impairs a cascade of cognitive functions during a sustained attention task.

In *Article* IV, we re-analyzed the EEG data from the Flanker task in the direction of vigilance and congruency. We also took into consideration a series of fundamental functions involved in a Flanker task. By utilizing the temporal PCA, we obtained some ERP components in the latency order of N1, P2, N2, P3a, P3b, and SW. We demonstrated that the P2, P3a, and SW decreased with mental fatigue increases. The P2 component has a close linkage with the functions of the identification of target features in the stimuli (Luck, 2005). N2 component has been widely reported to indicate conflict processing (Folstein & Van Petten, 2008), although many recent findings have argues that the P3a is a replacement indicator for conflict processing (Alderman, Olson, Brush, & Shors, 2016; Kałamała et al., 2018; Smith, Mattick, & Sufani, 2015). The P3b and SW have been demonstrated reflecting the functions of working memory and subsequent processing (Strüber & Polich, 2002). Our results seem to state that vigilance decrement affects the target stimuli process, the conflict stimulus process, and the subsequent further processing in a selective attention task. We further found the effects of congruency of ERP components of P3a and P3b. There were amplitude differences (e.g., P2, P3b, and SW) between vigilance and congruency. We also detected differences between these two main factors using the single-trial analysis.

Taken together, prolonged task engagement affects the fundamental cognitive functions involved either in a selective attention task or in a sustained attention task.

4.2 Theoretical framework of vigilance decrement

In the literature, many theoretical frameworks have been proposed including the underload (Manly et al., 1999), the overload (Helton & Warm, 2008), and motivational control (Kurzban et al., 2013), and the "resource-control" framework (Thomson et al., 2015), the synthesized theoretical frameworks combining the motivation and task unrelated thoughts (Seli et al., 2015), and the frameworks combining the motivational control and energetical costs (Boksem & Tops, 2008). However, no agreed theoretical framework has been determined until now.

In *Article* I, all indicators of ERP and ERSP in selective attention were weakened by time-on-task. In *Article* II, similarly, the indicators of fdFCs in sustained attention were impaired by prolonged task involvement. These results may indicate that the overload theoretical framework indicating that cognitive resources were limited and these resources were depleted during the long-lasting performance. These results may also verify the motivational control theoretical framework stating that task performance declines and mental fatigue increases when the costs outweigh the benefits. After manipulating motivation in the low vigilant state, the P300 amplitude and delta band power increased, but the P300 latency and theta band power were not modulated by motivation (*Article* I); some fdFCs were improved after providing rewards, but the beta left sensorimotor network was not restored from impairment. Although the beta right sensorimotor network was restored by the motivation, the restoration was transient showing that the improved network declined again in the last 10 minutes (*Article* II). These results seem to disagree with the overload theoretical framework because task performance and neural responses were improved after manipulating motivation. These restoration results seem to support the theoretical framework of motivational control owing to the role of motivation played on cognitive tasks in the fatigue state. However, partial restorations and transient improvement by motivation probably reaffirm that the motivational control framework cannot explain all these changes from *Articles* I and II. Our results are likely to provide evidence for the synthesized theoretical framework of motivational control and energetical costs.

4.3 Limitations

Mental fatigue is a subjective feeling of humans and it is a complex phenomenon affected by many factors, such as sleep, durations of task engagement, health situation, emotion, and nutrition, and environment. To explore the mechanism of mental fatigue, we should focus on one or two factors at the same time controlling confusion from other unrelated factors, which is such a hard problem. Besides, there is still no agreed definition of mental fatigue in the literature. In *Articles* I and IV, we regarded the early and late blocks as high vigilant and low vigilant states, respectively. In fact, the state of fatigue or vigilance dynamically varied during cognitive tasks even in a few seconds or minutes. Therefore, we should determine the vigilance states at the level of single-trial in both early and late blocks. In addition, subjective questionnaires and other modality data such as eye-tracking and ECG should also be used together to provide more evidence for mental states. *Article* II applied the TCA to extract fdFCs during a sustained attention task. In fact, the stability of the TCA is still a key question. To widely promote this method, the stability of TCA should be further studied. In this article, more appropriate approaches to select the task-related FC patterns remain to be established. Limited to the spatial resolution of EEG, we only analyze the activity in the sensor level rather than the source level, and we could not give

more explanations on the neuroimaging activations. *Article* III proposed an automatic single-trial identification system using prepocrssing, DWPT feature extraction, and MPCA dimensionality reduction methods, more efficient and generalized methods across participants and tasks should be developed in cognitive studies.

4.4 Future directions

To explore the mechanism of mental fatigue, we will consider as many factors (e.g., the experience working on specific tasks, different populations) related to fatigue state and control unrelated factors when conducting fatigue-related experiments.

Considering the complex of mental fatigue, we will also extend the EEG research to MEG, which has a higher spatial resolution relative to EEG data. We can analyze the data at both the sensor level and source level, providing underlying neural responses in rapid time scales and in brain regions.

To provide more indicators for the state of fatigue, we will also adopt other modality data such as eye-tracking, ECG, EOG, EMG, and video images. It is also recommended to fusion some modality data to provide precise results. However, the fusion approaches and the complexity should be considered and well developed in practical application.

Instead of averaged response exploration, we will also extend the mental fatigue analysis to single-trial responses. The averaged responses cannot reveal the transient changes during cognitive tasks and may leave out some important information after averaging.

Furthermore, subjective questionnaires should also be used because the mental fatigue is a subjective feeling. It should be noted the duration of providing questionnaires since the interruption of answering questionnaires can cause the fluctuations of mental state.

The sleep deprivation is closely related to the task performance of humans. Sleep deprivation should also be considered in studies of mental fatigue. In fact, lapses of attention usually emerge during task performance, we should also distinguish the differences between lapses of attention and too tiredness to conduct tasks

In this dissertation, we only observe the effects of prolonged task engagement on selective and sustained attention, and we will also extend the effects to other types of cognitive tasks (e.g., auditory tasks).

YHTEENVETO (SUMMARY IN FINNISH)

Tässä väitöskirjassa on tutkittu henkisen uupumuksen mekanismien vaikutuksia valikoivaan huomiota ja jatkuvaa huomiota liittyviin aika-tehtäviin. Lisäksi työssä on tutkittu myös hermostollisia eroja valppauden ja kongruenssin välillä.

Selektiivisessä visuaalisen tarkkailun tehtävässä selvitettiin aika-tehtävän vaikutuksia valikoivaan tarkkailuun ja tutkittiin myös motivaation modulaatioita valikoivaan tarkkailuun korkeassa ja matalassa valppaana olotilassa. Hyödyntämällä P300-amplitudin ja -viiveen elektrofysiologisia indikaattoreita ja ERSP:n delta-ja teeta-alueita on havaittu, että nämä indikaattorit heikensivät pitkäaikaista tehtävään sitoutumista, mikä osoitti, että tarkkaavaisuuden resurssit heikkenivät henkisen väsymyksen lisääntyessä. Rahallisten palkkioiden tarjoamisen jälkeen osittaiset indikaattorit (esim. P300-amplitudi ja delta-alue) palauttivat väsymystilasta, mutta eivät hälytystilasta, mikä viittaa siihen, että motivaatio parantaa tarkkaavaisuusresursseja väsymystilassa jossain määrin. Väitöskirjan tulokset tarjoavat näyttöä motivaatiokontrollin ja energiakustannusten teoreettisesta kehyksestä.

Jatkuvan tarkkailun tehtävässä on tutkittu valppauden vähentämisen vaikutuksia jatkuvaan tarkkaavaisuuteen ja motivaation modulaatioita siihen matalassa valppaustasossa. Jatkuvan tarkkaavaisuuden EEG-tietojoukko on julkaistu ERP:n ja aikataajuusanalyysin kanssa aikaisemmassa tutkimuksessa. Dynaamisen toiminnallisen liitettävyyden indikaattorit on johdettu tensorihajotuksella monitiefunktionaalisen liitettävyyden purkamiseksi ottaen huomioon samanaikaisesti dynaamisten vaihteluiden, oskillaattorisynkronoinnin ja aivojen alueiden vuorovaikutuksen ominaisuudet. Tuloksena on neljän tyyppinen taajuuskohtainen toiminnallinen liitettävyys jatkuvassa tarkkailutehtävässä, mukaan lukien stimuloinnin edeltävät alfa-FC, stimulanjälkeiset teeta-, delta- ja beeta-FC:t. Nämä neljä toiminnallista liitäntätyyppiä heikensivät valppauden heikkenemistä ja palautuivat osittain ja ohimenevästi motivaatiomenetelmillä. Tämä osoittaa, että jatkuvan huomion taustalla olevat kognitiiviset perustoiminnot heikkeni, mutta osittaiset toiminnot palautuivat ja osa palautuksista oli ohimeneviä. Nämä havainnot vahvistavat motivaation merkityksen tehtävän ohjaukseen.

Saman valikoivan tarkkailutehtävän aikana kerätyn tiedon kanssa analysoitiin neurologisia eroja valppauden ja yhdenmukaisuuden välillä. Päähavaintona oli, että sekä henkinen väsymys että konfliktien käsittely voivat johtaa pidempiin vasteaikoihin konfliktitehtävissä. Tässä analysoitiin myös yhtäläisten ja epäyhdenmukaisten olosuhteiden hermovasteita sekä korkeaa ja matalaa valpasta tilaa. Käyttämällä ajallista PCA:ta otettiin sarjan ERP:tä ajallisessa järjestyksessä N1,P2, N2, P3a, P3b ja SW. Tästä huomattiin, että P2, P3a, SW olivat herkkiä valppaan tilan heikkenemiselle, kun taas P3a ja P3b olivat herkkiä muutoksille. Tässä havaittiin myös erot valppauden ja yhdenmukaisuuden välillä yhden kokeen tasolla.

Yhteenvetona väitöskirja osoittaa pitkäaikaisen tehtävän sitoutumisen merkittävät vaikutukset erilaisiin tarkkaavaisuustehtäviin valikoivassa tarkkailussa ja jatkuvassa tarkkailussa. Tulokset vaikuttavat teoreettiseen kehykseen, jonka

mukaan valppauden vähennys liittyy motivaatioon ja energiakustannuksiin. Tämä mahdollistaa vertailun valppauden ja yhdenmukaisuuden välillä, mikä osoittaa, että hermosolujen perusta on erilainen valppauden vähennyksen ja konfliktien käsittelyn välillä. Kaikki väitöskirjassa tehdyt havainnot tarjoavat työkaluja sen ymmärtämiseen, mitä vaikutuksia on työstä toiseen siirtymisellä tai valppauden heikkenemisellä.

REFERENCES

Aaronson, L. S., Teel, C. S., Cassmeyer, V., Neuberger, G. B., Pallikkathayil, L., Pierce, J., … Wingate, A. (1999). Defining and measuring fatigue. *Journal of Nursing Scholarship*, *31*(1), 45–50. https://doi.org/10.1111/j.1547-5069.1999.tb00420.x

Adam, K. C. S., Mance, I., Fukuda, K., & Vogel, E. K. (2015). The Contribution of Attentional Lapses to Individual Differences in Visual Working Memory Capacity. *Journal of Cognitive Neuroscience*, *27*(8), 139. https://doi.org/10.1162/jocn

Ahn, M., & Jun, S. C. (2015). Performance variation in motor imagery brain-computer interface: A brief review. *Journal of Neuroscience Methods*, *243*, 103–110. https://doi.org/10.1016/j.jneumeth.2015.01.033

Åkerstedt, T., & Gillberg, M. (1990). Subjective and objective sleepiness in the active individual. *International Journal of Neuroscience*, *52*(1–2), 29–37. https://doi.org/10.3109/00207459008994241

Akerstedt, T., Kecklund, G., & Knutsson, A. (1991). Manifest sleepiness and the spectral content of the EEG during shift work. *Sleep*, *14*(3), 221–225. https://doi.org/10.1093/sleep/14.3.221

Alderman, B. L., Olson, R. L., Brush, C. J., & Shors, T. J. (2016). MAP training: Combining meditation and aerobic exercise reduces depression and rumination while enhancing synchronized brain activity. *Translational Psychiatry*, *6*(December 2015). https://doi.org/10.1038/tp.2015.225

Anderson, M. C., & Levy, B. J. (2009). Suppressing unwanted memories. *Current Directions in Psychological Science*, *18*(4), 189–194. https://doi.org/10.1111/j.1467-8721.2009.01634.x

Ang, K. K., Chin, Z. Y., Wang, C., Guan, C., & Zhang, H. (2012). Filter bank common spatial pattern algorithm on BCI competition IV datasets 2a and 2b. *Frontiers in Neuroscience*, *6*(MAR), 1–9. https://doi.org/10.3389/fnins.2012.00039

B.S.Oken, M.C.Salinsky, and S. M. E. (2006). Vigilance, alertness, or sustained attention: physiological basis and measurement. *Clinical Neurophysiology*, *117*(9), 1885–1901. https://doi.org/10.1038/jid.2014.371

Barry, R. J., Steiner, G. Z., De Blasio, F. M., Fogarty, J. S., Karamacoska, D., & MacDonald, B. (2020). Components in the P300: Don't forget the Novelty P3! *Psychophysiology*, *57*(7), 1–15. https://doi.org/10.1111/psyp.13371

Bastos, A. M., & Schoffelen, J. M. (2016). A tutorial review of functional connectivity analysis methods and their interpretational pitfalls. *Frontiers in Systems Neuroscience*, *9*(JAN2016), 1–23. https://doi.org/10.3389/fnsys.2015.00175

Belyavin, A., & Wright, N. A. (1987). Changes in electrical activity of the brain with vigilance. *Electroencephalography and Clinical Neurophysiology*, *66*(2), 137–144. https://doi.org/10.1016/0013-4694(87)90183-0

Benjamini, Y., & Yekutieli, D. (2001). The control of the false discovery rate under dependency. *The Annals of Statistics*, *29*(4), 1165–1188. Retrieved from

http://www.math.tau.ac.il/~ybenja/MyPapers/benjamini_yekutieli_ANNSTAT2001.pdf

Benjamini, Y., & Yekutieli, D. (2005). False Discovery Rate–Adjusted Multiple Confidence Intervals for Selected Parameters. *Journal of the American Statistical Association*, *100*(469), 71–81. https://doi.org/10.1198/016214504000001907

Blankertz, B., Lemm, S., Treder, M., Haufe, S., & Müller, K. R. (2011). Single-trial analysis and classification of ERP components - A tutorial. *NeuroImage*, *56*(2), 814–825. https://doi.org/10.1016/j.neuroimage.2010.06.048

Boksem, M. A. S., Meijman, T. F., & Lorist, M. M. (2005). Effects of mental fatigue on attention: An ERP study. *Cognitive Brain Research*, *25*(1), 107–116. https://doi.org/10.1016/j.cogbrainres.2005.04.011

Boksem, M. A. S., Meijman, T. F., & Lorist, M. M. (2006). Mental fatigue, motivation and action monitoring. *Biological Psychology*, *72*(2), 123–132. https://doi.org/10.1016/j.biopsycho.2005.08.007

Boksem, M. A. S., & Tops, M. (2008). Mental fatigue: Costs and benefits. *Brain Research Reviews*, *59*(1), 125–139. https://doi.org/10.1016/j.brainresrev.2008.07.001

Bola, M., & Sabel, B. A. (2015). Dynamic reorganization of brain functional networks during cognition. *NeuroImage*, *114*, 398–413. https://doi.org/10.1016/j.neuroimage.2015.03.057

Borja-Cacho, D., & Matthews, J. (2008). Influence lf cognitive control and mismatch on the N2 component of the ERP: A review. *Psychophysiology*, *6*(9), 2166–2171. https://doi.org/10.1021/nl061786n.Core-Shell

Bowers, M. E., Buzzell, G. A., Bernat, E. M., Fox, N. A., & Barker, T. V. (2018). Time-frequency approaches to investigating changes in feedback processing during childhood and adolescence. *Psychophysiology*, *55*(10), e13208. https://doi.org/10.1111/psyp.13208

Brookes, M. J., Hale, J. R., Zumer, J. M., Stevenson, C. M., Francis, S. T., Barnes, G. R., … Nagarajan, S. S. (2011). Measuring functional connectivity using MEG: Methodology and comparison with fcMRI. *NeuroImage*, *56*(3), 1082–1104. https://doi.org/10.1016/j.neuroimage.2011.02.054

Brudzynski, S. M. (2014). The ascending mesolimbic cholinergic system - A specific division of the reticular activating system involved in the initiation of negative emotional states. *Journal of Molecular Neuroscience*, *53*(3), 436–445. https://doi.org/10.1007/s12031-013-0179-1

Cattell, R. (1966). The Scree Test for the number of factors. Multivariate Behavioral Research. *Multivariate Behavioral Research. 1*, *1*(August), 116–141. https://doi.org/10.1207/s15327906mbr0102

Cavanagh, J. F., & Frank, M. J. (2014). Frontal theta as a mechanism for cognitive control. *Trends in Cognitive Sciences*, *18*(8), 414–421. https://doi.org/10.1016/j.tics.2014.04.012

Chaudhary, U., Birbaumer, N., & Ramos-Murguialday, A. (2016). Brain-computer interfaces for communication and rehabilitation. *Nature Reviews Neurology*, *12*(9), 513–525. https://doi.org/10.1038/nrneurol.2016.113

Chui, C. (1992). *An Introduction to Wavelets.* Academic Press. https://doi.org/10.2307/2153134

Chun, M. M., Golomb, J. D., & Turk-Browne, N. B. (2011). A Taxonomy of external and internal attention. *Annual Review of Psychology*, *62*, 73–101. https://doi.org/10.1146/annurev.psych.093008.100427

Clark, K., Gregory Appelbaum, L., van den Berg, B., Mitroff, S. R., & Woldorff, M. G. (2015). Improvement in visual search with practice: Mapping learning-related changes in neurocognitive stages of processing. *Journal of Neuroscience*, *35*(13), 5351–5359. https://doi.org/10.1523/JNEUROSCI.1152-14.2015

Cohen, M. X. (2014). *Analyzing neural time series data: theory and practice*. MIT Press.

Collins, A., & Koechlin, E. (2012). Reasoning, learning, and creativity: Frontal lobe function and human decision-making. *PLoS Biology*, *10*(3). https://doi.org/10.1371/journal.pbio.1001293

Conway, A. R. A., & Engle, R. W. (1994). Working Memory and Retrieval: A Resource-Dependent Inhibition Model. *Journal of Experimental Psychology: General*, *123*(4), 354–373. https://doi.org/10.1037/0096-3445.123.4.354

Corbetta, M., & Shulman, G. L. (2002). Control of goal-directed and stimulus-driven attention in the brain. *Nature Reviews Neuroscience*, *3*(3), 201–215. https://doi.org/10.1038/nrn755

Crowley, K. E., & Colrain, I. M. (2004). A review of the evidence for P2 being an independent component process: Age, sleep and modality. *Clinical Neurophysiology*, *115*(4), 732–744. https://doi.org/10.1016/j.clinph.2003.11.021

D R Davies;, & Parasurman, R. (1982). *The psychology of vigilance*. London□; New York□: Academic Press.

Daubechies, I. (1990). The Wavelet Transform, Time-Frequency Localization and Signal Analysis. *IEEE Transactions on Information Theory*, *36*(5), 961–1005. https://doi.org/10.1109/18.57199

David, O., Kilner, J. M., & Friston, K. J. (2006). Mechanisms of evoked and induced responses in MEG/EEG. *NeuroImage*, *31*(4), 1580–1591. https://doi.org/10.1016/j.neuroimage.2006.02.034

Dawson, D., Ian Noy, Y., Härmä, M., Kerstedt, T., & Belenky, G. (2011). Modelling fatigue and the use of fatigue models in work settings. *Accident Analysis and Prevention*, *43*(2), 549–564. https://doi.org/10.1016/j.aap.2009.12.030

Demiralp, T., Ademoglu, A., Comerchero, M., & Polich, J. (2001). Wavelet analysis of P3a and p3b. *Brain Topography*, *13*(4), 251–267. https://doi.org/10.1023/A:1011102628306

Diamond, A. (2013). Executive functions. *Annual Review of Psychology*, *64*, 135–168. https://doi.org/10.1146/annurev-psych-113011-143750

Dien, J. (1998). Addressing misallocation of variance in principal components analysis of event-related potentials. *Brain Topography*, *11*(1), 43–55. https://doi.org/10.1023/A:1022218503558

Dien, J. (2010). Evaluating two-step PCA of ERP data with Geomin, Infomax, Oblimin, Promax, and Varimax rotations. *Psychophysiology*, *47*(1), 170–183. https://doi.org/10.1111/j.1469-8986.2009.00885.x

Dien, J. (2012). Applying principal components analysis to event-related potentials: A tutorial. *Developmental Neuropsychology*, *37*(6), 497–517. https://doi.org/10.1080/87565641.2012.697503

Dien, J., Khoe, W., & Mangun, G. R. (2007). Evaluation of PCA and ICA of simulated ERPs: Promax vs. infomax rotations. *Human Brain Mapping*, *28*(8), 742–763. https://doi.org/10.1002/hbm.20304

Dien, J., Spencer, M. kevin., & Donchin, E. (2003). Localization of event-related potential novelty response as definded by principal components analysis. *Cognitive Brain Research*, *17*(2003), 637–650. https://doi.org/10.1016/S0926-6410(03)00188-5

Dimitrakopoulos, G. N., Member, S., & Kakkos, I. (2018). Fatigue Reveals Different Network Topological. *IEEE Transactions on Neural Systems and Rehabilitation Engineering*, *26*(4), 740–749.

Egeth, H. E., & Yantis, S. (1997). Visual Attention: Control, Representation, and Time Course. *Annual Review of Psychology*, *48*, 269–297. https://doi.org/10.1146/annurev.psych.48.1.269

Engel, A. K., Gerloff, C., Hilgetag, C. C., & Nolte, G. (2013). Intrinsic Coupling Modes: Multiscale Interactions in Ongoing Brain Activity. *Neuron*, *80*(4), 867–886. https://doi.org/10.1016/j.neuron.2013.09.038

Eoh, H. J., Chung, M. K., & Kim, S. H. (2005). Electroencephalographic study of drowsiness in simulated driving with sleep deprivation. *International Journal of Industrial Ergonomics*, *35*(4), 307–320. https://doi.org/10.1016/j.ergon.2004.09.006

Erickson, K. I., & Kramer, A. F. (2009). Aerobic exercise effects on cognitive and neural plasticity in older adults. *British Journal of Sports Medicine*, *43*(1), 22–24. https://doi.org/10.1136/bjsm.2008.052498

Eriksen, B. A., & Eriksen, C. W. (1974). Effects of noise letters upon the identification of a target letter in a nonsearch task. *Perception & Psychophysics*. https://doi.org/10.3758/BF03203267

Ernst Niedermeyer, & Silva, F. H. L. da. (2005). *Electroencephalography: Basic Principles, Clinical Applications, and Related Fields*. Lippincott Williams & Wilkins.

Escudero, J., Acar, E., Fernández, A., & Bro, R. (2015). Multiscale entropy analysis of resting-state magnetoencephalogram with tensor factorisations in Alzheimer's disease. *Brain Research Bulletin*, *119*, 136–144. https://doi.org/10.1016/j.brainresbull.2015.05.001

Faber, L. G., Maurits, N. M., & Lorist, M. M. (2012). Mental Fatigue Affects Visual Selective Attention. *PLoS ONE*, *7*(10), 1–10. https://doi.org/10.1371/journal.pone.0048073

Fan, J., Mccandliss, B. D., Sommer, T., Raz, A., & Posner, M. I. (2002). Testing the efficiency and independence of attentional networks. *Journal of Cognitive Neuroscience*, *14*(3), 340–347. https://doi.org/10.1162/089892902317361886

Fava, J. L., & Velicer, W. F. (1992). The Effects of Overextraction on Factor and Component Analysis. *Multivariate Behavioral Research*, *27*(3), 387–415. https://doi.org/10.1207/s15327906mbr2703_5

Fava, J. L., & Velicer, W. F. (1996). The effects of underextraction in factor and component analyses. *Educational and Psychological Measurement*, *56*(6), 907–929. https://doi.org/10.1177/0013164496056006001

Folstein, J. R., & Van Petten, C. (2008). Influence of cognitive control and mismatch on the N2 component of the ERP: A review. *Psychophysiology*, *45*(1), 152–170. https://doi.org/10.1111/j.1469-8986.2007.00602.x

Fries, P. (2005). A mechanism for cognitive dynamics: Neuronal communication through neuronal coherence. *Trends in Cognitive Sciences*, *9*(10), 474–480. https://doi.org/10.1016/j.tics.2005.08.011

Fries, P., & Str, E. (2015). Rhythms for Cognition : Communication through Coherence. *Neuron*, *88*(October 2015), 220–235. https://doi.org/10.1016/j.neuron.2015.09.034.

Gergelyfi, M., Jacob, B., Olivier, E., & Zénon, A. (2015). Dissociation between mental fatigue and motivational state during prolonged mental activity. *Frontiers in Behavioral Neuroscience*, *9*, 1–15. https://doi.org/10.3389/fnbeh.2015.00176

Gorsuch, R. L. (1983). *Factor analysis* (2nd editio). Hillsdale, NJ: Lawrence Erlbaum Associates. https://doi.org/10.1177/0145482x1711100313

Grandjean, E. (1979). Fatigue in industry. *British Journal of Industrial Medicine*, *36*(3), 175–186. https://doi.org/10.1136/oem.36.3.175

Grinband, J., Savitskaya, J., Wager, T. D., Teichert, T., Ferrera, V. P., & Hirsch, J. (2011). The dorsal medial frontal cortex is sensitive to time on task, not response conflict or error likelihood. *NeuroImage*, *57*(2), 303–311. https://doi.org/10.1016/j.neuroimage.2010.12.027

Gross, J., Kujala, J., Hämäläinen, M., Timmermann, L., Schnitzler, A., & Salmelin, R. (2001). Dynamic imaging of coherent sources: Studying neural interactions in the human brain. *Proceedings of the National Academy of Sciences of the United States of America*, *98*(2), 694–699. https://doi.org/10.1073/pnas.98.2.694

Guadagnoli, E., & Velicer, W. F. (1988). Relation of Sample Size to the Stability of Component Patterns. *Psychological Bulletin*, *103*(2), 265–275. https://doi.org/10.1037/0033-2909.103.2.265

Gui, D., Xu, S., Zhu, S., Fang, Z., Spaeth, A. M., Xin, Y., … Rao, H. (2015). Resting spontaneous activity in the default mode network predicts performance decline during prolonged attention workload. *NeuroImage*, *120*(01), 323–330. https://doi.org/10.1016/j.neuroimage.2015.07.030

Guo, Z., Chen, R., Liu, X., Zhao, G., Zheng, Y., Gong, M., & Zhang, J. (2018). The impairing effects of mental fatigue on response inhibition: An ERP study. *PLoS ONE*, *13*(6), 1–18. https://doi.org/10.1371/journal.pone.0198206

Harmony, T., Fernández, T., Silva, J., Bernal, J., Díaz-Comas, L., Reyes, A., … Rodríguez, M. (1996). EEG delta activity: An indicator of attention to internal processing during performance of mental tasks. *International Journal of*

Psychophysiology, *24*(1–2), 161–171. https://doi.org/10.1016/S0167-8760(96)00053-0

Hassan, M., Benquet, P., Biraben, A., Berrou, C., Dufor, O., & Wendling, F. (2015). Dynamic reorganization of functional brain networks during picture naming. *Cortex*, *73*, 276–288. https://doi.org/10.1016/j.cortex.2015.08.019

He, H., Tan, Y., & Xing, J. (2019). Unsupervised classification of 12-lead ECG signals using wavelet tensor decomposition and two-dimensional Gaussian spectral clustering. *Knowledge-Based Systems*, *163*, 392–403. https://doi.org/10.1016/j.knosys.2018.09.001

Helton, W. S., & Warm, J. S. (2008). Signal salience and the mindlessness theory of vigilance. *Acta Psychologica*, *129*(1), 18–25. https://doi.org/10.1016/j.actpsy.2008.04.002

Herrmann, C. S., Rach, S., Vosskuhl, J., & Strüber, D. (2014). Time-frequency analysis of event-related potentials: A brief tutorial. *Brain Topography*, *27*(4), 438–450. https://doi.org/10.1007/s10548-013-0327-5

Hillebrand, A., Barnes, G. R., Bosboom, J. L., Berendse, H. W., & Stam, C. J. (2012). Frequency-dependent functional connectivity within resting-state networks: An atlas-based MEG beamformer solution. *NeuroImage*, *59*(4), 3909–3921. https://doi.org/10.1016/j.neuroimage.2011.11.005

Himberg, J., & Hyvärinen, A. (2003). ICASSO: Software for investigating the reliability of ICA estimates by clustering and visualization. *Neural Networks for Signal Processing - Proceedings of the IEEE Workshop*, *2003–Janua*, 259–268. https://doi.org/10.1109/NNSP.2003.1318025

Hirvonen, K., Puttonen, S., Gould, K., Korpela, J., Koefoed, V. F., & Müller, K. (2010). Improving the saccade peak velocity measurement for detecting fatigue. *Journal of Neuroscience Methods*, *187*(2), 199–206. https://doi.org/10.1016/j.jneumeth.2010.01.010

Hobson, J. A., & Pace-Schott, E. F. (2002). The cognitive neuroscience of sleep: Neuronal systems, consciousness and learning. *Nature Reviews Neuroscience*, *3*(9), 679–693. https://doi.org/10.1038/nrn915

Hopstaken, J. F., van der Linden, D., Bakker, A. B., & Kompier, M. A. J. (2015). A multifaceted investigation of the link between mental fatigue and task disengagement. *Psychophysiology*, *52*(3), 305–315. https://doi.org/10.1111/psyp.12339

Hu, L., Zhang, Z. G., Hung, Y. S., Luk, K. D. K., Iannetti, G. D., & Hu, Y. (2011). Single-trial detection of somatosensory evoked potentials by probabilistic independent component analysis and wavelet filtering. *Clinical Neurophysiology*, *122*(7), 1429–1439. https://doi.org/10.1016/j.clinph.2010.12.052

Jagannathan, S. R., Ezquerro-Nassar, A., Jachs, B., Pustovaya, O. V., Bareham, C. A., & Bekinschtein, T. A. (2018). Tracking wakefulness as it fades: Micro-measures of alertness. *NeuroImage*, *176*(April), 138–151. https://doi.org/10.1016/j.neuroimage.2018.04.046

James, W. (1890). *The principles of psychology* (Vol. 1). .: Dover Publications. New York.

Jap, B. T., Lal, S., Fischer, P., & Bekiaris, E. (2009). Using EEG spectral components to assess algorithms for detecting fatigue. *Expert Systems with Applications*, *36*(2 PART 1), 2352–2359. https://doi.org/10.1016/j.eswa.2007.12.043

Jia, H., Peng, W., & Hu, L. (2015). A novel approach to identify time-frequency oscillatory features in electrocortical signals. *Journal of Neuroscience Methods*, *253*, 18–27. https://doi.org/10.1016/j.jneumeth.2015.05.026

Jones, B. E. (2008). Modulation of cortical activation and behavioral arousal by cholinergic and orexinergic systems. *Annals of the New York Academy of Sciences*, *1129*, 26–34. https://doi.org/10.1196/annals.1417.026

Kaiser, H. F. (1960). The application of electronic computers to factor analysis. *Educational and Psychological Measurement*, *XX*(1), 141–151. https://doi.org/10.1177/001316446002000116

Kałamała, P., Szewczyk, J., Senderecka, M., & Wodniecka, Z. (2018). Flanker task with equiprobable congruent and incongruent conditions does not elicit the conflict N2. *Psychophysiology*, *55*(2), 1–15. https://doi.org/10.1111/psyp.12980

Kane, M. J., & Engle, R. W. (2000). Working-Memory Capacity, Proactive Interference, and Divided Attention: Limits on Long-Term Memory Retrieval. *Journal of Experimental Psychology: Learning Memory and Cognition*, *26*(2), 336–358. https://doi.org/10.1037/0278-7393.26.2.336

Karbach, J., & Kray, J. (2009). How useful is executive control training? Age differences in near and far transfer of task-switching training. *Developmental Science*, *12*(6), 978–990. https://doi.org/10.1111/j.1467-7687.2009.00846.x

Käthner, I., Wriessnegger, S. C., Müller-Putz, G. R., Kübler, A., & Halder, S. (2014). Effects of mental workload and fatigue on the P300, alpha and theta band power during operation of an ERP (P300) brain-computer interface. *Biological Psychology*, *102*(1), 118–129. https://doi.org/10.1016/j.biopsycho.2014.07.014

Kato, Y., Endo, H., & Kizuka, T. (2009). Mental fatigue and impaired response processes: Event-related brain potentials in a Go/NoGo task. *International Journal of Psychophysiology*, *72*(2), 204–211. https://doi.org/10.1016/j.ijpsycho.2008.12.008

Kayser, J., & Tenke, C. E. (2003). Optimizing principal components analysis (PCA) methodology for ERP component identification and measurement□: Theoretical rationale and empirical evaluation. *Clinical Neurophysiology*, *12*(2307), 2325. https://doi.org/10.1016/s1388-2457(03)00241-4

Keller, A. S., Payne, L., & Sekuler, R. (2017). Characterizing the roles of alpha and theta oscillations in multisensory attention. *Neuropsychologia*, *99*, 48–63. https://doi.org/10.1016/j.neuropsychologia.2017.02.021

Klimesch, W. (1999). EEG alpha and theta oscillations reflect cognitive and memory performance. *Brain Research Reviews*, *29*(2–3), 169–195. https://doi.org/10.1016/S0165-0173(98)00056-3

Knyazev, G. G. (2012). EEG delta oscillations as a correlate of basic homeostatic and motivational processes. *Neuroscience and Biobehavioral Reviews*, *36*(1), 677–695. https://doi.org/10.1016/j.neubiorev.2011.10.002

Krusienski, D. J., McFarland, D. J., & Wolpaw, J. R. (2012). Value of Amplitude, Phase, and Coherence Features for a Sensorimotor Rhythm-Based Brain-Computer Interface. *Brain Research Bulletin*, *87*(1), 130–134. https://doi.org/10.1161/CIRCULATIONAHA.110.956839

Krusienski, D. J., Sellers, E. W., Bayoudh, S., Mcfarland, D. J., Vaughan, T. M., Wolpaw, J. R., … Mcfarland, D. J. (2006). A comparison of classification techniques for the P300 speller To cite this version□: A Comparison of Classification Techniques for the P300 Speller. *Journal of Neural Engineering*, *3*(4), 299–305. https://doi.org/10.1088/1741-2560/3/4/007

Kujala, J., Pammer, K., Cornelissen, P., Roebroeck, A., Formisano, E., & Salmelin, R. (2007). Phase coupling in a cerebro-cerebellar network at 8-13 Hz during reading. *Cerebral Cortex*, *17*(6), 1476–1485. https://doi.org/10.1093/cercor/bhl059

Kurzban, R., Duckworth, A., Kable, J. W., & Myers, J. (2013). An opportunity cost model of subjective effort and task performance. *Behavioral and Brain Sciences*, *36*(6), 661–679. https://doi.org/10.1017/S0140525X12003196

Lal, S. K. L., & Craig, A. (2001). A critical review of the psychophysiology of driver fatigue. Biological Psychology. *Biological Psychology*, *55*(2001), 173–194. https://doi.org/10.1016/S0301-0511(00)00085-5

Lal, S. K. L., & Craig, A. (2002). Driver fatigue: Electroencephalography and psychological assessment. *Psychophysiology*, *39*(3), 313–321. https://doi.org/10.1017/S0048577201393095

Lehto, J. E., Juujärvi, P., Kooistra, L., & Pulkkinen, L. (2003). Dimensions of executive functioning: Evidence from children. *British Journal of Developmental Psychology*, *21*(1), 59–80. https://doi.org/10.1348/026151003321164627

Leon, T., & Schultz, W. (1999). Relative reward preference in primate orbitofrontal cortex. *Nature*, *398*(6729), 704–708.

Leopold, D. A., Murayama, Y., & Logothetis, N. K. (2003). Very slow activity fluctuations in monkey visual cortex: Implications for functional brain imaging. *Cerebral Cortex*, *13*(4), 422–433. https://doi.org/10.1093/cercor/13.4.422

Liang, N., & Bougrain, L. (2012). Decoding finger flexion from band-specific ecog signals in humans. *Frontiers in Neuroscience*, *6*(JUN), 1–6. https://doi.org/10.3389/fnins.2012.00091

Liddle, E. B., Price, D., Palaniyappan, L., Brookes, M. J., Robson, S. E., Hall, E. L., … Liddle, P. F. (2016). Abnormal salience signaling in schizophrenia: The role of integrative beta oscillations. *Human Brain Mapping*, *37*(4), 1361–1374. https://doi.org/10.1002/hbm.23107

Lim, J., & Dinges, D. F. (2008). Sleep deprivation and vigilant attention. *Annals of the New York Academy of Sciences*, *1129*, 305–322. https://doi.org/10.1196/annals.1417.002

Lim, J., Wu, W., Wang, J., Detre, J. A., Dinges, D. F., & Hengyi, R. (2010). Imaging Brain Fatigue from Sustained Mental Workload: An ASL Perfusion Study of the Time-On-Task Effect. *Neuroimage*, *49*(4), 3426–3435. https://doi.org/10.1016/j.neuroimage.2009.11.020

Lin, C. T., Ko, L. W., Chung, I. F., Huang, T. Y., Chen, Y. C., Jung, T. P., & Liang, S. F. (2006). Adaptive EEG-based alertness estimation system by using ICA-based fuzzy neural networks. *IEEE Transactions on Circuits and Systems I: Regular Papers*, *53*(11), 2469–2476. https://doi.org/10.1109/TCSI.2006.884408

Linden, D. E. J. (2005). The P300: Where in the brain is it produced and what does it tell us? *Neuroscientist*, *11*(6), 563–576. https://doi.org/10.1177/1073858405280524

Liu, J., Zhang, C., Ristaniemi, T., & Cong, F. (2019). Detection of Myocardial Infarction from Multi-lead ECG using Dual-Q Tunable Q-Factor Wavelet Transform. In *Proceedings of the Annual International Conference of the IEEE Engineering in Medicine and Biology Society, EMBS* (pp. 1496–1499). IEEE. https://doi.org/10.1109/EMBC.2019.8857775

Liu, J., Zhang, C., Zhu, Y., Ristaniemi, T., Parviainen, T., & Cong, F. (2020). Automated detection and localization system of myocardial infarction in single-beat ECG using Dual-Q TQWT and wavelet packet tensor decomposition. *Computer Methods and Programs in Biomedicine*, *184*, 105120. https://doi.org/10.1016/j.cmpb.2019.105120

Lorist, M. M., Boksem, M. A. S., & Ridderinkhof, K. R. (2005). Impaired cognitive control and reduced cingulate activity during mental fatigue. *Cognitive Brain Research*, *24*(2), 199–205. https://doi.org/10.1016/j.cogbrainres.2005.01.018

Lorist, M. M., Klein, M., & Nieuwenhuis, S. (2000). Mental fatigue and task control□: Planning and preparation Mental fatigue and task control□: Planning and preparation. *Psychophysiology*, *37*(July 2017), 614–625. https://doi.org/10.1017/S004857720099005X

Lotte, B. F. (2015). Signal Processing Approaches Oscillatory Activity-Based Calibration Time in to Minimize or Suppress Brain–Computer Interfaces. In *Proceedings of the IEEE* (Vol. 103, pp. 871–890). IEEE. https://doi.org/10.1109/JPROC.2015.2404941

Lotte, F., Bougrain, L., Cichocki, A., Clerc, M., Congedo, M., Rakotomamonjy, A., & Yger, F. (2018). A review of classification algorithms for EEG-based brain-computer interfaces: A 10 year update. *Journal of Neural Engineering*, *15*(3). https://doi.org/10.1088/1741-2552/aab2f2

Lotte, F., Congedo, M., Lécuyer, A., Lamarche, F., & Arnaldi, B. (2007). A review of classification algorithms for EEG-based brain – computer interfaces. *Journal of Neural Engineering*, *4*(24). https://doi.org/10.1088/1741-2560/4/2/R01

Luck, S. J. (2005). *An introduction to the event-related potential technique*. MIT Press.

Luck, S. J., & Vogel, E. K. (1998). Electrophysiological Evidence for a Postperceptual Locus of Suppression during the Attentional Blink. *Journal of Experimental Psychology: Human Perception and Performance*, *24*(6), 1656–1674. https://doi.org/10.1037/0096-1523.24.6.1656

Mackworth, N. H. (1948). The breakdown of vigilance durning prolonged visual search. *Quarterly Journal of Experimental Psychology*, *1*(1), 6–21. https://doi.org/10.1080/17470214808416738

MacLean, K. A., Aichele, S. R., Bridwell, D. A., Mangun, G. R., Wojciulik, E., & Saron, C. D. (2009). Interactions between endogenous and exogenous attention during vigilance. *Attention, Perception, & Psychophysics*, *71*(5), 1042–1058. https://doi.org/10.3758/APP.71.5.1042

Mahyari, A. G., & Aviyente, S. (2014). Identification of dynamic functional brain network states through tensor decomposition. In *2014 IEEE International Conference on Acoustics, Speech and Signal Processing (ICASSP)* (pp. 2099–2103). IEEE. https://doi.org/10.1109/ICASSP.2014.6853969

Manly, T., Robertson, I. H., Galloway, M., & Hawkins, K. (1999). The absent mind: Further investigations of sustained attention to response. *Neuropsychologia*, *37*(6), 661–670. https://doi.org/10.1016/S0028-3932(98)00127-4

Marcora, S. M., Staiano, W., & Manning, V. (2009). Mental fatigue impairs physical performance in humans. *Journal of Applied Physiology*, *106*(3), 857–864. https://doi.org/10.1152/japplphysiol.91324.2008

May, J. F., & Baldwin, C. L. (2009). Driver fatigue: The importance of identifying causal factors of fatigue when considering detection and countermeasure technologies. *Transportation Research Part F: Traffic Psychology and Behaviour*, *12*(3), 218–224. https://doi.org/10.1016/j.trf.2008.11.005

McFarland, D. J., McCane, L. M., David, S. V., & Wolpaw, J. R. (1997). Spatial filter selection for EEG-based communication. *Electroencephalography and Clinical Neurophysiology*, *103*(3), 386–394. https://doi.org/10.1016/S0013-4694(97)00022-2

McKay, C. C., van den Berg, B., & Woldorff, M. G. (2017). Neural cascade of conflict processing: Not just time-on-task. *Neuropsychologia*, *96*(December 2016), 184–191. https://doi.org/10.1016/j.neuropsychologia.2016.12.022

Mistlberger, R. E., & Mumby, D. G. (1992). The limbic system and food-anticipatory circadian rhythms in the rat: ablation and dopamine blocking studies. *Behavioural Brain Research*, *47*(2), 159–168. https://doi.org/10.1016/S0166-4328(05)80122-6

Miyake, A., Friedman, N. P., Emerson, M. J., Witzki, A. H., Howerter, A., & Wager, T. D. (2000). The Unity and Diversity of Executive Functions and Their Contributions to Complex "Frontal Lobe" Tasks: A Latent Variable Analysis. *Cognitive Psychology*, *41*(1), 49–100. https://doi.org/10.1006/cogp.1999.0734

Möckel, T., Beste, C., & Wascher, E. (2015). The Effects of Time on Task in Response Selection - An ERP Study of Mental Fatigue. *Scientific Reports*, *5*, 1–9. https://doi.org/10.1038/srep10113

Mørup, M., Hansen, L. K., Herrmann, C. S., Parnas, J., & Arnfred, S. M. (2006). Parallel Factor Analysis as an exploratory tool for wavelet transformed event-related EEG. *NeuroImage*, *29*(3), 938–947. https://doi.org/10.1016/j.neuroimage.2005.08.005

O'Neill, G. C., Tewarie, P. K., Colclough, G. L., Gascoyne, L. E., Hunt, B. A. E., Morris, P. G., … Brookes, M. J. (2017). Measurement of dynamic task related functional networks using MEG. *NeuroImage*, *146*, 667–678. https://doi.org/10.1016/j.neuroimage.2016.08.061

O'Neill, G. C., Tewarie, P., Vidaurre, D., Liuzzi, L., Woolrich, M. W., & Brookes, M. J. (2018). Dynamics of large-scale electrophysiological networks: A technical review. *NeuroImage*, *180*(October 2017), 559–576. https://doi.org/10.1016/j.neuroimage.2017.10.003

Okogbaa, O. G., Shell, R. L., & Filipusic, D. (1994). On the investigation of the neurophysiological correlates of knowledge worker mental fatigue using the EEG signal. *Applied Ergonomics*, *25*(6), 355–365. https://doi.org/10.1016/0003-6870(94)90054-X

Ozdemir, A., Bernat, E. M., & Aviyente, S. (2017). Recursive tensor subspace tracking for dynamic brain network analysis. *IEEE Transactions on Signal and Information Processing over Networks*, *3*(4), 669–682. https://doi.org/10.1109/TSIPN.2017.2668146

Papadelis, C., Chen, Z., Kourtidou-Papadeli, C., Bamidis, P. D., Chouvarda, I., Bekiaris, E., & Maglaveras, N. (2007). Monitoring sleepiness with on-board electrophysiological recordings for preventing sleep-deprived traffic accidents. *Clinical Neurophysiology*, *118*(9), 1906–1922. https://doi.org/10.1016/j.clinph.2007.04.031

Parasuraman, R. (1979). Memory Load and Event Rate Control Sensitivity Decrements in Sustained Attention. *Science*, *205*(2209), 924–927. https://doi.org/10.1126/science.472714

Peled, A., Geva, A. B., Kremen, W. S., Blankfeld, H. M., Esfandiarfard, R., & Nordahl, T. E. (2001). Functional connectivity and working memory in schizophrenia: An EEG study. *International Journal of Neuroscience*, *106*(1–2), 47–61. https://doi.org/10.3109/00207450109149737

Pester, B., Ligges, C., Leistritz, L., Witte, H., & Schiecke, K. (2015). Advanced insights into functional brain connectivity by combining tensor decomposition and partial directed coherence. *PLoS ONE*, *10*(6), 1–18. https://doi.org/10.1371/journal.pone.0129293

Phillies, G. D. J. (1996). Wavelets: a New Alternative to Fourier Transforms. *Computers in Physics*, *10*(3), 247. https://doi.org/10.1063/1.168573

Picton, T. W., Bentin, S., Berg, P., Donchin, E., Hillyard, S. A., Johnson, R., … Taylor, M. J. (2000). Guidelines for using human event-related potentials to study cognition: Recording standards and publication criteria. *Psychophysiology*, *37*(2), 127–152. https://doi.org/10.1017/S0048577200000305

Polich, J. (2007). Updating P300:An Integrative Theory of P3a and P3b. *Clinical Neurophysiology*, *118*(10), 2128–2148. https://doi.org/10.1016/j.clinph.2007.04.019.Updating

Polich, J. (2020). 50+ years of P300: Where are we now? *Psychophysiology*, *57*(7), 2–3. https://doi.org/10.1111/psyp.13616

Polich, J., & Criado, J. R. (2006). Neuropsychology and neuropharmacology of P3a and P3b. *International Journal of Psychophysiology*, *60*(2), 172–185. https://doi.org/10.1016/j.ijpsycho.2005.12.012

Polich, J., & Kok, A. (1995). Cognitive and biological determinants of P300: an integrative review. *Biological Psychology*, *41*(2), 103–146. https://doi.org/10.1016/0301-0511(95)05130-9

Posner, M. I., & Boies, S. J. (1971). Components of attention. *Psychological Review*, *78*(5), 391–408. https://doi.org/10.1037/h0031333

Qi, P., Ru, H., Gao, L., Zhang, X., Zhou, T., Tian, Y., … Sun, Y. (2019). Neural Mechanisms of Mental Fatigue Revisited: New Insights from the Brain Connectome. *Engineering*, *5*(2), 276–286. https://doi.org/10.1016/j.eng.2018.11.025

Quotb, A., Bornat, Y., & Renaud, S. (2011). Wavelet transform for real-time detection of action potentials in neural signals. *Frontiers in Neuroengineering*, *4*(JULY), 1–10. https://doi.org/10.3389/fneng.2011.00007

Ramoser, H., Müller-Gerking, J., & Pfurtscheller, G. (2000). Optimal spatial filtering of single trial EEG during imagined hand movement. *IEEE Transactions on Rehabilitation Engineering*, *8*(4), 441–446. https://doi.org/10.1109/86.895946

Reteig, L. C., van den Brink, R. L., Prinssen, S., Cohen, M. X., & Slagter, H. A. (2019). Sustaining attention for a prolonged period of time increases temporal variability in cortical responses. *Cortex*, *117*, 16–32. https://doi.org/10.1016/j.cortex.2019.02.016

Robert, D., & Duncan, J. (1995). Neural Mechanisms of Selective Visual Attention. *Annual Review of Neuroscience*, *18*, 193–222. https://doi.org/10.1146/annurev.ne.18.030195.001205

Rose, J. E., & Woolsey, C. N. (1949). Organization of the mammalian thalamus and its relationships to the cerebral cortex. *Electroencephalography and Clinical Neurophysiology*, *1*(1–4), 391–404. https://doi.org/10.1016/0013-4694(49)90212-6

Rosenberg, M. D., Finn, E. S., Scheinost, D., Papademetris, X., Shen, X., Constable, R. T., & Chun, M. M. (2016). A neuromarker of sustained attention from whole-brain functional connectivity. *Nature Neuroscience*, *19*(1), 165–171. https://doi.org/10.1038/nn.4179.

Sabine, K., & Ungerleider, L. G. (2000). Mechanisms of visial attention in the human cortex. *Annual Review of Neuroscience*, *23*, 315–341. https://doi.org/10.1146/annurev.neuro.23.1.315

Salinas, E., & Sejnowski, T. J. (2001). Correlated neuronal activity and the flow of neural information. *Nature Reviews Neuroscience*, *2*, 539–550.

Salvucci, D. D., & Goldberg, J. H. (2000). Identifying fixations and saccades in eye-tracking protocols. *Proceedings of the Eye Tracking Research and Applications Symposium 2000*, (October 2014), 71–78. https://doi.org/10.1145/355017.355028

Santamaria, J., & Chiappa, K. H. (1987). The EEG of drowsiness in normal adults. *Journal of Clinical Neurophysiology*. https://doi.org/10.1097/00004691-198710000-00002

Sarter, M., Givens, B., & Bruno, J. P. (2001). The cognitive neuroscience of sustained attention: Where top-down meets bottom-up. *Brain Research Reviews*, *35*(2), 146–160. https://doi.org/10.1016/S0165-0173(01)00044-3

Schleicher, R., Galley, N., Briest, S., & Galley, L. (2008). Blinks and saccades as indicators of fatigue in sleepiness warnings: Looking tired? *Ergonomics*, *51*(7), 982–1010. https://doi.org/10.1080/00140130701817062

Schölvinck, M. L., Leopold, D. A., Brookes, M. J., & Khader, P. H. (2013). The contribution of electrophysiology to functional connectivity mapping. *NeuroImage*, *80*, 297–306. https://doi.org/10.1016/j.neuroimage.2013.04.010

See, J. E., Howe, S. R., Warm, J. S., & Dember, W. N. (1995). Meta-analysis of the sensitivity decrement in vigilance. *Psychological Bulletin*, *117*(2), 230–249. https://doi.org/10.1037/0033-2909.117.2.230

Seli, P., Cheyne, J. A., Xu, M., Purdon, C., & Smilek, D. (2015). Motivation, intentionality, and mind wandering: Implications for assessments of task-unrelated thought. *Journal of Experimental Psychology: Learning Memory and Cognition*, *41*(5), 1417–1425. https://doi.org/10.1037/xlm0000116

Shen, J., Barbera, J., & Shapiro, C. M. (2006). Distinguishing sleepiness and fatigue: Focus on definition and measurement. *Sleep Medicine Reviews*, *10*(1), 63–76. https://doi.org/10.1016/j.smrv.2005.05.004

Shenoy, P., Krauledat, M., Blankertz, B., Rao, R. P. N., & Müller, K. R. (2006). Towards adaptive classification for BCI. *Journal of Neural Engineering*, *3*(1), 13–23. https://doi.org/10.1088/1741-2560/3/1/R02

Slagter, H. A., Prinssen, S., Reteig, L. C., & Mazaheri, A. (2016). Facilitation and inhibition in attention: Functional dissociation of pre-stimulus alpha activity, P1, and N1 components. *NeuroImage*, *125*, 25–35. https://doi.org/10.1016/j.neuroimage.2015.09.058

Smallwood, J., & Schooler, J. W. (2006). The restless mind. *Psychological Bulletin*, *132*(6), 946–958. https://doi.org/10.1037/0033-2909.132.6.946

Smith, J. L., Mattick, R. P., & Sufani, C. (2015). Female but not male young heavy drinkers display altered performance monitoring. *Psychiatry Research - Neuroimaging*, *233*(3), 424–435. https://doi.org/10.1016/j.pscychresns.2015.07.014

Spencer, K. M., Dien, J., & Donchin, E. (2001). Spatiotemporal analysis of the late ERP responses to deviant stimuli. *Psychophysiology*, *38*(2), 343–358. https://doi.org/10.1017/S0048577201000324

Sporns, O. (2010). *Networks of the Brain*. *Networks of the Brain*. The MIT Press. https://doi.org/10.7551/mitpress/8476.001.0001

Stewart, A. X., Nuthmann, A., & Sanguinetti, G. (2014). Single-trial classification of EEG in a visual object task using ICA and machine learning. *Journal of Neuroscience Methods*, *228*, 1–14. https://doi.org/10.1016/j.jneumeth.2014.02.014

Stokes, M., & Spaak, E. (2016). The Importance of Single-Trial Analyses in Cognitive Neuroscience. *Trends in Cognitive Sciences*, *20*(7), 483–486. https://doi.org/10.1016/j.tics.2016.05.008

Strüber, D., & Polich, J. (2002). P300 and slow wave from oddball and single-stimulus visual tasks: Inter-stimulus interval effects. *International Journal of Psychophysiology*, *45*(3), 187–196. https://doi.org/10.1016/S0167-8760(02)00071-5

Sturm, W., & Willmes, K. (2001). On the functional neuroanatomy of intrinsic and phasic alertness. *NeuroImage*, *14*(1 II), 76–84. https://doi.org/10.1006/nimg.2001.0839

Stuss, D. T., Levine, B., Alexander, M. P., Hong, J., Palumbo, C., Hamer, L., … Izukawa, D. (2000). Wisconsin Card Sorting Test performance in patients with focal frontal and posterior brain damage: Effects of lesion location and test structure on separable cognitive processes. *Neuropsychologia*, *38*(4), 388–402. https://doi.org/10.1016/S0028-3932(99)00093-7

Sun, Y., Lim, J., Kwok, K., & Bezerianos, A. (2014). Functional cortical connectivity analysis of mental fatigue unmasks hemispheric asymmetry and changes in small-world networks. *Brain and Cognition*, *85*(1), 220–230. https://doi.org/10.1016/j.bandc.2013.12.011

Tanaka, H., Hayashi, M., & Hori, T. (1997). Topographical characteristics and principal component structure of the hypnagogic EEG. *Sleep*, *20*(7), 523–534. https://doi.org/10.1093/sleep/20.7.523

Tewarie, P., Bright, M. G., Hillebrand, A., Robson, S. E., Gascoyne, L. E., Morris, P. G., … Brookes, M. J. (2016). Predicting haemodynamic networks using electrophysiology: The role of non-linear and cross-frequency interactions. *NeuroImage*, *130*, 273–292. https://doi.org/10.1016/j.neuroimage.2016.01.053

Theeuwes, J. (1991). Exogenous and endogenous control of attention: The effect of visual onsets and offsets. *Perception & Psychophysics*, *49*(1), 83–90. https://doi.org/10.3758/BF03211619

Thiffault, P., & Bergeron, J. (2003). Monotony of road environment and driver fatigue: A simulator study. *Accident Analysis and Prevention*, *35*(3), 381–391. https://doi.org/10.1016/S0001-4575(02)00014-3

Thomson, D. R., Besner, D., & Smilek, D. (2015). A Resource-Control Account of Sustained Attention: Evidence From Mind-Wandering and Vigilance Paradigms. *Perspectives on Psychological Science*, *10*(1), 82–96. https://doi.org/10.1177/1745691614556681

Trejo, L. J., Kubitz, K., Rosipal, R., Kochavi, R. L., & Montgomery, L. D. (2015). EEG-Based Estimation and Classification of Mental Fatigue. *Psychology*, *06*(05), 572–589. https://doi.org/10.4236/psych.2015.65055

Van Dongen, H. P. A., Maislin, G., Mullington, J. M., & Dinges, D. F. (2003). The cumulative cost of additional wakefulness: Dose-response effects on neurobehavioral functions and sleep physiol. *Sleep*, *26*(2), 117–126. https://doi.org/10.1093/sleep/26.2.117

Varela, F., Lachaux, J. P., Rodriguez, E., & Martinerie, J. (2001). The brainweb: Phase synchronization and large-scale integration. *Nature Reviews Neuroscience*, *2*(4), 229–239. https://doi.org/10.1038/35067550

Verleger, R. (1997). On the utility of P3 latency as an index of mental chronometry. *Psychophysiology*. https://doi.org/10.1111/j.1469-8986.1997.tb02125.x

Vidaurre, D., Hunt, L. T., Quinn, A. J., Hunt, B. A. E., Brookes, M. J., Nobre, A. C., & Woolrich, M. W. (2018). Spontaneous cortical activity transiently organises into frequency specific phase-coupling networks. *Nature Communications*, *9*(1). https://doi.org/10.1038/s41467-018-05316-z

Vinck, M., Oostenveld, R., Van Wingerden, M., Battaglia, F., & Pennartz, C. M. A. (2011). An improved index of phase-synchronization for electrophysiological data in the presence of volume-conduction, noise and sample-size bias. *NeuroImage*, *55*(4), 1548–1565. https://doi.org/10.1016/j.neuroimage.2011.01.055

Warm, J. S., Parasuraman, R., & Matthews, G. (2008). Vigilance requires hard mental work and is stressful. *Human Factors*, *50*(3), 433–441. https://doi.org/10.1518/001872008X312152

Williams, A. H., Kim, T. H., Wang, F., Vyas, S., Ryu, S. I., Shenoy, K. V., … Ganguli, S. (2018). Unsupervised Discovery of Demixed, Low-Dimensional Neural Dynamics across Multiple Timescales through Tensor Component Analysis. *Neuron*, *98*(6), 1099–1115.e8. https://doi.org/10.1016/j.neuron.2018.05.015

Wolpaw, J. R., Birbaumer, N., Heetderks, W. J., McFarland, D. J., Peckham, P. H., Schalk, G., … Vaughan, T. M. (2000). Brain-computer interface technology: a review of the first international meeting. *IEEE Transactions on Rehabilitation Engineering*, *8*(2), 164–173. https://doi.org/10.1109/TRE.2000.847807

Yin, Z., & Zhang, J. (2017). Cross-session classification of mental workload levels using EEG and an adaptive deep learning model. *Biomedical Signal Processing and Control*, *33*, 30–47. https://doi.org/10.1016/j.bspc.2016.11.013

Yin, Z., Zhao, M., Wang, Y., Yang, J., & Zhang, J. (2017). Recognition of emotions using multimodal physiological signals and an ensemble deep learning model. *Computer Methods and Programs in Biomedicine*, *140*, 93–110. https://doi.org/10.1016/j.cmpb.2016.12.005

Zhang, C., Cong, F., Kujala, T., Liu, W., Liu, J., Parviainen, T., & Ristaniemi, T. (2018). Network Entropy for the Sequence Analysis of Functional Connectivity Graphs of the Brain. *Entropy*, *20*(5), 311. https://doi.org/10.3390/e20050311

Zhang, C., Wang, H., & Fu, R. (2014). Automated detection of driver fatigue based on entropy and complexity measures. *IEEE Transactions on Intelligent Transportation Systems*, *15*(1), 168–177. https://doi.org/10.1109/TITS.2013.2275192

Zhou, S. M., Gan, J. Q., & Sepulveda, F. (2008). Classifying mental tasks based on features of higher-order statistics from EEG signals in brain-computer interface. *Information Sciences*, *178*(6), 1629–1640. https://doi.org/10.1016/j.ins.2007.11.012

Zhu, Y., Liu, J., Mathiak, K., Ristaniemi, T., & Cong, F. (2019). Deriving electrophysiological brain network connectivity via tensor component

analysis during freely listening to music. *IEEE Transactions on Neural Systems and Rehabilitation Engineering*.
https://doi.org/10.1109/TNSRE.2019.2953971

Zhu, Y., Liu, J., Ye, C., Mathiak, K., Astikainen, P., Ristaniemi, T., & Cong, F. (2020). Discovering dynamic task-modulated functional networks with specific spectral modes using MEG. *NeuroImage*, *116924*.
https://doi.org/10.1016/j.neuroimage.2020.116924

ORIGINAL PAPERS

I

DISSOCIABLE EFFECTS OF REWARD ON P300 AND EEG SPECTRA UNDER CONDITIONS OF HIGH VS. LOW VIGILANCE DURING A SELECTIVE VISUAL ATTENTION TASK

by

Jia Liu, Chi Zhang, Yongjie Zhu, Yunmeng Liu, Hongjin Sun, Tapani Ristaniemi, Fengyu Cong, and Tiina Parviainen, 2020

Frontiers in human neuroscience, 14, 207

https://doi.org/10.3389/fnhum.2020.00207

frontiers in Human Neuroscience

ORIGINAL RESEARCH
published: 24 June 2020
doi: 10.3389/fnhum.2020.00207

Dissociable Effects of Reward on P300 and EEG Spectra Under Conditions of High vs. Low Vigilance During a Selective Visual Attention Task

Jia Liu[1,2], Chi Zhang[1], Yongjie Zhu[1,2], Yunmeng Liu[1], Hongjin Sun[3], Tapani Ristaniemi[2], Fengyu Cong[1,2,4,5] and Tiina Parviainen[6]**

[1]School of Biomedical Engineering, Dalian University of Technology, Dalian, China, [2]Faculty of Information Technology, University of Jyväskylä, Jyväskylä, Finland, [3]Department of Psychology, Neuroscience and Behaviour, McMaster University, Hamilton, ON, Canada, [4]School of Artificial Intelligence, Faculty of Electronic Information and Electrical Engineering, Dalian University of Technology, Dalian, China, [5]Key Laboratory of Integrated Circuit and Biomedical Electronic System, Dalian University of Technology, Dalian, China, [6]Centre for Interdisciplinary Brain Research, Department of Psychology, Faculty of Education and Psychology, University of Jyvaskyla, Jyvaskyla, Finland

OPEN ACCESS

Edited by:
Benjamin Cowley,
University of Helsinki, Finland

Reviewed by:
Kirk R. Daffner,
Brigham and Women's Hospital and Harvard Medical School, United States
Edmund Wascher,
Leibniz Research Centre for Working Environment and Human Factors (IfADo), Germany

***Correspondence:**
Fengyu Cong
cong@dlut.edu.cn
Tiina Parviainen
tiina.m.parviainen@jyu.fi

Specialty section:
This article was submitted to Cognitive Neuroscience, a section of the journal Frontiers in in Human Neuroscience

Received: 15 September 2019
Accepted: 07 May 2020
Published: 24 June 2020

Citation:
Liu J, Zhang C, Zhu Y, Liu Y, Sun H, Ristaniemi T, Cong F and Parviainen T (2020) Dissociable Effects of Reward on P300 and EEG Spectra Under Conditions of High vs. Low Vigilance During a Selective Visual Attention Task. Front. Hum. Neurosci. 14:207. doi: 10.3389/fnhum.2020.00207

The influence of motivation on selective visual attention in states of high vs. low vigilance is poorly understood. To explore the possible differences in the influence of motivation on behavioral performance and neural activity in high and low vigilance levels, we conducted a prolonged 2 h 20 min flanker task and provided monetary rewards during the 20- to 40- and 100- to 120-min intervals of task performance. Both the behavioral and electrophysiological measures were modulated by prolonged task engagement. Moreover, the effect of reward was different in high vs. low vigilance states. The monetary reward increased accuracy and decreased the reaction time (RT) and number of omitted responses in the low but not in the high vigilance state. The fatigue-related decrease in P300 amplitude recovered to its level in the high vigilance state by manipulating motivation, whereas the fatigue-related increase in P300 latency was not modulated by reward. Additionally, the fatigue-related increase in event-related spectral power at 1–4 Hz was sensitive to vigilance decrement and reward. However, the spectral power at 4–8 Hz was only affected by the decrease in vigilance. These electrophysiological measures were not influenced by motivation in the state of high vigilance. Our results suggest that neural processing capacity, but not the timing of processing, is sensitive to motivation. These findings also imply that the fatigue-related impairments in behavioral performance and neural activity underlying selective visual attention only partly recover after manipulating motivation. Furthermore, our results provide evidence for the dissociable neural mechanisms underlying the fatigue-related decrease vs. reward-related increase in attentional resources.

Keywords: vigilance, mental fatigue, motivation, selective visual attention, event-related potential, event-related spectral perturbation

HIGHLIGHTS

- Time-on-task impairs performance in a selective visual attention task.
- Lower vigilance is associated with decreased amplitude and increased latency of P300.
- Monetary rewards improve P300 amplitude, but not P300 latency.
- The event-related spectral power at 1–4 Hz is sensitive to vigilance decrement and reward, whereas the spectral power at 4–8 Hz is sensitive only to vigilance decrement.
- Reward improves P300 amplitude and spectral power at 1–4 Hz only in the low and not in the high vigilance state.

INTRODUCTION

Although we are subjected to constant visual information in daily life, our visual capacity to process this information is limited. To perform in an efficient and goal-directed manner, we need to continuously distinguish the relevant information from the visual environment and allocate our limited attentional capacity to the selected target objects, a phenomenon referred to as selective visual attention (Moore and Zirnsak, 2017). As outlined by Robert and Duncan (1995), selective visual attention is characterized by two basic phenomena: the ability to filter out task-irrelevant stimuli and the limited capacity for task-relevant information processing, both of which leading to reduced accuracy when the target number increases. We experience selective visual attention in many daily activities. For example, customers find the target objects among colorful irrelevant sales; car drivers filter out irrelevant surroundings and detect the relevant road marks and traffic lights. However, prolonged engagement in selective attention tasks inevitably leads to increased errors, deactivated performance goals, diminished motivation to continue performing the task (Boksem et al., 2005), and an increase in mental fatigue (Kok, 2001; Lal and Craig, 2001; Gergelyfi et al., 2015; Benoit et al., 2019).

Mental fatigue is caused by prolonged cognitive task performance (Gergelyfi et al., 2015). It is considered a related concept but distinct from arousal, which often refers to a physiological state and is closely linked with the transition between wakefulness and sleep (Shen et al., 2006). Mental fatigue is a cumulative process, accompanied by a feeling of indolence, reduced motivation, and impaired performance (Lal and Craig, 2001). What is more, mental fatigue exhibits more cognitive elements than arousal. Based on different causal factors, two types of mental fatigue can be identified: sleep- and task-related (May and Baldwin, 2009). The former results from accumulated sleep debt, whereas the latter from prolonged task engagement (May and Baldwin, 2009). In the present study, we aimed to examine the task-related mental fatigue, specifically related to attentional resources. The attention-requiring task performance over a prolonged duration pointedly refers to vigilance decrement (Mackworth et al., 1964), which is likely identical or very closely related to mental fatigue (Oken et al., 2006). For this reason, both terms have been used interchangeably in previous studies (Taya et al., 2018; Reteig et al., 2019).

Vigilance decrement has been reported as a major factor in a large proportion of road crashes due to the reduction of attentional resources. Although the risks of vigilance decrement have received much attention, the underlying neurophysiological mechanisms have not yet been established (Lorist et al., 2005; Tops et al., 2006; Benoit et al., 2019). In earlier research, three core concepts around vigilance decrement or mental fatigue have emerged, namely, active fatigue, passive fatigue, and motivational control. Active fatigue is a result of an excessive workload—needed to carry out a task over a prolonged duration, resulting in the depletion of cognitive resources (Helton and Warm, 2008). Passive fatigue is a result of a lower workload—needed to engage in prolonged, but relatively easy tasks (May and Baldwin, 2009). Motivational control plays an important role in vigilance decrement, as it reflects the level of willingness to perform a task. Motivational control is linked with the process of subconscious balancing between costs and benefits to expend or conserve energy (Kurzban et al., 2013a). For instance, Kurzban and colleagues suggested that people experienced performance reductions over time when the costs outweighed the benefits (Kurzban et al., 2013b). Recent studies recognize that these three core concepts are not mutually exclusive, and there are still limitations in the core concepts account for changes induced by fatigue (Boksem and Tops, 2008; Seli et al., 2015; Thomson et al., 2015). Therefore, the hybrid models synthesizing different concepts have emerged to complement the limitations. For example, Boksem and Tops (2008) proposed a framework of mental fatigue that integrated the motivational control and energetical costs, suggesting that people would no longer maintain their performance when the energetical resources depleted, although the costs outweighed the benefits. All in all, it is still unclear why task performance deteriorates with time-on-task.

The influence of motivation on prolonged task performance has been studied by subsequently providing monetary rewards. The effects on response selection (Möckel et al., 2015), action monitoring (Boksem et al., 2006), and sustained attention (Reteig et al., 2019) have been previously shown. Although numerous studies have demonstrated that monetary rewards can improve performance when provided after long-term tasks (Lorist et al., 2005; Boksem et al., 2006; Hopstaken et al., 2015), the neural mechanisms upon which this improvement builds on are not established. Moreover, the effect of reward on performance in different (i.e., high vs. low) vigilance states has rarely been approached.

To explore the effects of motivation on behavioral performance and brain electrophysiology in high and low vigilance states, we conducted a 140-min selective visual attention task and provided monetary rewards for successful task performance in the early stage (during the 20- to 40-min interval) and in the late stage (during the 100- to 120-min interval; **Figure 1**). By utilizing brain electrophysiological measures derived from high-temporal-resolution electroencephalograms (EEGs), we focused on time domain [event-related potential (ERP) P300 amplitude and latency] and time-frequency

domain [event-related spectral perturbations (ERSPs)] variables as electrophysiological markers of visually induced neural activations. We further quantified the degree of recovery of behavioral and electrophysiological measures in the low vigilance state after motivation manipulation.

The stimulus-locked ERP component P300 has received much attention as a potential indicator of mental workload in a selective visual attention task (Faber et al., 2012). The amplitude of P300 was proved to be a useful measure of processing capacity that correlates positively with the accuracy of the memory search task (Kok, 2001). Furthermore, the latency of P300 was suggested to be an indicator of mental chronometry as demonstrated by its positive correlation with reaction time (RT; Verleger, 1997). While reports about the effect of time-on-task on the P300 component are diverse, the study of Faber et al. (2012) did not find a significant decrease in the P3b amplitude during prolonged engagement in a selective visual attention task. Boksem et al. (2006) also showed that the P300 amplitude did not change with time-on-task, but the P300 latency increased with vigilance decrement. Although the P300 amplitude and latency have been widely used in studies on vigilance (Kato et al., 2009; Käthner et al., 2014; Hopstaken et al., 2015), most results are limited to conventional ERP analysis.

It is also valuable to explore how the oscillatory dynamics reflect changes in attentional allocation and information processing during a selective visual attention task. Frontal theta oscillations have been shown to be related to the allocation of attention to task-relevant visual and auditory stimuli (Keller et al., 2017). Oscillations in the delta band have been implicated in attention and salience detection and are associated with vigilance levels and motivation (Knyazev, 2012). It has also been suggested that EEG delta oscillations are an indicator of attention to internal processing during the performance of mental tasks (Harmony et al., 1996). Compared with traditional time- and phase-locked ERP analysis, the changes in spectral power provided by two-dimensional time-frequency analysis could provide a better account of the neural mechanisms involved in selective visual attention. In the current study, besides the evoked P300 component, we will analyze the ERSPs.

We hypothesize that vigilance decrement induced by prolonged engagement in a selective visual attention task impairs behavioral performance and neural activity and is evident in P300 latency and amplitude. We further hypothesize that monetary rewards improve the behavioral performance and neural activity in the low vigilance state. We apply a variant of the Eriksen Flanker Task conducted over 2 h 20 min (seven blocks) and assume that the subjects are in a lower vigilance state at the end of the task (blocks 5 and 6) than at the beginning (blocks 1 and 2). To compare the effects of motivation on performance in states of high vs. low vigilance, we introduce rewards in block 2 (during 20–40 min after task onset) and block 6 (during 100–120 min after task onset). The behavioral performance, evoked ERPs, and ERSPs were compared between high and low vigilance states with and without rewards.

MATERIALS AND METHODS

Subjects

Twenty healthy participants (eight males), ranging from 18 to 28 [mean = 21.9, standard deviation (SD) = 2.4] years of age, were recruited from the university population. Participants reported that they had no history of smoking, sleep problems, or use of prescription medication. None worked the night shift. Furthermore, they all had normal or corrected-to-normal visual acuity, and they were right-handed according to their own report. The participants were compensated for their participation. The study was conducted in accordance with the Declaration of Helsinki and was approved by the ethics committee of Liaoning Normal University. Informed consent was obtained from each subject prior to the study.

Measures

Task and Stimuli

A version of the Eriksen Flanker Task (Eriksen and Eriksen, 1974) was adopted. A five-letter string stimuli with a central target letter (M/N) and four-remaining flanker letters (N/M) were used. The letters M and N were more similar with increased complexity in comparison to the original version with the letters H and S (Gulbinaite et al., 2014). In congruent trials (MMMMM or NNNNN), the target letter (the middle letter in the five-letter string) was identical to the flankers, whereas in incongruent trials (MMNMM or NNMNN), the target letter differed from the flankers. The participants were instructed to press the left button with the left index finger if the target was M and the right button with the right index finger if the target was N as soon as possible while maintaining a high level of accuracy.

All stimuli were presented as white against a black background on a computer screen. At the beginning of the task, there was a fixation cross in the center of the screen (0.32° × 0.32°). Each letter of the string had a height and width of 0.24° visual angle. The letters were 0.05° apart to increase the error rates (Boksem et al., 2008). After 1,000 ms, the fixation cross was replaced by the five-letter string. The stimuli disappeared after 200 ms and—for the subjects to provide the response—were followed by a time interval, which elapsed until the response button was pressed or until 600 ms. An additional 200-ms interval was provided for the subjects to realize a possible erroneous response. Finally, the feedback indicating task performance was presented for 1,000–1,500 ms, depending on the response time. Feedback was presented with given responses (“Correct,” “Error,” or “Miss”) at a width of 0.5 cm. Each trial lasted 3 s in total. The trial structures are depicted in **Figure 1**. Congruent (60%) and incongruent (40%) trials were presented in random order (Tops et al., 2006).

Reward

Although individuals present differences in sensitivity to reward, the monetary reward has been corroborated to be an effective means of motivation manipulation (Paschke et al., 2015). Participants were told that in one or some blocks, for each correct response, they would receive bonus money, and they would not lose money for errors or misses. Participants could earn up to

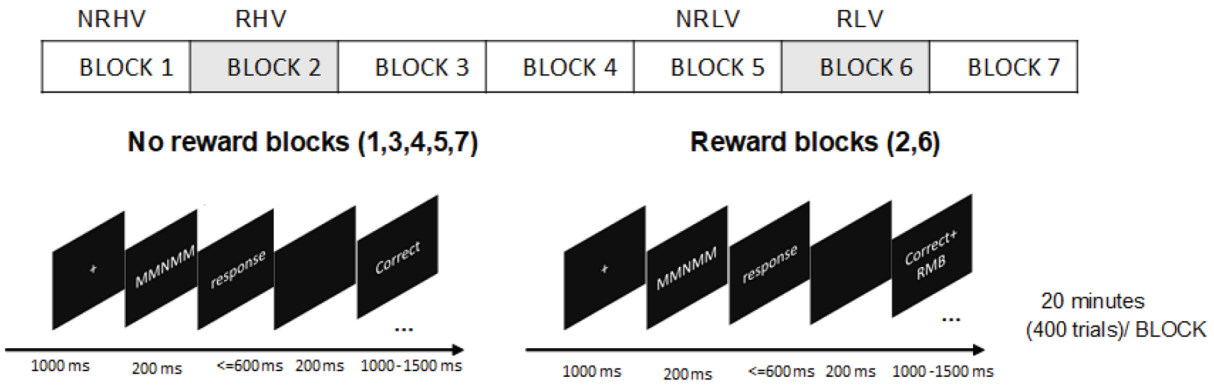

FIGURE 1 | The procedure of experiment design and the trial structure of flanker task.

100 RMB (approximately 12.8€) in addition to a basic sum of 50 RMB (approximately 6.4€) payment. The amount of money was evaluated proportionally to students' monthly expenses when manipulating motivation. To maintain the effectiveness of the reward, it was stressed that they would receive the bonus if the average accuracy of the reward blocks was more than 90%; otherwise, they would lose it. For the feedback in the reward blocks, the correct responses "Correct" coupled with "+ RMB" were 1 cm in width, and the "Error" or "Miss" responses were similar to the nonreward blocks (**Figure 1**).

Procedure

The participants were informed that they should abstain from alcohol, tea, and coffee for 24 h before the experiment. After arriving at the laboratory, they were given the written task instructions. They were asked to leave their watches and mobile phones outside the laboratory so that they had no indication of time during the measurement. The participants were then seated in front of a 19-inch PC monitor (1,280 × 1,024 pixels) at a distance of 0.9 m in a dimly lit, sound-attenuated, and electrically shielded room. Participants practiced the task before the formal experiment day to achieve an accuracy of 90% (those with an accuracy of <90% were not included in this study). Moreover, the reward was introduced in the practice experiment to build the association between task performance and monetary reward already prior to the experiment to avoid different time of reward exposure in high vs. low vigilance states in the formal experiment. On the experiment day, prior to the start of the formal experiment, participants performed the task for 10 min (200 trials) to adapt to the task. In the formal experiment, they were instructed to respond to the target letter presented in seven blocks of 20 min, for a total of 2 h 20 min (2,800 trials). Among the seven blocks, the monetary reward was introduced in blocks 2 and 6. The procedures can be found in **Figure 1**. The task blocks 1–4 were performed to induce vigilance decrement. To avoid any anticipatory effect of experiment ending, the additional no-reward block 7 was performed after the rewarded block 6. There was no rest during the experiment or any subjective questionnaires to maintain task performance and avoid the effects of short breaks alleviating fatigue. Prior studies have shown that even short breaks can increase task performance, making it difficult to evaluate whether the performance recovery results from motivation or the short break (Helton and Russell, 2015; Lim and Kwok, 2016). To maintain task performance, subjects were asked to focus their attention on the target letter presented in the center of the screen. The subjects were informed of the beginning and end of the reward blocks by instructions displayed on the screen. At the end of the task, the average accuracy of reward blocks was calculated to determine whether they would receive the bonus money or not.

EEG Recording and Processing

The EEGs were recorded using 64 Ag/AgCl electrodes attached to an electro cap according to the International 10-20 System. An ANT Neuro EEG amplifier was used to record EEG signals sampled at a digitization rate of 500 Hz. Horizontal and vertical electrooculograms were recorded from the outer canthi of the eyes and above and below the left eye. The electrode impedance was kept below 10 kΩ, and the EEG was online referenced to the CPz channel.

In the offline analysis, EEG data were notch filtered at 50 Hz. Next, a digital high-pass filter of 0.5 Hz and a low-pass filter of 30 Hz were applied. After removing the direct current (DC) component, the EEG signals were denoised using the wavelet threshold method (Zhang et al., 2018), wherein the wavelet coefficient threshold was set to *abs* (mean ± 3 × SD). If the absolute value of the wavelet coefficients exceeded the threshold, the coefficients were reset to one-quarter of the average value. The data were re-referenced to the average of the mastoid references (M1, M2). The ERP epochs from 200 ms before to 800 ms after stimulus onset were extracted. Finally, by using the Icasso software (Himberg and Hyvärinen, 2003), independent artifact components (e.g., blinks, movements, etc.) were removed through visual inspection.

Data Analysis

To study the effects of the reward state (i.e., no-reward vs. reward) on the behavioral and electrophysiological measures

in the states of high vs. low vigilance, four blocks (blocks 1, 2, 5, and 6) were selected. The subjects were provided with monetary rewards in blocks 2 and 6. In both high (blocks 1 and 2) and low (blocks 5 and 6) vigilance states, the reward blocks were introduced after the no-reward blocks. In summary, the analysis was based on 2 × 2 comparisons, representing the no-reward high vigilance (NRHV) condition in block 1, reward high vigilance (RHV) condition in block 2, no-reward low vigilance (NRLV) condition in block 5, and reward low vigilance (RLV) condition in block 6.

Behavioral Performance

For each participant, the accuracy, mean RT, and number of omitted responses were calculated. Only responses occurring between 100 and 600 ms were included in the RT analysis. A response time equal to zero was regarded as an omitted response. The accuracy was calculated as the percentage of correct responses in each block. We addressed the main effects and interactions of the vigilance state and the reward state on task performance. In addition, the effect of congruency (congruent vs. incongruent) was also tested for accuracy, RT, and omitted responses.

Event-Related Potentials

ERPs were analyzed with MATLAB 2015b. First, the individual correct trials whose amplitude was out of range (max >75 μv, baseline max >30 μv) were rejected, and then the baseline 200 ms before stimulus onset was subtracted from the waveforms. Next, trials were averaged across blocks for each subject. The mean (with SD in parentheses) number of trials across all subjects for NRHV, RHV, NRLV, and RLV were 236 (82), 232 (65), 234 (64), and 238 (64), respectively. The P300 amplitude and latency were quantified for further analysis. Based on some earlier studies (Polich and Kok, 1995; Kuba et al., 2012; van Dinteren et al., 2014) and topographic activations in our study, eight electrodes (FC1, FC2, FCz, C1, C2, Cz, CP1, and CP2) were chosen for the P300 analysis. A time window of 440–660 ms for the P300 component was selected. The P300 latency values were calculated as the time of maximum amplitude within the time window of the P300 component (Luck, 2005).

EEG Spectra

The EEG spectral power was assessed by calculating the ERSP using the continuous wavelet transform (CWT; Zhang et al., 2018). The complex Morlet wavelet was adopted for the CWT analysis, by which the time-dependent signals were evaluated at each sampling instant with a central frequency band of 1.5 Hz covering frequencies from 1 to 30 Hz, with a frequency step of 0.5 Hz. Additionally, we normalized the power spectra with the subtraction change from −1,000- to 0-ms baseline. For quantifying the oscillatory dynamics, we focused on separate time windows in the analysis of two frequency bands (**Figure 5**). According to the maximum power of the different frequency bands, statistical analysis was performed within the time window of 440–660 ms for the delta band (1–4 Hz) and within the time window of 300–600 ms for the theta band (4–8 Hz). In order to account for the effect of phase-locked (evoked response) activity in the induced oscillations, we also analyzed the induced activations by subtracting the averaged evoked response from each epoch prior to the wavelet analysis. The results of this analysis are provided in the **Supplementary Materials**.

Statistical Analysis

Data were analyzed using the IBM SPSS software (version 22.0), Chicago: SPSS Inc. The significance level $p < 0.05$ was used, and all results were reported under the 2-tailed condition. One-way repeated-measures analysis of variance (ANOVA) with the blocks 1, 3, 4, and 5 was used to test the hypothesis that behavioral performance deteriorates with time-on-task. Blocks 2 and 6 with an additional influence of motivation and block 7 with an effect of approaching the end of the task were excluded to capture the changes purely due to time-on-task. Moreover, behavioral, time domain, and time-frequency domain data were subjected to 2 × 2 [vigilance states (high and low) × reward states (no-reward and reward)] repeated-measures ANOVA. In case of significant interaction and/or main effects, a follow-up ANOVA was applied to separately test the effect of the vigilance state in no-reward and reward conditions (NRLV vs. NRHV indicates the effects of vigilance decrement) and the effect of reward in low and high vigilance states (RHV vs. NRHV and RLV vs. NRLV indicate the effects of motivation in the high and low vigilance states, respectively). The Greenhouse–Geisser correction was used as the adjusted report, and the effect size was determined using adjusted partial η^2 (η^2_{ap}; Mordkoff, 2019).

The effect of congruency was initially tested with 2 × 2 × 2 ANOVA (congruency, vigilance state, and reward state). However, as no interaction was found for congruency, the effects of the reward and vigilance states were tested with congruent and incongruent trials integrated together. The correlations between performance (accuracy, RT, and omitted response) and ERPs (P300 amplitude and latency) were calculated using the Pearson Correlation Coefficient to study the association between the behavioral and electrophysiological measures in different vigilance and reward states.

RESULTS

Behavioral Performance

Figure 2 illustrates the alterations of behavioral performance (accuracy, RT, and number of omitted responses) with time-on-task. Based on the one-way repeated-measures ANOVA, we found that the accuracy significantly decreased ($F_{(1.37,25.93)} = 4.44$, $p = 0.02$, $\eta^2_{ap} = 0.15$) with time-on-task. Meanwhile, the RT ($F_{(2.37,44.99)} = 3.97$, $p = 0.03$, $\eta^2_{ap} = 0.13$) and the number of omitted responses ($F_{(2.55,48.45)} = 4.12$, $p = 0.02$, $\eta^2_{ap} = 0.14$) significantly increased along with the prolonged task performance.

Accuracy

In the 2 (vigilance states) × 2 (reward states) ANOVA analysis, there was a significant main effect of the reward state ($F_{(1,19)} = 6.02$, $p = 0.03$, $\eta^2_{ap} = 0.21$ and a significant vigilance state × reward state interaction ($F_{(1,19)} = 7.38$, $p = 0.01$, $\eta^2_{ap} = 0.24$). When the vigilance states were contrasted separately for reward and no-reward conditions, the accuracy was lower

FIGURE 2 | The mean values and standard deviations (SDs)/sqrt (subjects) of **(A)** the accuracy (ACC), **(B)** the reaction time (RT), and **(C)** the omitted responses (OMIT) in seven blocks. B indicates block (e.g., B1 is block1); B2 and B6 were introduced with monetary rewards.

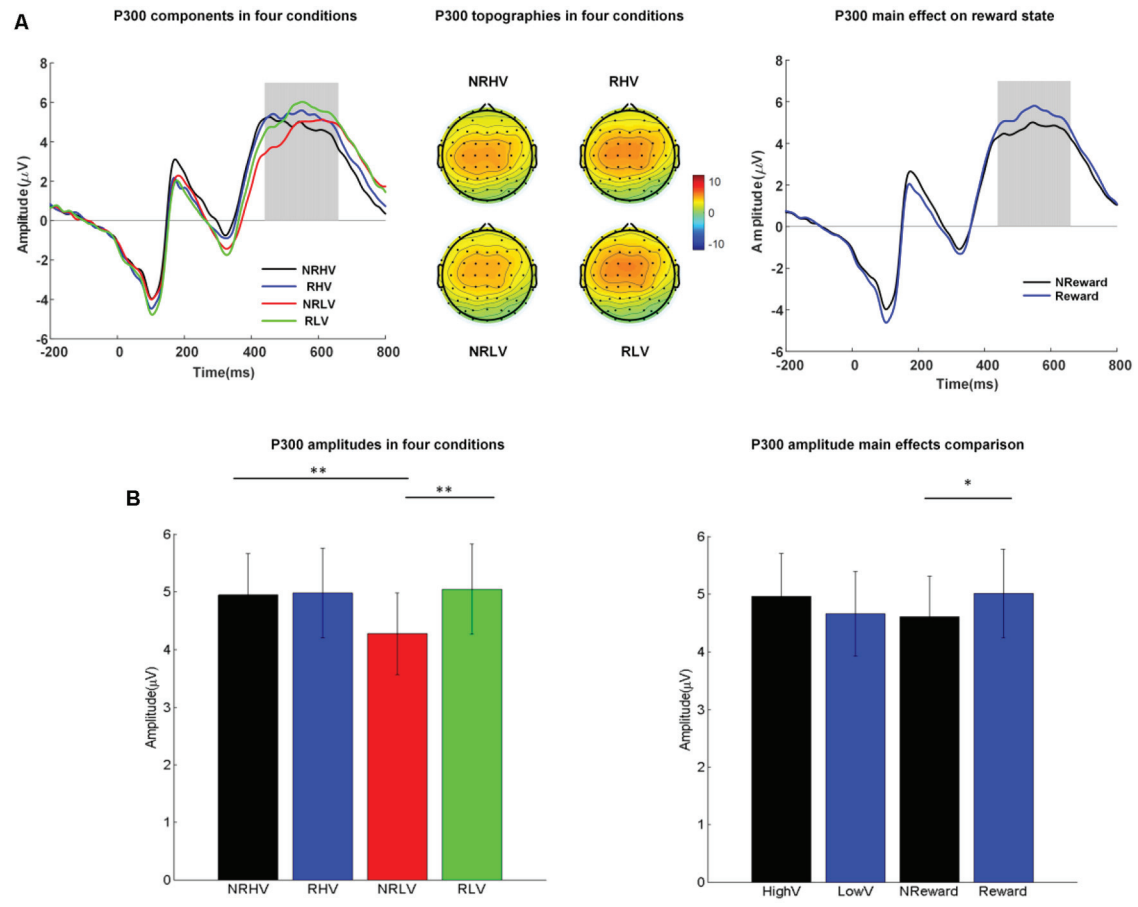

FIGURE 3 | (A) The P300 waveforms (left) averaged from electrodes of FC1, FC2, FCz, C1, C2, Cz, CP1, and CP2, the topographies (middle) in the four conditions, and P300 waveforms coalesced for the reward vs. non-reward states (right). **(B)** Mean values and standard error of the P300 amplitude in the four conditions (left) and in the two main factors (right). HighV (high vigilance blocks) = (NRHV + RHV)/2, LowV (low vigilance blocks) = (NRLV + RLV)/2, NReward (no-reward blocks) = (NRHV + NRLV)/2, and reward (reward blocks) = (RHV + RLV)/2. Analysis of variance (ANOVA) results were marked by $*p < 0.05$ and $**p < 0.01$.

in the low vigilance state than in the high vigilance state in the no-reward condition (NRLV: mean = 0.88, SD = 0.12, NRHV: mean = 0.93, SD = 0.06, $F_{(1,19)}$ = 5.24, p = 0.03, η^2_{ap} = 0.17). There was no difference between the rewarded low and high vigilance states (RLV: mean = 0.94, SD = 0.05, RHV: mean = 0.94, SD = 0.05, $F_{(1,19)}$ = 0.00, p = 1.00, η^2_{ap} = 0.00). The monetary

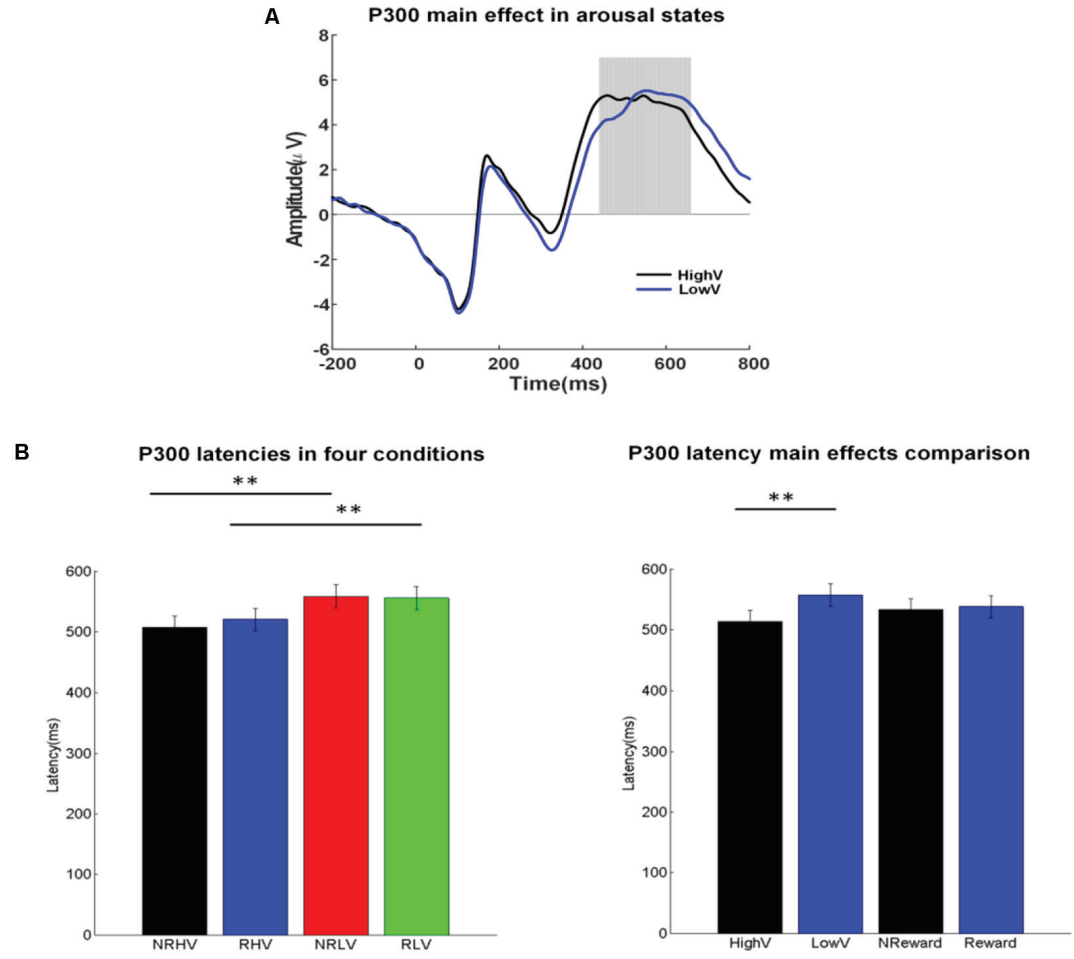

FIGURE 4 | (A) P300 waveforms coalesced for the high vs. low vigilance states. **(B)** Mean values and standard error for the P300 latency in the four conditions (left) and for the two main factors (right). The ANOVA results were marked by $*p < 0.05$ and $**p < 0.01$.

reward played a role only in the low vigilance state. The accuracy was higher in the rewarded than in the no-rewarded low vigilance condition ($F_{(1,19)} = 7.37$, $p = 0.01$, $\eta^2_{ap} = 0.24$), although there was no significant difference between the rewarded and the no-rewarded high vigilance conditions ($F_{(1,19)} = 0.47$, $p = 0.50$, $\eta^2_{ap} = -0.03$).

Reaction Time

There was a significant main effect of the reward state on the RT ($F_{(1,19)} = 10.95$, $p < 0.01$, $\eta^2_{ap} = 0.33$). The follow-up ANOVA indicated that the RT increased with vigilance decrement in the no-reward condition (NRLV: mean = 319.22, $SD = 49.15$, NRHV: mean = 311.02, $SD = 46.42$, $F_{(1,19)} = 5.52$, $p = 0.03$, $\eta^2_{ap} = 0.18$). There was no significant difference between the low and high vigilance states in the reward condition (RLV: mean = 308.58, $SD = 45.25$, RHV: mean = 309.83, $SD = 47.25$, $F_{(1,19)} = 0.21$, $p = 0.65$, $\eta^2_{ap} = -0.04$). When rewards were provided in the states of low and high vigilance, the RT was faster in the low vigilance state ($F_{(1,19)} = 8.38$, $p = 0.01$, $\eta^2_{ap} = 0.27$) but was not improved in the high vigilance state ($F_{(1,19)} = 1.75$, $p = 0.20$, $\eta^2_{ap} = 0.04$).

Omitted Responses

There was a significant main effect of the reward state on the number of omitted responses ($F_{(1,19)} = 9.22$, $p = 0.01$, $\eta^2 = 0.29$). The follow-up ANOVA revealed that the omitted responses increased with the decrease in vigilance in the no-reward condition ($F_{(1,19)} = 5.39$, $p = 0.03$, $\eta^2_{ap} = 0.18$). No difference was found between low and high vigilance states in the reward condition ($F_{(1,19)} = 0.07$, $p = 0.80$, $\eta^2_{ap} = -0.05$). The number of omitted responses decreased in the state of low vigilance ($F_{(1,19)} = 10.94$, $p = 0.01$, $\eta^2_{ap} = 0.33$) after motivation manipulation, although it did not change in the state of high vigilance ($F_{(1,19)} = 1.97$, $p = 0.18$, $\eta^2_{ap} = 0.05$).

Congruency

Regarding the congruency (congruent × incongruent), we found significant main effects of congruency on accuracy ($F_{(1,19)} = 18.07$, $p < 0.01$, $\eta^2_{ap} = 0.46$), RT ($F_{(1,19)} = 32.75$, $p < 0.01$, $\eta^2_{ap} = 0.61$), and omitted responses ($F_{(1,19)} = 9.65$, $p = 0.01$, $\eta^2_{ap} = 0.30$). The congruent condition showed a higher accuracy (congruent: mean = 0.94, $SD = 0.01$, incongruent: mean = 0.91,

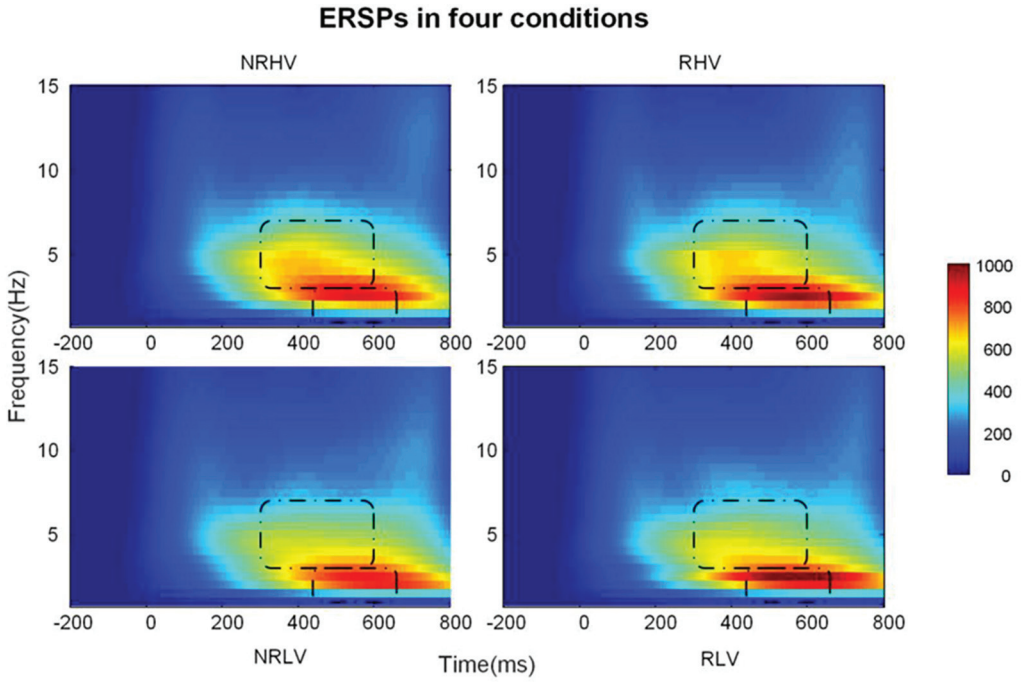

FIGURE 5 | The time-frequency representations in the four conditions averaged over subjects.

SD = 0.02), faster RTs (congruent: mean = 306.93, *SD* = 10.08, incongruent: mean = 315.28, *SD* = 9.84), and less omitted responses (congruent: mean = 2.98, *SD* = 0.69, incongruent: mean = 5.45, *SD* = 1.31) than the incongruent condition. However, no significant interaction between congruency and vigilance state or between congruency and reward state was observed in behavioral performance.

Event-Related Potentials

P300 Components

Amplitude

The left part of **Figure 3A** shows the averaged ERP amplitude waveforms with the time window of interest (P300 response at 440–660 ms after stimulus onset) depicted by a gray rectangle. The middle part of **Figure 3A** shows the corresponding topographies in the four experimental conditions, whereas **Figure 3B** illustrates the differences in P300 amplitude between the four conditions (left) and between the two main factors of vigilance state and reward state (right).

The repeated-measures ANOVA showed a significant main effect of the reward state on the P300 amplitude ($F_{(1,19)}$ = 7.08, p = 0.02, η^2_{ap} = 0.23) and a significant interaction between the vigilance state and reward state ($F_{(1,19)}$ = 6.78, p = 0.02, η^2_{ap} = 0.22). The follow-up ANOVA revealed that the P300 amplitude decreased with vigilance decrement (NRLV: mean = 4.17, *SD* = 2.68, NRHV: mean = 4.81, *SD* = 2.74, $F_{(1,19)}$ = 9.99, p = 0.01, η^2_{ap} = 0.31) in the no-reward condition, although no significant difference was found between the low and high vigilance states in the reward condition (RLV: mean = 4.96, *SD* = 3.01, RHV: mean = 4.89, *SD* = 2.98, $F_{(1,19)}$ = 0.07, p = 0.80, η^2_{ap} = −0.05). When the effect of reward was tested in states of low and high vigilance separately, the reward improvement presented only in the low vigilance state ($F_{(1,19)}$ = 15.88, $p < 0.01$, η^2_{ap} = 0.43) and not in the high vigilance state ($F_{(1,19)}$ = 0.12, p = 0.74, η^2_{ap} = −0.05).

Regarding the congruency (congruent vs. incongruent), a significant main effect of congruency was found for the P300 amplitude ($F_{(1,19)}$ = 22.19, $p < 0.01$, η^2_{ap} = 0.51). The amplitude was higher in the congruent condition (mean = 5.07, *SD* = 1.15) than in the incongruent condition (mean = 4.35, *SD* = 1.14). No interaction from congruency × vigilance state or congruency × reward state was detected.

Latency

Figure 4A illustrates the ERP waveforms in high and low vigilance states (reward and nonreward blocks coalesced), and **Figure 4B** shows the differences in P300 latency in the four experimental conditions (left) and the two main factors of vigilance state and reward state (right).

There was a significant main effect of the vigilance state on the P300 latency ($F_{(1,19)}$ = 52.20, $p < 0.01$, η^2_{ap} = 0.72) and an interaction between the vigilance state and the reward state ($F_{(1,19)}$ = 6.55, p = 0.02, η^2_{ap} = 0.22). Separate ANOVAs revealed the clear effects of vigilance states regardless of rewards. The P300 latency increased in the low vigilance state compared with the high vigilance state in both the no-reward (NRLV: mean = 557.45, *SD* = 84.71, NRHV: mean = 506.85, *SD* = 81.31, $F_{(1,19)}$ = 45.52, $p < 0.01$, η^2_{ap} = 0.69) and reward conditions (RLV: mean = 554.65, *SD* = 83.94, RHV: mean = 519.55, *SD* = 80.44,

$F_{(1,19)} = 37.97$, $p < 0.01$, $\eta^2_{ap} = 0.65$). When the effect of reward was tested in the states of low and high vigilance, there was no difference between reward and no-reward conditions in the low vigilance state ($F_{(1,19)} = 0.37$, $p = 0.55$, $\eta^2_{ap} = -0.03$), but we did find a decrease in the high vigilance state ($F_{(1,19)} = 6.81$, $p = 0.02$, $\eta^2_{ap} = 0.23$) after manipulating motivation.

Regarding congruency (congruent vs. incongruent), a significant main effect was found on the P300 latency ($F_{(1,19)} = 8.91$, $p = 0.01$, $\eta^2_{ap} = 0.28$). The latency was shorter in the congruent (mean = 465.59, *SD* = 8.43) than in the incongruent conditions (mean = 471.48, *SD* = 9.41). For P300 latency, no interaction from congruency × vigilance state or from congruency × reward state was detected.

Correlations Between ERPs and Behavioral Performance

To investigate the associations between task performance and ERPs affected by motivation and vigilance states, the correlations between the behavioral measures (accuracy, RT, and number of omitted responses) and ERPs (the amplitude and latency of P300) were calculated (**Table 1**). Significant negative correlations between the accuracy and P300 latency and significant positive correlations between the accuracy and P300 amplitude were detected. Additionally, the number of omitted responses and the RT were negatively correlated with the P300 amplitude and positively correlated with the P300 latency. Scatter diagrams showing the relationships between the behavioral measures and P300 amplitude and latency can be found in **Supplementary Figure S1**.

ERSP Analysis

Figure 5 illustrates the time-frequency representations (averaged over electrodes F1, F2, Fz, FC1, FC2, FCz, C1, C2, Cz, CP1, and CP2) in the four experimental conditions. A clear modulation of frequencies of approximately 1–4 Hz is visible in the time window of 440–660 ms. Separable modulations of approximately 4–8 Hz (in the time window of 300–500 ms) appear visually earlier than 1–4 Hz over the four conditions. The corresponding frequency bands and time windows are indicated by the dotted-line boxes. We also calculated the induced time-frequency representations after removing the phase-locked evoked responses from the total power (**Supplementary Figure S2**). **Figure 6A** illustrates the topographic distribution (right) and power waveforms (left) averaged across the electrodes (referred above) corresponding to the delta band (averaged over 1–4 Hz). **Figure 6B** draws the topographic distribution (right) and power waveforms (left) of the theta band (averaged over 4–8 Hz), with activations in the frontal electrodes (F1, F2, Fz, FC1, FC2, and FCz).

TABLE 1 | Correlations between behavioral performance and P300 measures in the four conditions.

	NRHV	RHV	NRLV	RLV
Model	*r*	*r*	*r*	*r*
ACC vs. AMP	0.40	0.57*	0.60*	0.59*
ACC vs. LAN	−0.52*	−0.53*	−0.53*	−0.41
RT vs. AMP	−0.65**	−0.68**	−0.82**	−0.83**
RT vs. LAN	0.54*	0.51*	0.53*	0.64*
OMIT vs. AMP	−0.39	−0.45*	−0.65**	−0.65**
OMIT vs. LAN	0.54*	0.46*	0.71**	0.59*

*Note: The AMP and LAN represent the amplitude and latency of P300. ACC and OMIT represent the accuracy and number of omitted responses. Correlation cofficients in 2-tailed condition were marked by *p < 0.05 and **p < 0.01. The correlations were corrected by executing the Benjamini and Hochberg procedure for controlling the false discovery rate (FDR; Benjamini and Hochberg, 1995).*

In the 2 (vigilance states) × 2 (reward states) ANOVAs, for the delta band power, we found a significant interaction between the vigilance state and reward state ($F_{(1,19)} = 7.28$, $p = 0.01$, $\eta^2_{ap} = 0.24$). When the effect of the vigilance state was tested in the no-reward and reward conditions, the delta band power decreased with vigilance decrement in the no-reward condition (NRLV: mean = 703.43, *SD* = 162.89, NRHV: mean = 768.16, *SD* = 153.49, $F_{(1,19)} = 8.72$, $p = 0.01$, $\eta^2_{ap} = 0.28$), but no significant difference was detected between low and high vigilance states in the reward condition (RLV: mean = 750.86, *SD* = 206.30, RHV: mean = 757.08, *SD* = 200.46, $F_{(1,19)} = 0.05$, $p = 0.82$, $\eta^2_{ap} = -0.05$). When the effect of reward was separately tested in the states of low and high vigilance, the effect of reward on delta band power was detected only in the low vigilance state ($F_{(1,19)} = 4.57$, $p = 0.04$, $\eta^2_{ap} = 0.19$) and not in the high vigilance state ($F_{(1,19)} = 0.23$, $p = 0.64$, $\eta^2_{ap} = 0.01$).

For the theta band, vigilance state had a significant main effect ($F_{(1,19)} = 18.56$, $p < 0.01$, $\eta^2_{ap} = 0.47$). Follow-up ANOVA revealed that theta power was weaker in low vigilance state than in high vigilance state in both no-reward condition (NRLV: mean = 432.43, *SD* = 115.29, NRHV: mean = 512.47, *SD* = 169.54, $F_{(1,19)} = 11.38$, $p < 0.01$, $\eta^2_{ap} = 0.34$) and reward condition (RLV: mean = 455.70, *SD* = 118.69, RHV: mean = 498.61, *SD* = 137.47, $F_{(1,19)} = 6.36$, $p = 0.02$, $\eta^2_{ap} = 0.21$). The separate ANOVAs revealed that reward did not play a role in low vigilance state ($F_{(1,19)} = 1.73$, $p = 0.20$, $\eta^2_{ap} = 0.03$) or in high vigilance state ($F_{(1,19)} = 0.21$, $p = 0.65$, $\eta^2_{ap} = -0.04$).

DISCUSSION

We examined the alterations in behavioral performance and brain electrophysiology produced by the vigilance level and reward during a prolonged period of selective visual attention tasks. Behavioral measures (accuracy, RT, and number of omitted responses), evoked responses (P300 amplitude and latency), and spectral power (delta and theta bands) were analyzed. A clear deterioration in behavioral performance was demonstrated over time (**Figure 2**). The monetary reward improved the performance in accuracy, RT, and number of omitted responses only in the low vigilance state. The P300 amplitude was smaller in low than in high vigilance state; however, in the low vigilance state, reward increased the P300 amplitude to its level in the high vigilance state. The P300 latency was sensitive to vigilance decrement but insensitive to rewards, with longer latency in low than in high vigilance states. Changes in spectral power at 4–8 Hz purely reflected the vigilance level, being stronger in the high vigilance state than in the low vigilance state. Similarly, the spectral responses at 1–4 Hz also decreased with vigilance decrement. However, the reward selectively increased the spectral power at 1–4 Hz

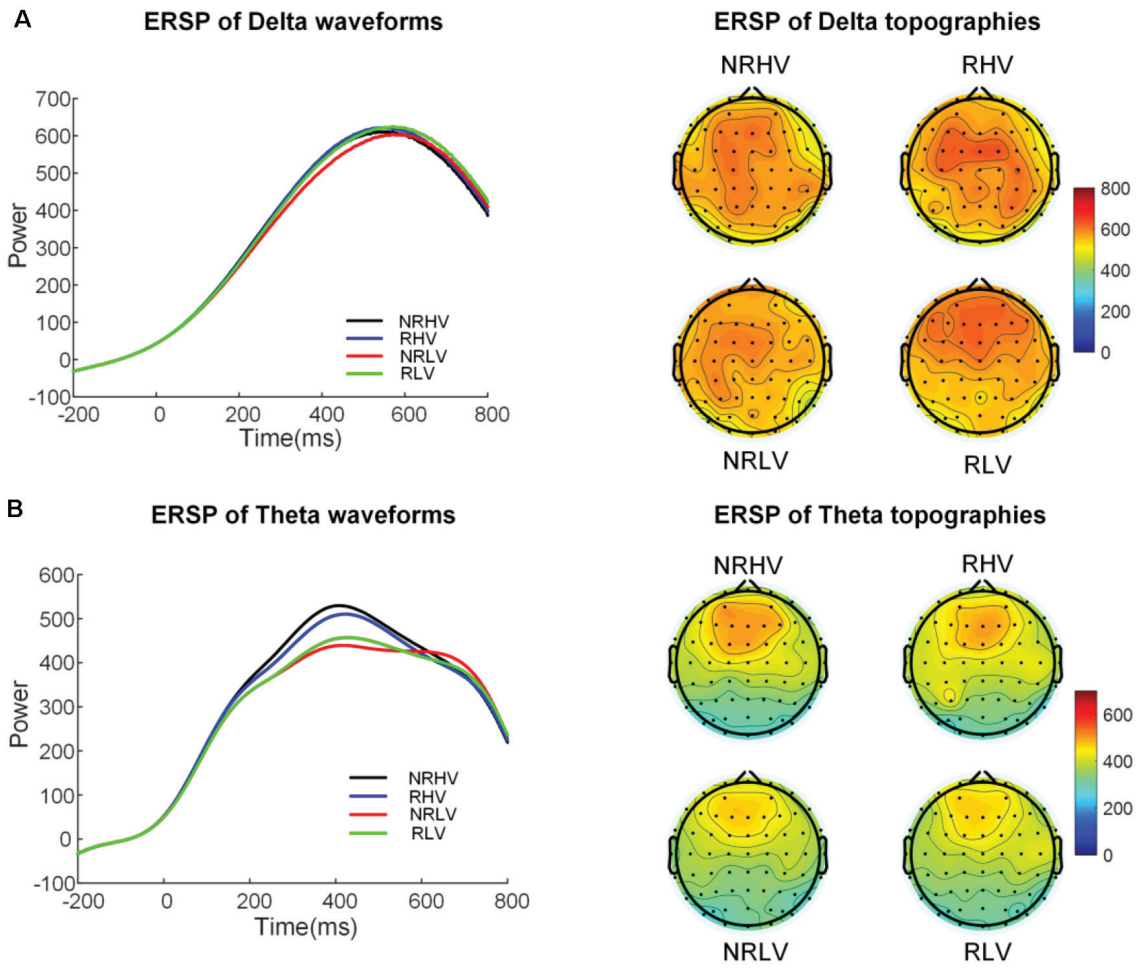

FIGURE 6 | The temporal waveforms of power modulation and topographies of the delta **(A)** and the theta band **(B)** in the four experimental conditions.

in the low vigilance state to the strength levels in the high vigilance state.

Although the time of emergence of fatigue during the prolonged performance of cognitive tasks has not been defined, earlier studies suggest cumulative effects in performance and neurophysiology with time-on-task (Boksem et al., 2005, 2006; Lorist et al., 2005; Faber et al., 2012; Möckel et al., 2015; Reteig et al., 2019). In line with these findings, our study found a significant decrease in accuracy and an increase in RT and the number of omitted responses with time-on-task (**Figure 2**). The decline of behavioral performance in prolonged attention tasks is in line with our assumption that time-on-task is associated with the decrement of vigilance levels. These results provided justification for testing the interactions between vigilance and reward states, where blocks 1 and 2 (first 40 min) were regarded as representing the high vigilance state, whereas blocks 5 (80–100 min) and 6 (100–120 min) were regarded as the low vigilance state. This selection was also supported by earlier findings of the effects of mental fatigue after 60- to 90-min tasks (Kastner and Ungerleider, 2000; Lorist et al., 2000; Marcora et al., 2009).

The limited processing capacity biased toward goal-directed selection is the core of selective visual attention (Robert and Duncan, 1995; Polich, 2009). The P300 component is considered as an important indicator of attentional capacity in visual tasks (Polich, 2009). In line with earlier results showing a fatigue-related decrease in P300 amplitude during brain-computer interface performance (Käthner et al., 2014), our results demonstrated that the P300 amplitude decreased with vigilance decrement during a selective visual attention task, presumably reflecting a less efficient engagement or limited capacity of attentional resources. The insufficient attention resources allocation in the low vigilance state has also been reflected by the P300 latency, which is thought to provide a specific index for the timing of information processing and stimulus evaluation (Polich and Kok, 1995; Verleger, 1997; Käthner et al., 2014). In our study, the P300 latency was significantly prolonged in the state of low vigilance, in line with earlier studies (Kutas et al., 1977; Boksem et al., 2006; Kato et al., 2009). The result indicates that prolonged task performance accompanies longer evaluation time for processing information. Therefore, in agreement with existing studies, our

results demonstrated a decrease in P300 amplitude and an increase in latency along with vigilance decrement.

The close link between the modulations in behavioral performance and the changes in brain electrophysiology is demonstrated by strong correlations between the behavioral and P300 measures (**Table 1**). It is noteworthy that, although the RT correlates with both P300 amplitude and latency, the association between the decrease of P300 amplitude and the increase in RT in particular is clear (**Supplementary Figure S1**).

After reward manipulation, the P300 amplitude increased only in the low vigilance state, reaching the same level as in the high vigilance state. Our results are consistent with earlier studies demonstrating a monetary-reward based improvement of neural measures in mental fatigue (Boksem et al., 2006; Hopstaken et al., 2015). We further provide quantitative evidence for the recovery of attentional resources from low vigilance to high vigilance states. Our results verify that, when rewards are provided, the capacity of attentional resources in the low vigilance state can reach the level of capacity in the high vigilance state, at least within the limited time duration of 2 h 20 min for a visual attention task.

Interestingly, there was no significant reward-induced improvement in P300 latency either in high or low vigilance states despite the reward-related improvement in RT in the low vigilance state. These results are in line with a previous study (Boksem et al., 2006), suggesting that the P300 latency is an unstable electrophysiological marker of motivation compared with the P300 amplitude. These diverging results concerning the RT and P300 latency could be interpreted to indicate improvement in motor response generation (as reflected by the RT) but not in the preceding stage of information processing (as reflected by the P300 latency). However, these results might also reflect the complex composition (subcomponents) of the P300 responses. The P300 component has been shown to comprise two subcomponents—P3a and P3b—with different functional correlations (Demiralp et al., 2001). The P3a with frontal topography has been suggested to contribute to attention engagement in top-down task-relevant processing, whereas the P3b with centroparietal topography has been linked to the level of cognitive workload and memory encoding (Polich, 2009). They are activated in different time windows, and P3a usually emerges earlier than P3b (Polich, 2009). Although we fail to disentangle the two subcomponents in this study, it is possible that, in addition to changes in the amplitude, also changes in the emphasis of these neural subprocesses are associated with vigilance decrement. This complicates the interpretation of latency measures.

The topography of the P300 component in the present study is more anterior than that in some earlier studies (Demiralp et al., 2001; Käthner et al., 2014). This likely reflects the task requirements of the present study. To successfully perform a selective visual attention task, humans are able to filter out task-irrelevant stimuli and engage their limited capacity in task-relevant processing (Robert and Duncan, 1995). Our task is likely to harness—although it was not designed to differentiate—these two subprocesses. The modified Eriksen Flanker Task applied in our study required responses for every trial and was specifically adapted to make the target letter distinction visually hard, emphasizing the need for the active inhibition of the flankers. Some interpretations, especially in studies showing anteriorly located P300 generators, emphasize the role of the inhibitory control underlying the modulation of P300 responses, for example, as a result of aging (Kuba et al., 2012; van Dinteren et al., 2014). Importantly for the present findings, this interpretation is also sensible in the context of vigilance decrement, which is often accompanied by a reduction in the capacity for top-down inhibitory control (Guo et al., 2018).

P300 seems to provide a reliable measure of cognitive performance, but the analysis of phase-locked ERP offers only limited windows to explore the underlying neural processes in more detail. Previous studies have indicated that both delta (Keller et al., 2017) and frontal theta oscillations (Knyazev, 2012) are involved in visual attention tasks, although the influence of time-on-task was not studied in these studies. Focusing on the spectral patterns and the power modulations at different frequency bands may provide additional sensitivity to separate vigilance- and reward-related processes in the brain. The oscillatory activity at low-frequency bands [i.e., the delta (1–4 Hz) and theta (4–8 Hz) bands] has been shown to increase during the transition to the low vigilance state in spontaneous conditions (Lal and Craig, 2001). Although the modulations of the oscillatory activity triggered by cognitive tasks are different from those from spontaneous activity, the temporal variations in the power of these frequency bands triggered by a visual attention task may tap on the same underlying processes as reported based on more spontaneous conditions.

In the present study, the changes in the spectral power at 1–4 Hz and 4–8 Hz reflected different topographies, with the delta band distributed in the centroparietal electrodes and the theta band distributed more focally in the frontal electrodes. In addition, the temporal characteristics of the changes in power in these two frequency bands differed, with an earlier emergence of the modulation at 1–4 Hz (300–600 ms) than at 4–8 Hz (440–660 ms). Therefore, it is likely that the two separable changes in spectral power reflect two distinct cognitive functions involved in selective visual attention. The theta band has been shown to be an indicator of attention allocation to task-relevant stimuli (Keller et al., 2017), whereas the delta band has been linked with internal processing in an attention task (Harmony et al., 1996). Prolonged engagement in a selective visual attention task led to the reduced spectral power in both delta and theta bands. These results are in line with the analysis of the evoked P300 responses and suggest that vigilance decrement impairs both attention allocation and information processing. In the rewarded low vigilance condition, the spectral power at approximately 1–4 Hz increased to the same level as that recorded in the high vigilance state. However, the spectral power at approximately 4–8 Hz did not increase in the rewarded low vigilance state compared to the rewarded high vigilance state. Consequently, the power in these two frequency bands was thus differently modulated by motivation. It would be tempting to associate the current findings with the distinct roles suggested for the theta and delta bands, suggesting that intrinsically driven regulation of information processing can be influenced by reward

(as reflected by delta-band changes, Knyazev, 2012), but the top-down attentional control (reflected by theta-band changes, Cavanagh and Frank, 2014) is insensitive to reward. Interestingly, accumulating evidence exists linking theta oscillations with the attentional sampling of the environment, especially during higher task demands (Bastiaansen and Hagoort, 2003; Landau et al., 2015; Spyropoulos et al., 2018; Karamacoska et al., 2019). Interpreted in the context of the current results suggesting the insensitivity of the theta band to reward manipulation, theta power might subserve rather low-level attentional sampling, which is not directly linked with the reward system, at least in the context of nonprimary, extrinsic rewards such as money. On the contrary, delta band oscillations may reflect a separate compensatory mechanism (Knyazev, 2012), which supports the recovery of functions after manipulating motivation.

However, these interpretations must be treated with caution, especially regarding the role of fatigue-related oscillatory dynamics. The current experimental paradigm is not optimal for studying ongoing oscillations, and the changes in rhythmic activation are strongly linked with the visual trigger. It is important to distinguish between ongoing oscillations and stimulus-related changes in spectral power. This fact is highlighted by the detected decrease in the spectral power by the decrease in vigilance in the present study, while ongoing oscillations at low-frequency bands generally show a fatigue-related increase (Lal and Craig, 2001). When the influence of phase-locked evoked activation (**Supplementary Figure S2**) was removed from the spectral responses, the theta-band modulations strongly decreased. Rather than reflecting neural computation in the theta band, the time-frequency results might be at least partly driven by the phase-locked evoked responses. Our analysis can be seen as advancing the interpretability of evoked responses, and different experimental paradigms are needed to focus purely on the fatigue-related changes in oscillatory dynamics.

Based on our results, vigilance decrement changes the neural processes underlying selective visual attention, as demonstrated by the changes in the spectral power at 1–4 Hz and at 4–8 Hz, as well as evoked P300 response. Motivation plays a different role in the high and low vigilance states, with improvement of performance only in the low vigilance state. This appears inconsistent with the active fatigue framework (which states that the vigilance decrement is the result of the depletion of cognitive resources, and motivation cannot improve the performance impaired by vigilance decrement, Helton and Warm, 2008) because the impairment in the state of low vigilance is improved after motivation manipulation. On the other hand, our results seem to agree with the motivation control framework—that vigilance decrement is a subconscious balancing between the costs and benefits to expend or conserve energy (Kurzban et al., 2013a). When the cost of efforts to carry out a task outweighs the benefits, humans are unwilling to do so, leading to vigilance decrement. However, not all of the neural measures are improved after providing reward. The P300 latency in the low vigilance state was not modulated by reward. Furthermore, the spectral power in the delta but not in the theta band was modulated by motivation manipulation, which means that motivation partially alleviates neural activity in the low vigilance state. In general, our results imply that motivation is not enough to completely restore the impairment induced by vigilance decrement and provide support for the mental fatigue framework, which integrates the evaluation of expected rewards and energetic costs (Boksem and Tops, 2008).

Further studies are inevitably needed to establish a more comprehensive picture of the underlying neural processes affected by motivation and vigilance states. We only analyze the changes in high vs. low vigilance states; nevertheless, focusing on the ongoing changes while performing the task can significantly advance the understanding of the dynamic emergence of mental fatigue. Our study did not consider the effects of monetary values during a long period of attention task engagement. It is also not possible to completely disengage the dimensions of vigilance and motivation, as it is likely that a decrease in vigilance is also accompanied by decreased motivation to perform a task. Furthermore, providing rewards is not the only method to motivate individuals. Further studies should further elaborate the particular differences in sensitivity to reward (positive) and punishment (negative).

CONCLUSION

Both the behavioral and electrophysiological measures were modulated by vigilance decrement. The neurocognitive processes were only partially recovered by manipulating rewards. In particular, increasing motivation using rewards differentially influenced brain activations in the high vs. low vigilance states, with more evident improvement in the low than in the high vigilance state. The fatigue-related decrease in latency of P300 responses did not recover with rewards, whereas the P300 amplitude increased to the same level as in the high vigilance state. The spectral power of the delta band was specifically increased by motivation, whereas the decrease of the theta band was not recovered by reward. These findings provide evidence for the dissociable effects of motivation in the states of low and high vigilance and might validate the mental fatigue framework integrating the evaluation of expected rewards and energetic costs.

DATA AVAILABILITY STATEMENT

The datasets generated and analyzed during the present study are available from the corresponding author on reasonable request.

ETHICS STATEMENT

The studies involving human participants were reviewed and approved by Liaoning Normal University. The participants provided their written informed consent to participate in this study.

AUTHOR CONTRIBUTIONS

JL, HS, and TP designed the experiment. JL, CZ, and YZ analyzed the data. JL and YL collected the data. JL and TP conducted the

statistics. JL, FC, TP, and TR wrote the manuscript. FC, TR, and TP provided the fundings and guidance for all the conduction of work.

FUNDING

This work was supported by the National Science Foundation of China (No. 91748105, No. 61703069), the Fundamental Research Funds for the Central Universities in Dalian University of Technology in China (DUT2019), the Academy of Finland grant (No. 295076), and the scholarships from China Scholarship Council (No. 201600090044; No. 201600090042). Open access funding was provided by the University of Jyväskylä (JYU).

ACKNOWLEDGMENTS

We thank Dr. Tengfei Liang for the help with E-prime programming and the editor and reviewers for their constructive comments to improve the manuscript.

SUPPLEMENTARY MATERIAL

The Supplementary Material for this article can be found online at: https://www.frontiersin.org/articles/10.3389/fnhum.2020.00207/full#supplementary-material.

FIGURE S1 | Scatter diagrams showing the relationships between the behavioral measures (accuracy, reaction time, and number of omitted responses) and the P300 amplitude and latency in the four conditions. NRHV is block 1 in the no-reward high vigilance state, RHV is block 2 in the reward high vigilance state, NRLV is block 5 in the no-reward low vigilance state, and RLV is block 6 in the reward low vigilance state.

FIGURE S2 | Comparison of different ways of calculating time-frequency representation changes for the current data. **(A)** Calculation of the power with the continuous wavelet transform (CWT) in each trial, and then averaged (presented in the present study). **(B)** Calculation of the power with the CWT from epochs, from which the contribution of averaged evoked responses are removed from each trial (averaged ERP is subtracted from each trial). **(C)** Calculation of the power with the CWT from epochs averaged in the evoked responses (spectra power of averaged ERP).

REFERENCES

Bastiaansen, M., and Hagoort, P. (2003). Event-induced theta responses as a window on the dynamics of memory. *Cortex* 39, 967–992. doi: 10.1016/s0010-9452(08)70873-6

Benjamini, Y., and Hochberg, Y. (1995). Controlling the false discovery rate? A practical and powerful approach to multiple testing. *J. R. Stat. Soc. Ser. B* 57, 289–300. doi: 10.1111/j.2517-6161.1995.tb02031.x

Benoit, C.-E., Solopchuk, O., Borragán, G., Carbonnelle, A., Van Durme, S., and Zénon, A. (2019). Cognitive task avoidance correlates with fatigue-induced performance decrement but not with subjective fatigue. *Neuropsychologia* 123, 30'40. doi: 10.1016/j.neuropsychologia.2018.06.017

Boksem, M. A. S., Meijman, T. F., and Lorist, M. M. (2005). Effects of mental fatigue on attention: an ERP study. *Cogn. Brain Res.* 25, 107–116. doi: 10.1016/j.cogbrainres.2005.04.011

Boksem, M. A. S., Meijman, T. F., and Lorist, M. M. (2006). Mental fatigue, motivation and action monitoring. *Biol. Psychol.* 72, 123–132. doi: 10.1016/j.biopsycho.2005.08.007

Boksem, M. A. S., and Tops, M. (2008). Mental fatigue: costs and benefits. *Brain Res. Rev.* 59, 125–139. doi: 10.1016/j.brainresrev.2008.07.001

Boksem, M. A. S., Tops, M., Kostermans, E., and De Cremer, D. (2008). Sensitivity to punishment and reward omission: evidence from error-related ERP components. *Biol. Psychol.* 79, 185–192. doi: 10.1016/j.biopsycho.2008.04.010

Cavanagh, J. F., and Frank, M. J. (2014). Frontal theta as a mechanism for affective and effective control. *Trends Cogn. Sci.* 18, 414–421. doi: 10.1016/j.tics.2014.04.012

Demiralp, T., Ademoglu, A., Comerchero, M., and Polich, J. (2001). Wavelet analysis of P3a and p3b. *Brain Topogr.* 13, 251–267. doi: 10.1023/a:1011102628306

Eriksen, B. A., and Eriksen, C. W. (1974). Effects of noise letters upon the identification of a target letter in a nonsearch task. *Percept. Psychophys.* 16, 143–149. doi: 10.3758/bf03203267

Faber, L. G., Maurits, N. M., and Lorist, M. M. (2012). Mental fatigue affects visual selective attention. *PLoS One* 7:e48073. doi: 10.1371/journal.pone.0048073

Gergelyfi, M., Jacob, B., Olivier, E., and Zénon, A. (2015). Dissociation between mental fatigue and motivational state during prolonged mental activity. *Front. Behav. Neurosci.* 9:176. doi: 10.3389/fnbeh.2015.00176

Gulbinaite, R., Johnson, A., de Jong, R., Morey, C. C., and van Rijn, H. (2014). Dissociable mechanisms underlying individual differences in visual working memory capacity. *NeuroImage* 99, 197–206. doi: 10.1016/j.neuroimage.2014.05.060

Guo, Z., Chen, R., Liu, X., Zhao, G., Zheng, Y., Gong, M., et al. (2018). The impairing effects of mental fatigue on response inhibition: an ERP study. *PLoS One* 13:e0198206. doi: 10.1371/journal.pone.0198206

Harmony, T., Fernández, T., Silva, J., Bernal, J., Díaz-Comas, L., Reyes, A., et al. (1996). EEG delta activity: an indicator of attention to internal processing during performance of mental tasks. *Int. J. Psychophysiol.* 24, 161–171. doi: 10.1016/s0167-8760(96)00053-0

Helton, W. S., and Russell, P. N. (2015). Rest is best: the role of rest and task interruptions on vigilance. *Cognition* 134, 165–173. doi: 10.1016/j.cognition.2014.10.001

Helton, W. S., and Warm, J. S. (2008). Signal salience and the mindlessness theory of vigilance. *Acta Psychol.* 129, 18–25. doi: 10.1016/j.actpsy.2008.04.002

Himberg, J., and Hyvärinen, A. (2003). "ICASSO: software for investigating the reliability of ICA estimates by clustering and visualization," in *In Proceedings of the IEEE Workshop on Neural Networks for Signal Processing (NNSP'2003)* (Toulouse, France: IEEE), 259–268.

Hopstaken, J. F., van der Linden, D., Bakker, A. B., and Kompier, M. A. J. (2015). A multifaceted investigation of the link between mental fatigue and task disengagement. *Psychophysiology* 52, 305–315. doi: 10.1111/psyp.12339

Karamacoska, D., Barry, R. J., De Blasio, F. M., and Steiner, G. Z. (2019). EEG-ERP dynamics in a visual continuous performance test. *Int. J. Psychophysiol.* 146, 249–260. doi: 10.1016/j.ijpsycho.2019.08.013

Kastner, S., and Ungerleider, L. G. (2000). Mechanisms of visual attention in the human cortex. *Annu. Rev. Neurosci.* 23, 315–341. doi: 10.1146/annurev.neuro.23.1.315

Käthner, I., Wriessnegger, S. C., Müller-Putz, G. R., Kübler, A., and Halder, S. (2014). Effects of mental workload and fatigue on the P300, alpha and theta band power during operation of an ERP (P300) brain-computer interface. *Biol. Psychol.* 102, 118–129. doi: 10.1016/j.biopsycho.2014.07.014

Kato, Y., Endo, H., and Kizuka, T. (2009). Mental fatigue and impaired response processes: event-related brain potentials in a Go/NoGo task. *Int. J. Psychophysiol.* 72, 204–211. doi: 10.1016/j.ijpsycho.2008.12.008

Keller, A. S., Payne, L., and Sekuler, R. (2017). Characterizing the roles of alpha and theta oscillations in multisensory attention. *Neuropsychologia* 99, 48–63. doi: 10.1016/j.neuropsychologia.2017.02.021

Knyazev, G. G. (2012). EEG delta oscillations as a correlate of basic homeostatic and motivational processes. *Neurosci. Biobehav. Rev.* 36, 677–695. doi: 10.1016/j.neubiorev.2011.10.002

Kok, A. (2001). On the utility of P3 amplitude as a measure of processing capacity. *Psychophysiology* 38, 557–577. doi: 10.1017/s0048577201990559

Kuba, M., Kremlácek, J., Langrová, J., Kubová, Z., Szanyi, J., and Vít, F. Š. (2012). Aging effect in pattern, motion and cognitive visual evoked potentials. *Vision Res.* 62, 9–16. doi: 10.1016/j.visres.2012.03.014

Kurzban, R., Duckworth, A., Kable, J. W., and Myers, J. (2013a). An opportunity cost model of subjective effort and task performance. *Behav. Brain Sci.* 36, 661–679. doi: 10.1017/s0140525x12003196

Kurzban, R., Duckworth, A., Kable, J. W., and Myers, J. (2013b). Cost-benefit models as the next, best option for understanding subjective effort. *Behav. Brain Sci.* 36, 707–726. doi: 10.1017/s0140525x13001532

Kutas, M., McCarthy, G., and Donchin, E. (1977). Augmenting mental chronometry?: the P300 as a measure of stimulus evaluation time. *Science* 197, 792–795. doi: 10.1126/science.887923

Lal, S. K. L., and Craig, A. (2001). A critical review of the psychophysiology of driver fatigue. *Biol. Psychol.* 55, 173–194. doi: 10.1016/s0301-0511(00)00085-5

Landau, A. N., Schreyer, H. M., Van Pelt, S., and Fries, P. (2015). Distributed attention is implemented through theta-rhythmic gamma modulation. *Curr. Biol.* 25, 2332–2337. doi: 10.1016/j.cub.2015.07.048

Lim, J., and Kwok, K. (2016). The effects of varying break length on attention and time on task. *Hum. Factors* 58, 472–481. doi: 10.1177/0018720815617395

Lorist, M. M., Boksem, M. A. S., and Ridderinkhof, K. R. (2005). Impaired cognitive control and reduced cingulate activity during mental fatigue. *Cogn. Brain Res.* 24, 199–205. doi: 10.1016/j.cogbrainres.2005.01.018

Lorist, M. M., Klein, M., and Nieuwenhuis, S. (2000). Mental fatigue and task control? planning and preparation mental fatigue and task control?: planning and preparation. *Psychophysiology* 37, 614–625. doi: 10.1111/1469-8986.3750614

Luck, S. J. (2005). *An Introduction to the Event-Related Potential Technique.* Cambridge, MA: MIT Press.

Mackworth, N. H., Kaplan, I. T., and Metlay, W. (1964). Eye movements during vigilance. *Percept. Mot. Skills* 18, 397–402. doi: 10.2466/pms.1964.18.2.397

Marcora, S. M., Staiano, W., and Manning, V. (2009). Mental fatigue impairs physical performance in humans. *J Appl. Physiol.* 106, 857–864. doi: 10.1152/japplphysiol.91324.2008

May, J. F., and Baldwin, C. L. (2009). Driver fatigue: the importance of identifying causal factors of fatigue when considering detection and countermeasure technologies. *Transp. Res. Part F Traffic Psychol. Behav.* 12, 218–224. doi: 10.1016/j.trf.2008.11.005

Möckel, T., Beste, C., and Wascher, E. (2015). The effects of time on task in response selection—an ERP study of mental fatigue. *Sci. Rep.* 5:10113. doi: 10.1038/srep10113

Moore, T., and Zirnsak, M. (2017). Neural mechanisms of selective visual attention. *Ann. Rev. Psychol.* 68, 47–72. doi: 10.1146/annurev-psych-122414-033400

Mordkoff, J. T. (2019). A simple method for removing bias from a popular measure of standardized effect size: adjusted partial eta squared. *Adv. Methods Pract. Psychol. Sci.* 2, 228–232. doi: 10.1177/2515245919855053

Oken, B. S., Salinsky, M. C., and S. Elsas, M. (2006). Vigilance, alertness, or sustained attention: physiological basis and measurement. *Clin. Neurophysiol.* 117, 1885–1901. doi: 10.1016/j.clinph.2006.01.017

Paschke, L. M., Walter, H., Steimke, R., Ludwig, V. U., Gaschler, R., Schubert, T., et al. (2015). Motivation by potential gains and losses affects control processes *via* different mechanisms in the attentional network. *NeuroImage* 111, 549–561. doi: 10.1016/j.neuroimage.2015.02.047

Polich, J. (2009). Updating P300: an integrative theory of P3a and P3b. *Clin. Neurophysiol.* 118, 2128–2148. doi: 10.1016/j.clinph.2007.04.019

Polich, J., and Kok, A. (1995). Cognitive and biological determinants of P300: an integrative review. *Biol. Psychol.* 41, 103–146. doi: 10.1016/0301-0511(95)05130-9

Reteig, L. C., van den Brink, R. L., Prinssen, S., Cohen, M. X., and Slagter, H. A. (2019). Sustaining attention for a prolonged period of time increases temporal variability in cortical responses. *Cortex* 117, 16–32. doi: 10.1016/j.cortex.2019.02.016

Robert, D., and Duncan, J. (1995). Neural mechanisms of selective visual attention. *Annu. Rev. Neurosci.* 18, 193–222.

Seli, P., Cheyne, J. A., Xu, M., Purdon, C., and Smilek, D. (2015). Motivation, intentionality and mind wandering: implications for assessments of task-unrelated thought. *J. Exp. Psychol. Learn. Mem. Cogn.* 41, 1417–1425. doi: 10.1037/xlm0000116

Shen, J., Barbera, J., and Shapiro, C. M. (2006). Distinguishing sleepiness and fatigue: focus on definition and measurement. *Sleep Med. Rev.* 10, 63–76. doi: 10.1016/j.smrv.2005.05.004

Spyropoulos, G., Bosman, C. A., and Fries, P. (2018). A theta rhythm in macaque visual cortex and its attentional modulation. *Proc. Natl. Acad. Sci. U S A* 115, E5614–E5623. doi: 10.1073/pnas.1719433115

Taya, F., Dimitriadis, S. I., Dragomir, A., Lim, J., Sun, Y., Wong, K. F., et al. (2018). Fronto-parietal subnetworks flexibility compensates for cognitive decline due to mental fatigue. *Hum. Brain Mapp.* 39, 3528–3545. doi: 10.1002/hbm.24192

Thomson, D. R., Besner, D., and Smilek, D. (2015). A resource-control account of sustained attention: evidence from mind-wandering and vigilance paradigms. *Perspect. Psychol. Sci.* 10, 82–96. doi: 10.1177/1745691614556681

Tops, M., Boksem, M. A. S., Wester, A. E., Lorist, M. M., and Meijman, T. F. (2006). Task engagement and the relationships between the error-related negativity, agreeableness, behavioral shame proneness and cortisol. *Psychoneuroendocrinology* 31, 847–858. doi: 10.1016/j.psyneuen.2006.04.001

van Dinteren, R., Arns, M., Jongsma, M. L. A., and Kessels, R. P. C. (2014). P300 development across the lifespan: a systematic review and meta-analysis. *PLoS One* 9:e87347. doi: 10.1371/journal.pone.0087347

Verleger, R. (1997). On the utility of P3 latency as an index of mental chronometry. *Psychophysiology* 34, 131–156. doi: 10.1111/j.1469-8986.1997.tb02125.x

Zhang, C., Cong, F., Kujala, T., Liu, W., Liu, J., Parviainen, T., et al. (2018). Network entropy for the sequence analysis of functional connectivity graphs of the brain. *Entropy* 20:311. doi: 10.3390/e20050311

Conflict of Interest: The authors declare that the research was conducted in the absence of any commercial or financial relationships that could be construed as a potential conflict of interest.

II

SUSTAINING ATTENTION FOR A PROLONGED DURATION AFFECTS DYNAMIC ORGANIZATIONS OF FREQUENCY-SPECIFIC FUNCTIONAL CONNECTIVITY

by

Jia Liu, Yongjie Zhu, Hongjin Sun, Tapani Ristaniemi, Fengyu Cong, 2020

Brain Topography

DOI: 10.1007/s10548-020-00795-0

Brain Topography
https://doi.org/10.1007/s10548-020-00795-0

ORIGINAL PAPER

Sustaining Attention for a Prolonged Duration Affects Dynamic Organizations of Frequency-Specific Functional Connectivity

Jia Liu[1,2,3] · Yongjie Zhu[1,2] · Hongjin Sun[3] · Tapani Ristaniemi[2] · Fengyu Cong[1,2,4,5]

Received: 13 May 2020 / Accepted: 1 September 2020

Abstract
Sustained attention encompasses a cascade of fundamental functions. The human ability to implement a sustained attention task is supported by brain networks that dynamically formed and dissolved through oscillatory synchronization. The decrement of vigilance induced by prolonged task engagement affects sustained attention. However, little is known about which stage or combinations are affected by vigilance decrement. Here, we applied an analysis framework composed of weighted phase lag index (wPLI) and tensor component analysis (TCA) to an EEG dataset collected during 80 min sustained attention task to examine the electrophysiological basis of such effect. We aimed to characterize the phase-coupling networks to untangle different phases involved in sustained attention and study how they are modulated by vigilance decrement. We computed the time–frequency domain wPLI from each block and subject and constructed a fourth-order tensor, containing the time, frequency, functional connectivity (FC), and blocks × subjects. This tensor was subjected to the TCA to identify the interacted and low-dimensional components representing the frequency-specific dynamic FC (fdFC). We extracted four types of neuromakers during a sustained attention task, namely the pre-stimulus alpha right-lateralized parieto-occipital FC, the post-stimulus theta fronto-parieto-occipital FC, delta fronto-parieto-occipital FC, and beta right/left sensorimotor FCs. All these fdFCs were impaired by vigilance decrement. These fdFCs, except for the beta left sensorimotor network, were restored by rewards, although the restoration by reward in the beta right sensorimotor network was transient. These findings provide implications for dissociable effects of vigilance decrement on sustained attention by utilizing the tensor-based framework.

Keywords Sustained attention · Vigilance decrement · Motivation · Frequency-specific dynamic functional connectivity · Weighted phase lag index · Tensor component analysis

Introduction

Human attentional resources are not limitless. Sustaining attention on stimuli for a prolonged duration results in task performance declines and mental fatigue increases. This effect is known as time-on-task effect or vigilance decrement (Davies and Parasurman 1982; Gillberg and Åkerstedt 1998; Lim and Dinges 2008; Mackworth 1948; See et al.

Handling editor: Christoph M. Michel .

Electronic supplementary material The online version of this article (https://doi.org/10.1007/s10548-020-00795-0) contains supplementary material, which is available to authorized users.

✉ Jia Liu
jialiu15@foxmail.com

✉ Fengyu Cong
cong@dlut.edu.cn

[1] School of Biomedical Engineering, Faculty of Electronic Information and Electrical Engineering, Dalian University of Technology, Dalian 116024, China

[2] Faculty of Information Technology, University of Jyvaskyla, 40014 Jyvaskyla, Finland

[3] Department of Psychology, Neuroscience and Behavior, MacMaster University, Hamilton, ON L8S4K1, Canada

[4] School of Artificial Intelligence, Faculty of Electronic Information and Electrical Engineering, Dalian University of Technology, Dalian 116024, China

[5] Key Laboratory of Integrated Circuit and Biomedical Electronic System, Dalian University of Technology, Dalian 116024, China

Published online: 14 September 2020

1995). Vigilance decrement leads to increased safety risks and decreased productivity at work. Efforts have been made to explore the mechanisms of vigilance decrement. In particular, three theoretical categories—underload, overload, and motivational control—have emerged in the mechanisms of vigilance decrement (Liu et al. 2020a; Reteig et al. 2019). The underload theories maintain that cognitive tasks are too monotonous to maintain task performance for a prolonged period of time (Manly et al. 1999). Whereas the overload theories hold that a limited pool of cognitive resources is depleted during a long period of task performance (Caggiano and Parasuraman 2004). Furthermore, the motivational control theories insist that the decrement of vigilance is associated with mental representations of costs and benefits and the task performance decreases when the costs outweigh the benefits (Kurzban et al. 2013). However, these three theories still have limitations to interpret all fatigue-related changes. In recent years there have been theoretical frameworks synthesizing different theoretical categories. For instance, Boksem and colleagues (Boksem and Tops 2008) proposed a hybrid model synthesizing the motivational control and energetical costs, stating that human task performance is determined by the energetical state and the mental representations of costs and benefits. Other hybrid models synthesizing underload and overload theories (Thomson et al. 2015) and synthesizing underload and motivational control theories (Seli et al. 2015) have also been proposed in the literature. Despite substantial efforts have been made for this, the mechanisms of vigilance decrement are still ambiguous.

Sustained attention has been widely used in the studies of vigilance decrement in the laboratory because tests of sustained attention are reliable and the neural mechanisms of sustained attention have been fairly well acknowledged. Sustained attention studies using perfusion functional magnetic resonance imaging (fMRI) and fMRI have uncovered that the fronto-parietal attention network decreases during prolonged sustained attention task engagement (Lim et al. 2010; Taya et al. 2018). Previous electroencephalogram (EEG) work of sustained attention has implicated that the theta and alpha frequency bands mainly at frontal and parietal brain regions are associated with vigilance decrement (Sauseng et al. 2007; Sun et al. 2014). While the summarized attention network and oscillations are useful neuromakers of vigilance decrement, few studies have addressed the frequency-specific dynamic functional connectivity (fdFC) without a prior selection of time windows, frequency bands or brain regions in the functional connectivity (FC) or oscillatory analysis.

In essence, whole-brain interactions through phase synchronization in specific frequency band form and dissolve dynamically and transiently to support cognitive processes (Bola and Sabel 2015; Fries and Str 2015; O'Neill et al. 2017; Rosenberg et al. 2016; Vidaurre et al. 2018). Sustained attention encompasses a variety of fundamental cognitive processes, including attentional preparatory, attentional stability, working memory, and enhancement or inhibition of selected or unselected information (Clark et al. 2015; Reteig et al. 2019; Rosenberg et al. 2016; Slagter et al. 2016). Brain regions rapidly shift the patterns of FC on the basis of the cognitive process demands (Cole et al. 2013). To successfully execute a sustained attention task, the fdFCs should emerge dynamically, with the temporal scale of milliseconds (Bola and Sabel 2015). Nevertheless, it is still unclear how oscillations are involved in brain networks during a sustained attention task. Little is known which stage or a combination of stages are impaired by vigilance decrement.

High-temporal resolution modality matching the rapid timescales of the brain is efficient for tracking the dynamics of FC. In the present study, we adopt a high-temporal resolution EEG dataset collected when participants performed a sustained attention task as long as 80 min and they were provided with unexpected monetary rewards 20 min before the end of the task (Reteig et al. 2019; Slagter et al. 2016). A different set of results based on this dataset extracted three univariate neuromarkers of vigilance decrement, consisting of the pre-stimulus alpha power, the early post-stimulus P1/N1 component, and the post-stimulus theta phase (Reteig et al. 2019). However, they did not use multivariate fashion through the integrity of the whole-brain networks. By utilizing the analysis framework composed of the weighted phase lag index (wPLI) and tensor component analysis (TCA), we aim to characterize the fdFC corresponding to temporal-spectral-spatial signatures that can be used to interpret the neural mechanisms of different phases of sustained attention and to reflect the modulations by vigilance decrement.

The wPLI is used to estimate the contributions of phase leads and lags, with the advantage of being insensitive to the volume-conduction or noise (Vinck et al. 2011). The TCA is applied to characterize the interacted and low-dimensional components. Compared with the matrix decomposition analysis, the TCA provides a good approach for identifying brain activities in multiple domains simultaneously without stacking or concatenating the data (Cong et al. 2015 2014; Liu et al. 2020b). The analysis framework was firstly proposed by our team and successfully derived the temporal, spectral, and spatial modes of covariation (third-order tensor) during freely listening to music (Zhu et al. 2019). The reliability and stability of this analysis framework (third-order tensor) was further validated using the MEG data collected during a hand movement task and a working memory task (Zhu et al. 2020a). We then apply this framework to track the temporal, spectral, spatial, and feature modes of covariation (fourth-order tensor) simultaneously during a prolonged sustained attention task. In order to find the divergences between different responses during sustained attention, we perform the same framework in conditions of correct rejections, hits,

and misses, respectively. We compute the time–frequency domain wPLI between whole-brain electrodes from each block and subject. Considering the equalization of the trial numbers, we perform the wPLI for 100 times and then average the time–frequency domain FC. We construct a fourth-order tensor including time points, frequency bins, pairs of connections, and subjects × blocks. The fourth order tensor is subjected to the TCA to derive the interacted and low-dimensional TCA components, consisting of the temporal factor (dynamic temporal fluctuations), spectral factor (oscillatory distributions), connectivity factor (FC), and features (representations of fdFC influenced by time-on-task and motivation). With the use of the tensor-based framework, we seek to identify which frequency bands, in which time windows, and how the FC patterns involved in cognitive tasks and provide evidence for the modulations by complex factors.

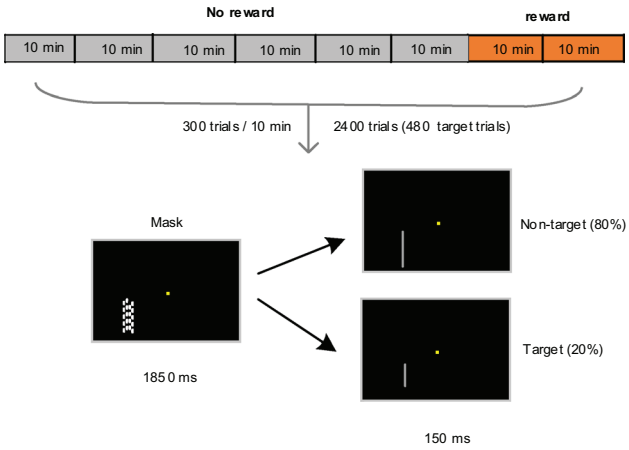

Fig. 1 Outline of the experiment procedure and an example of one trial in the sustained attention task

Materials and Methods

Data Description

We adopted a sustained attention EEG dataset published on the Open Science Framework (OSF) platform, which is a free, open platform to support our research and enable collaboration. The contributors of this dataset have reported a different set of results in a prior study (Reteig et al. 2019). The description of the data and preprocessing procedure in detail could be found at the link: https://doi.org/10.17605/OSF.IO/EMF9H.

The EEG data of twenty-one participants (ten males, aged 21.6 ± 3.4 years) collected during a modified version of sustained attention task (Maclean et al. 2009) was reported on the OSF platform. All stimuli were presented on a 17–inch monitor at a viewing distance of 100 cm. Participants were asked to maintain their fixation on a central yellow square (0.11° × 0.11°) against a black background throughout the task and covertly and continuously direct their attention to the stimuli located at 3° to the left and 1.5° lower than the fixation. The stimuli were presented only in the left hemifield, with the right hemifield never relevant. The outline of each trial is presented in Fig. 1. In each trial of 2 s, a light gray line was shortly presented at the to-be-attended location for 150 ms and was followed by a mask stimulus for the remaining 1850 ms. The light gray line with a width of 0.03° could either be a long (non-target, 80%) or short line (target, 20%). The long line was fixed on 1.89° in length, whereas the short one was calibrated individually before the main task. Participants were instructed to conduct a response to the rare target with their right index figure and withhold a response to the non-target. The mask stimulus was composed of many lines (0.03° × 0.12°), positioned with a space of 0.21° × 2.44°. These lines were randomly shifted in a small height (within ± 0.06°) on each presentation to prevent participants from recognizing the length of (non-) target line relative to the mask lines.

The Parameter Estimation by Sequential Testing (PEST) (Maclean et al. 2009; Taylor and Creelman 1967) was adopted to adjust the length of the short (target) line for individual participants, achieving a minimum accuracy of 80% in the task. The short line length ranged from 1.21° to 1.59° (1.40° ± 0.01°). After the execution of PEST (7–13 min), participants performed the main task for an interval of 80 min, consisting of 2400 trials (480 target trials) in total (Fig. 1). At the beginning of the task and every 10 min (300 trials), participants were provided with two 7–point scales to evaluate their levels of motivation (1: "not motivated", 7: "highly motivated") and aversion (1: "no aversion", 7: "strong aversion"). In the last 20 min of the main task, participants were informed an additional monetary reward of €30 (unknown to them until then) if they outperformed 65% of the other participants (Lorist et al. 2009). The instruction of monetary rewards—appeared at 60 min task-onset—disappeared until a button click or until a maximum of 60 s.

Data Acquisition and Preprocessing

EEG data was recorded using the BioSemi ActiveTwo with 64 Ag/AgCl electrodes arranged according to the international 10–10 system. The EEG signals were digitized at a sampling rate of 512 Hz. Each electrode was referenced to a common mode sense electrode online. Two additional channels were placed to the left and the right earlobes and four other external electrodes were used to record the horizontal (left and right outer canthi) and vertical (below and above the left eye) EOGs.

The preprocessing was conducted in MATLAB with the EEGLAB toolbox (Delorme and Makeig 2004). The EEG signals were high-pass filtered at 0.1 Hz and then segmented into epochs from − 2000 to 3000 ms peri-stimulus with buffer zones to reconcile the edge effects. Bad channels were interpolated using the spherical spline interpolation. With a visual inspection, parts of epochs containing eye movements, muscle activities, and other artifacts were removed. By running the independent component analysis (ICA), artificial components distinguishable from the neural activities were removed. Epochs were average referenced and segmented into − 1000 to 1000 ms peri-stimulus. Based on the markers of stimuli and responses, epochs were divided into four conditions, namely correct rejections, false alarms, hits, and misses. The condition of false alarms was not analyzed because the number of trials was too small.

Data Processing

The segmented epochs were further analyzed following the main steps of data processing. A schematic of the data analysis is demonstrated in Fig. 2.

Trial Binning

Consistent with previous analysis (Reteig et al. 2019), trials were split into eight 10–min blocks in the condition of correct rejections and binned into four 20–min blocks in conditions of hits and misses as the number of trials was too small. Obviously, the number of trials were different in each block for each participant, which might have a significant effect on results, especially the phase-based analysis results (Cohen 2014). Therefore, the number of trials was equalized across blocks for each participant by randomly selecting a minimum number of trials over blocks. Using the subsampling process, the number of trials in the correct rejections condition (167 ± 22.5, range = 124–213) and in the hits and misses conditions (24 ± 5.4, range = 11–33) was determined. The subsampling process was repeated 100 times. We computed the wPLI connectivity (Dynamic functional connectivity analysis section) at each time. The wPLI measures of all 100 times were further averaged to achieve the final value.

Dynamic Functional Connectivity Analysis

Time–Frequency Representations The spectral densities were estimated from each trial using the continuous wavelet transform with the complex Morlet wavelets. The frequency band from 1 to 30 Hz was linearly spaced in a resolution of 1 Hz. To preserve the temporal precision in low and high frequency bands, the number of wavelet cycles was adjusted from 2 to 11. A total of $n_f = 30$ linearly spaced frequencies and $n_t = 1024$ time points (− 1000 to 1000 ms peri-stimulus) were estimated. Thus, we derived the time frequency representations $S_c^n(t,f)$ in time point $t \in [1, n_t]$ and frequency bin $f \in [1, n_f]$ for trial n, where $n \in [1, N]$, N is the number of

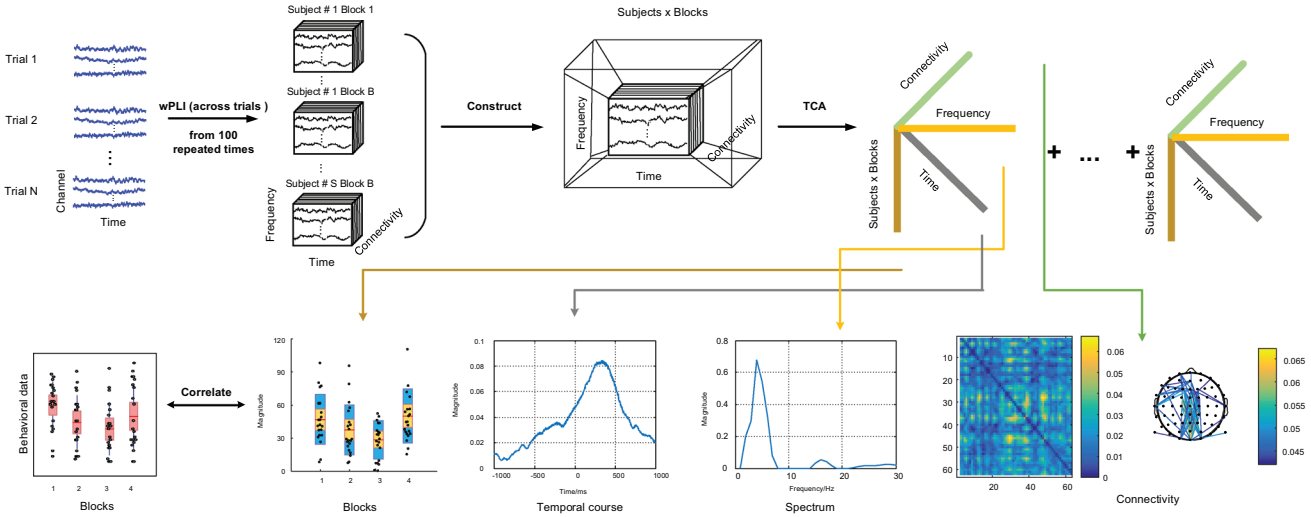

Fig. 2 The pipeline of data processing. The number of stimulus-locked trials were equalized over blocks for each participant. The subsampling process was repeated for 100 times. For each time, the signals from all trials were decomposed with the complex Morlet wavelet and then calculated with the wPLI, generating a third-order tensor (Time by frequency by connectivity) for each block and participant. An average third-order tensor was obtained by averaging all third-order tensors from 100 repeated times. Based on the average tensor of each block and participant, we constructed a fourth-order tensor by concatenating the blocks and subjects together. The fourth-order tensor was subjected to the TCA to extract the demixed components containing temporal course, spectrum, connectivity, and representations of blocks and subjects (features). The related components involved in the sustained attention were selected based on prior knowledge in the literature and the significant correlations with behavioral data

trials, $c \in [1, n_c]$, n_c is the number of channels, $n_c = 63$ after removing the on-line reference channel.

Weighted Phase Lag Index The wPLI was used to quantify phase differences by the magnitude of imaginary of the cross-spectrum (Vinck et al. 2011). Compared with the phase lag index (PLI) (Stam et al. 2007), the wPLI is less sensitivity to noise and volume conduction because of the contribution of weighted phase leads and lags. We computed wPLIs between all pairs of channels in each time point and frequency bin:

$$wPLI_{(c1,c2)}(t,f) = \frac{\left|\sum_{n=1}^{N} im\left(S_{c1}^{n}(t,f)S_{c2}^{n*}(t,f)\right)\right|}{\sum_{n=1}^{N}\left|im\left(S_{c1}^{n}(t,f)S_{c2}^{n*}(t,f)\right)\right|} \quad (1)$$

where $S_{c1}^{n}(t,f)$ and $S_{c2}^{n}(t,f)$ are time–frequency representations from two different channels $c1, c2 \in [1, n_c]$ in time point $t \in [1, n_t]$ and frequency bin $f \in [1, n_f]$ at trial $n \in [1, N]$. $im()$ represents the imaginary part of a complex value. $*$ is the complex conjugate and $||$ is an absolute operation. We then constructed a third-order tensor $\mathcal{P}$ with the dimensions of $n_t \times n_f \times C$ in each block and participant, where $C = 1953$ denotes the number of pairs of channels $(63 \times (63-1)/2)$. We computed the wPLI for 100 repeated times (Trial binning section) and averaged these 100 third-order tensors forming a final third-order tenor in each block and subject. In view of the blocks and subjects, we created a fifth-order tensor $\mathcal{O}$ with dimension of $n_t \times n_f \times C \times S \times B$, where $S = 21$ is the number of participants and B is the block amount, $B = 8$ in the correct rejections condition and $B = 4$ in the hits and misses conditions. Finally, we reshaped the tensor $\mathcal{O}$ into fourth-order tensor $\mathcal{X}\left(n_t \times n_f \times C \times M\right)$ by concatenating the blocks and participants together, where $M = S \times B$.

Tensor Component Analysis

In general, the multi-mode data were stacked or concatenated to facilitate two-way processing methods (e.g., independent component analysis (ICA) and principal component analysis (PCA)) for extracting interested brain activities (Bernat et al. 2005; Cong et al. 2010; Dien 2010; Tenke and Kayser 2005; Vigário and Oja 2008; Zhu et al. 2020b). The procedures of stacking and concatenating inevitably lost potential interaction information (Cong et al. 2015 2013a). The TCA can be directly applied to the multi-way data, exploiting the interacted information among multiple modes (Hitchcock 1927). As one of the most fundamental models of TCA, the canonical polyadic (CP) model (A.Harshman 1970; Hitchcock 1927) was applied to extract demixed components in our study. As all elements in the fourth-order tensor $\mathcal{X} \in \mathbb{R}_{+}^{n_t \times n_f \times C \times M}$ were nonnegative, the nonnegative constraint was used in the canonical polyadic decomposition (CPD) (Cichocki et al. 2009). For the input $\mathcal{X}$, the CPD is defined as an approximation of the sum of the outer products:

$$\mathcal{X} \approx \sum_{j=1}^{J} \mathcal{X}_j = \sum_{j=1}^{J} a_j \circ b_j \circ c_j \circ d_j \quad (2)$$

where $\mathcal{X}_j$ is the component $j \in [1, J]$ of $\mathcal{X}$, and J is the number of TCA components. The outer product of four factor-vectors $\boldsymbol{a}_j \circ \boldsymbol{b}_j \circ \boldsymbol{c}_j \circ \boldsymbol{d}_j$ produces the rank-one tensor $\mathcal{X}_j$. The operator $\circ$ is the outer product of the factor-vectors. In this application (Fig. 2), $\boldsymbol{a}_j$ is the temporal factor illustrating the temporal fluctuations, and $\boldsymbol{b}_j$ is the spectral factor characterizing the involvement of specific frequency band, and $\boldsymbol{c}_j$ is the connectivity factor representing whole-brain FC, and $\boldsymbol{d}_j$ is the feature factor indicating the alterations of specific time points, frequency bins, and FC affected by vigilance decrement and motivation.

The realization of CPD is to solve the following minimization problem:

$$\min_{\boldsymbol{A},\boldsymbol{B},\boldsymbol{C},\boldsymbol{D}} \frac{1}{2}\left\| \mathcal{X} - \sum_{j=1}^{J} \boldsymbol{a}_j \circ \boldsymbol{b}_j \circ \boldsymbol{c}_j \circ \boldsymbol{d}_j \right\|_F^2 \quad (3)$$

where $\boldsymbol{A} = [\boldsymbol{a}_1, \boldsymbol{a}_2, \ldots, \boldsymbol{a}_j], \boldsymbol{B} = [\boldsymbol{b}_1, \boldsymbol{b}_2, \ldots, \boldsymbol{b}_j], \boldsymbol{C} = [\boldsymbol{c}_1, \boldsymbol{c}_2, \ldots, \boldsymbol{c}_j]$, and $\boldsymbol{D} = [\boldsymbol{d}_1, \boldsymbol{d}_2, \ldots, \boldsymbol{d}_j]$ are factor matrixes of the temporal course, spectrum, FC, and features. The operator $\|\|_F$ is the Frobenius norm. The minimization problem in Eq. (3) can be solved by iterative optimization methods. The hierarchical alternating least squares (HALS) was applied in our study because the validity and high performance of HALS have been confirmed by extensive studies (Cichocki et al. 2009, 2008, 2007). The component number J was determined by the difference of fits (DIFFIT) (Cong et al. 2014, 2013b). The DIFFIT measures the differences in data fitting and is obtained by relative error and the explained sum of squares (Mørupa and Hansena 2009). The number of component J was chosen from 1 to 40 and the data fitting was averaged across 10 repetitions of CPD. In theoretical, the optimal component number J corresponds to the local maximum value of DIFFIT and a high data fit value.

Selection of TCA Components Modulated by Sustained Attention Tasks

By using the DIFFT, we determined J TCA components containing temporal course, spectrum, FC, and variations of blocks over subjects. Here, we aimed to select the related components modulated by the sustained attention task from the determined J components. Different methods

of selecting task-modulated TCA components have been described in previous studies such as a method integrating the prior knowledge of multi-domain components with a significant difference between experimental conditions (Cong et al. 2013b), a method combining the prior knowledge with significant correlations between variations of components and musical features (Zhu et al. 2019), and a method matching prior knowledge and significant task-modulation FC (empirical null distribution constructed based on phase randomization) (Zhu et al. 2020a). In the present study, we performed the selection procedure based on the prior knowledge of temporal windows, frequency bands, and brain networks involved in sustained attention tasks and the significant correlations between representations of components and behavioral data.

On the one hand, prior knowledge has revealed that implanting a sustained attention task involves different neural functions such as attentional preparatory, attentional stability, working memory, and enhancement/inhibition of selected/ unselected information (Clark et al. 2015; Reteig et al. 2019; Rosenberg et al. 2016; Slagter et al. 2016). Regarding the multi-domain TCA components, the FC patterns at different frequency bands should emerge in different time windows to subserve a variety of functions in sustained attention. Previous studies have demonstrated that preparatory orienting of attention is indexed by the pre-stimulus alpha, activated in the right-lateralized visual hemifield (Reteig et al. 2019; Worden et al. 2000). The variability of attention processing has been associated with the post-stimulus theta phase coherence, activated in frontal and parieto-occipital brain regions (Lutz et al. 2009; Reteig et al. 2019). The FC between frontal, parietal, and occipital brain regions in delta and theta bands has been linked to the working memory (Düzel et al. 2010; Gulbinaite et al. 2014; Harper et al. 2017). Numerous research work has demonstrated that the beta power (13–30 Hz) in the motor cortex is related to movement execution and response inhibition (Pfurtscheller and Aranibar 1977; Pfurtscheller and Lopes Da Silva 1999; Zabielska-Mendyk et al. 2018). The 20 Hz (mu) rhythm in particular is associated with the motor cortical function of the hand, and even unimanual finger movement relates to the bilateral somatomotor cortex (Hari and Salmelin 1997).

On the other hand, behavioral measurements—hit rate, a variant of accuracy, and response time—and motivation and aversion ratings have been illustrated as reliable markers, reflecting the effects of time-on-task and motivation (Reteig et al. 2019). The changes in behavioral and questionnaire data are shown in Fig. 3. The hit rate, accuracy, and response time rather than the false alarm rate deteriorated with time-on-task and transiently restored by motivation. Consequently, these three behavioral measurements were used for association analysis to select task-modulated TCA components. Although the ratings of motivation and aversion were significantly modulated by vigilance decrement and motivation, they were not applied for component selection because these ratings were not correctly corresponding to the values of each block.

We conducted correlation analyses between behavioral measurements and features of TCA components by connecting these measurements and features from all blocks (a total of 168 samples in the correct rejection condition and 84 samples in the hits and misses conditions). We selected the desirable TCA components that both consistent with prior knowledge with a visual inspection and closely related to the behavioral measurements. The component which only meets the criterion of prior knowledge or only meets the criterion of significant correlations were not selected, as shown in Figs. S1–3.

Statistics

In order to examine the changes of fdFC caused by vigilance decrement, the elements in feature factor were subjected to the one-way analysis of variances (ANOVAs) with the within-subject factor block (first 60 min without reward) and results were corrected by the Greenhouse–Geisser. We also conducted the pair-wise comparisons between blocks 6 and 1 in the correct rejections condition and between blocks 3 and 1 in the hits and misses conditions to directly reveal the differences of fdFC between low and high vigilance state (without considering variations in different blocks). We performed the pair-wise comparisons between blocks 7 and 6 in the correct rejections condition and between blocks 4 and 3 in the hits and misses conditions to indicate the modulations of fdFC produced by motivation. When the effects of reward on specific component were detected, we ran pair-wise comparisons between blocks 7 and 1 in the correct rejections condition and between blocks 4 and 1 in the hits and misses conditions to quantitatively investigate the improvement of fdFC by motivation relative to that in the high vigilance state. In case of significant differences between blocks 7 and 1, we further ran the comparisons between blocks 8 and 1 to explore the continuous effect of motivation on fdFC. Both paired-sample t-test and Kruskal–Wallis test were applied to pair-wise comparisons. When the representations of the specific component followed the Gaussian distribution measured by the Jarque–Bera test, we used the paired-sample t-test, otherwise the Kruskal–Wallis test.

After testing the distribution of behavioral data and representations of component with Jarque–Bera test, the Pearson correlation (following the Gaussian distribution) or Spearman rank correlation (non-parametric test) were used for correlation analysis between behavioral measurements (e.g., hit rate, accuracy, and response time) and the features of TCA components.

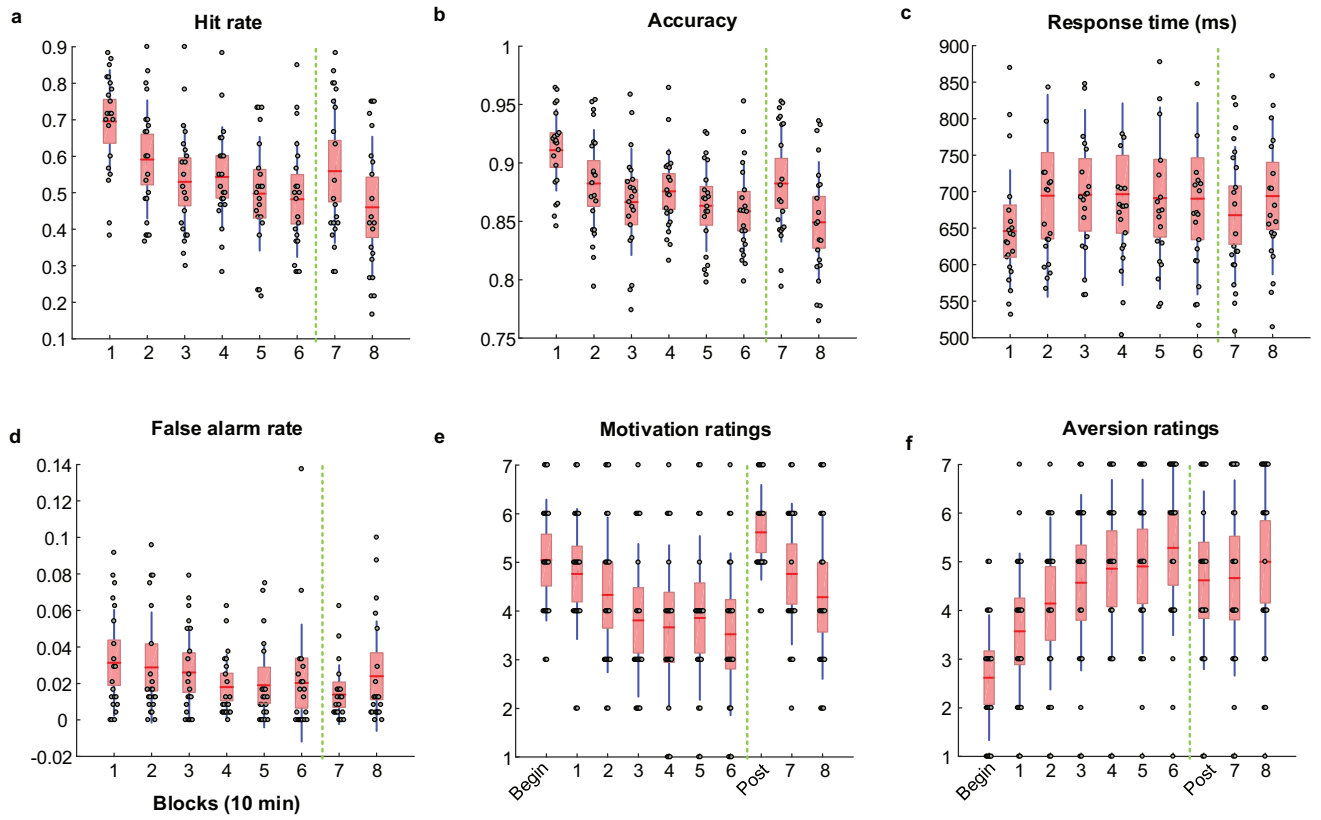

Fig. 3 The changes in behavioral measurements and questionnaire ratings affected by time-on-task and motivation. **a** Hit rate and **b** Accuracy declined with time-on-task and transiently recovered (block 7) after providing rewards (after 60 min, as marked with the vertical dotted green line). **c** Response time decreased with time-on-task and showed a partial restoration pattern in block 7 although no significant difference. **d** False alarm rate did not change with time-on-task. **e** Motivation ratings and **f** Aversion ratings were influenced by time-on-task, and the motivation ratings restored to the initial level whereas the aversion ratings remained high compared to the initial level. The ratings of motivation and aversion were conducted before the task performance (begin) and after providing the reward instructions (post), as well as every 10 min task performance. The red line in the box represents the mean value, the light red box represents the standard deviation (SD), and the blue line corresponds to the 95% confidence interval. Note: The statistical results of the behavioral measurements and questionnaire ratings have been presented (Reteig et al. 2019). We only displayed the changes of them with scatter and boxplot to directly reveal the reliability for correlation analysis to select the TCA components

The type I errors should be controlled during multiple comparisons when more than one TCA component was selected and multiple pair-wise comparisons were conducted. The p-values from selected components were corrected by the false discovery rate (FDR) to control the false discoveries (Benjamini and Yekutieli 2005, 2001; Benjamini and Hochberg 1995). The p-values (under one-tailed condition) from multiple pair-wise comparisons were further corrected. In sum, the statistics were conducted in MATLAB 2018b and IBM SPSS Statistics version 22. All tests applied a significance level of 0.05.

Results

The number of TCA components were determined by the DIFFIT, and the components modulated by the sustained attention task were selected from the retained TCA components using the criterion of prior knowledge and the significant correlations with behavioral measurements. We presented the multi-domain TCA components involved in the sustained attention task in the conditions of correct

rejections, hits, and misses, and showed the variations of fdFC affected by vigilance decrement and motivation.

TCA Components in the Correct Rejections Condition

According to the DIFFIT, a total of 25 TCA components were determined in the inhibition of the correct rejections condition. Among the 25 components, we selected 5 task-modulated components using the criterion based on prior knowledge and significant associations between representations of components and behavioral data. The five task components could be considered four types of neuromakers: (I) the pre-stimulus alpha right-lateralized parieto-occipital FC, (II) the post-stimulus theta fronto-parieto-occipital FC, (III) the post-stimulus delta fronto-parieto-occipital FC, (IV) the post-stimulus beta right sensorimotor FC, and (V) the post-stimulus beta left sensorimotor FC, as shown in Fig. 4.

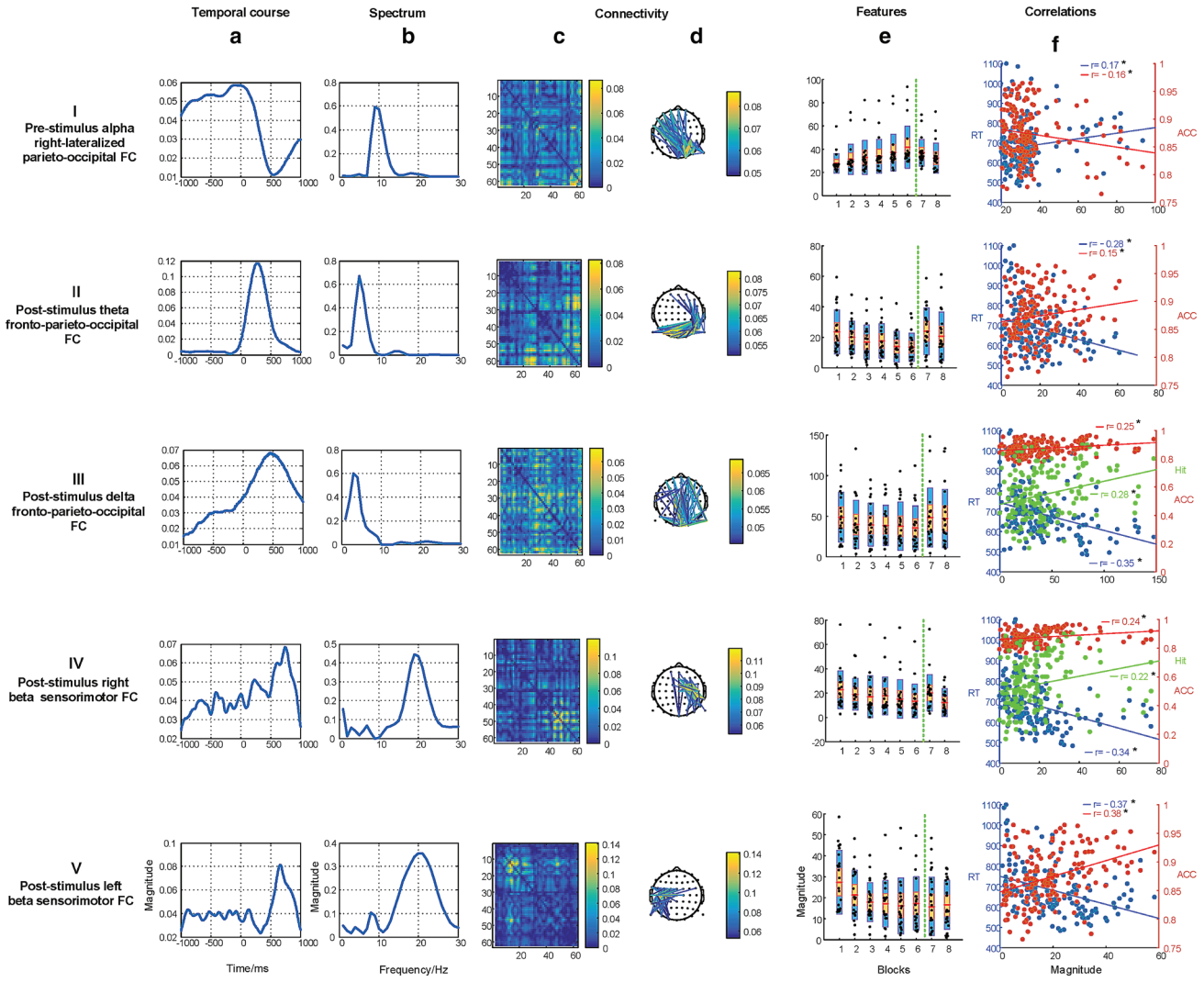

Fig. 4 The selected five TCA components in the correct rejections condition. Each row represents one component, consisting of four dimensional information: the temporal factor showing the temporal course during sustained attention (**a**); the spectral factor showing the involvement of specific spectrum (**b**); the connectivity factor representing the symmetrical weighted FC matrix (**c**) and the 2D weighted connectivity visualization (showing the top 2% of the links with highest values, and the 2% thresholding was only used for visualization), with different colors related to different connectivity strengths (**d**); the features of fdFC affected by time-on-task (blocks 1–6, marked with the vertical dotted green line) and motivation (blocks 7 and 8), and the red line in the bar represents the mean value, the yellow bar represents the standard deviation (SD), and the blue bar corresponds to the 95% confidence interval (Loftus and Masson 1994) (**e**). Correlations between behavioral measurements, namely the response time (RT, in blue line), accuracy (ACC, in red line), and Hit rate (Hit, in green line) and variations of blocks across all subjects are displayed, significant relationships ($p < 0.05$) marked with * (**f**). Note that the insignificant correlations between the hit rate and features are not presented in scatters but in Fig. S1

Pre-stimulus Alpha Parieto-Occipital FC

The component as shown in row I of Fig. 4 had significant associations with the response time ($r = 0.17, p = 0.03$) and accuracy ($r = -0.16, p = 0.04$). The FC that activated in the parietal and occipital brain regions, was right-lateralized. This FC emerged in the time window of − 1000 to 0 ms stimulus-onset was dominated by the alpha band. The strength of the fdFC was affected by vigilance decrement, with a slight increase with time-on-task ($F(3.07, 61.31) = 2.86, p_{corr} = 0.057$). Moreover, the strength was stronger in block 6 than in block 1 ($t(20) = 2.47, p_{corr} = 0.024$). There was no significant difference between blocks 7 and 6, although the strength of the fdFC showed a decrease pattern ($t(20) = 1.22, p_{corr} = 0.149$). Neither a significant difference between blocks 1 and 7 ($t(20) = 1.57, p_{corr} = 0.124$) nor between blocks 1 and 8 ($t(20) = 1.08, p_{corr} = 0.184$) was detected.

Post-stimulus Theta Fronto-Parieto-Occipital FC

The component in Row II of Fig. 4 was significantly correlated with the response time ($r = -0.28, p < 0.01$) and accuracy ($r = 0.15, p = 0.05$). The temporal window of the fronto-parieto-occipital FC ranged from 100 to 500 ms stimulus-onset, and the spectrum of it spanned the theta band. The strength of the fdFC decreased slightly during a long period of task engagement ($F(3.47, 69.41) = 2.61, p_{corr} = 0.057$). The strength was weaker in block 6 than in block 1 ($t(20) = 2.32, p_{corr} = 0.024$). Monetary reward increased the strength in block 7 relative to block 6 ($t(20) = 2.59, p_{corr} = 0.022$). The strength of the fdFC in block 1 was comparable to that in block 7 ($t(20) = 0.57, p_{corr} = 0.358$) and block 8 ($t(20) = 1.11, p_{corr} = 0.184$).

Post-stimulus Delta Fronto-Parieto-Occipital FC

The component (row III of Fig. 4) was positively associated with the hit rate ($r = 0.28, p < 0.01$) and accuracy ($r = 0.25, p < 0.01$), and negatively associated with the response time ($r = -0.35, p < 0.01$). The fronto-parieto-occipital FC peaked around 460 ms in the temporal course with the spectral modes ranging from 1–4 Hz corresponding to the delta band. There was a slight deterioration of the fdFC strength during a prolonged duration of task involvement ($F(3.83, 76.61) = 2.01, p_{corr} = 0.092$). The strength was weaker in block 6 than in block 1 ($t(20) = 2.26, p_{corr} = 0.024$). The strength of the fdFC in block 7 increased relative to block 6 after providing rewards ($t(20) = 2.78, p_{corr} = 0.022$). There was no significant difference either between blocks 1 and 7 ($t(20) = 0.01, p_{corr} = 0.500$) or between blocks 1 and 8 ($t(20) = 0.28, p_{corr} = 0.392$).

Post-stimulus Right and Left Beta Sensorimotor FCs

The component (row IV of Fig. 4) had a positive relationship with the hit rate ($r = 0.22, p < 0.01$) and accuracy ($r = 0.24, p < 0.01$), and had a negative relationship with the response time ($r = -0.34, p < 0.01$). The right-lateralized sensorimotor FC that peaked around 740 ms stimulus onset in the temporal course and was dominated by 20 Hz in the spectrum. The strength of the fdFC was weaker in block 6 than in block 1 ($t(20) = 2.07, p_{corr} = 0.026$) and it was stronger in block 7 than in block 6 after providing rewards ($t(20) = 2.30, p_{corr} = 0.033$). There was no significant difference between blocks 1 and 7 ($t(20) = 0.86, p_{corr} = 0.333$), whereas the strength of this fdFC was weaker in block 8 than in block 1 ($t(20) = 2.35, p_{corr} = 0.044$).

The component (row V of Fig. 4) was closely related to the response time ($r = -0.37, p < 0.01$) and accuracy ($r = 0.38, p < 0.01$). The left-lateralized sensorimotor FC that peaked around 670 ms stimulus onset was dominated by 20 Hz in the spectrum. A slight deterioration of the left sensorimotor FC was detected with time-on-task ($F(2.32, 46.36) = 2.53, p_{corr} = 0.057$). The strength of it was weaker in block 6 than in block 1 ($t(20) = 2.21, p_{corr} = 0.024$). There was no improvement of the strength in block 7 after manipulating motivation ($t(20) = 0.46, p_{corr} = 0.326$).

TCA Components in the Hits Condition

In the condition of hits, we extracted 35 TCA components based on the DIFFIT criterion and finally selected 3 task-modulated components according to the mentioned criterions. We derived three neuromarkers including the pre-stimulus alpha right-lateralized parieto-occipital FC (row I of Fig. 5), the post-stimulus theta fronto-parieto-occipital FC (row II of Fig. 5), and the post-stimulus delta fronto-parieto-occipital FC (row III of Fig. 5). These three neuromarkers were also discovered in the correct rejections condition. However, the beta right/left sensorimotor FCs were not detected in the hits condition.

Pre-stimulus Alpha Parieto-Occipital FC

The component as shown in row I of Fig. 5 was significantly correlated with the response time ($r = 0.34, p < 0.01$) and accuracy ($r = -0.27, p = 0.01$). The FC was mainly activated in the right-lateralized parietal and occipital brain regions. The FC emerged in the time window of –1000 to 0 ms was dominated by the alpha band. The

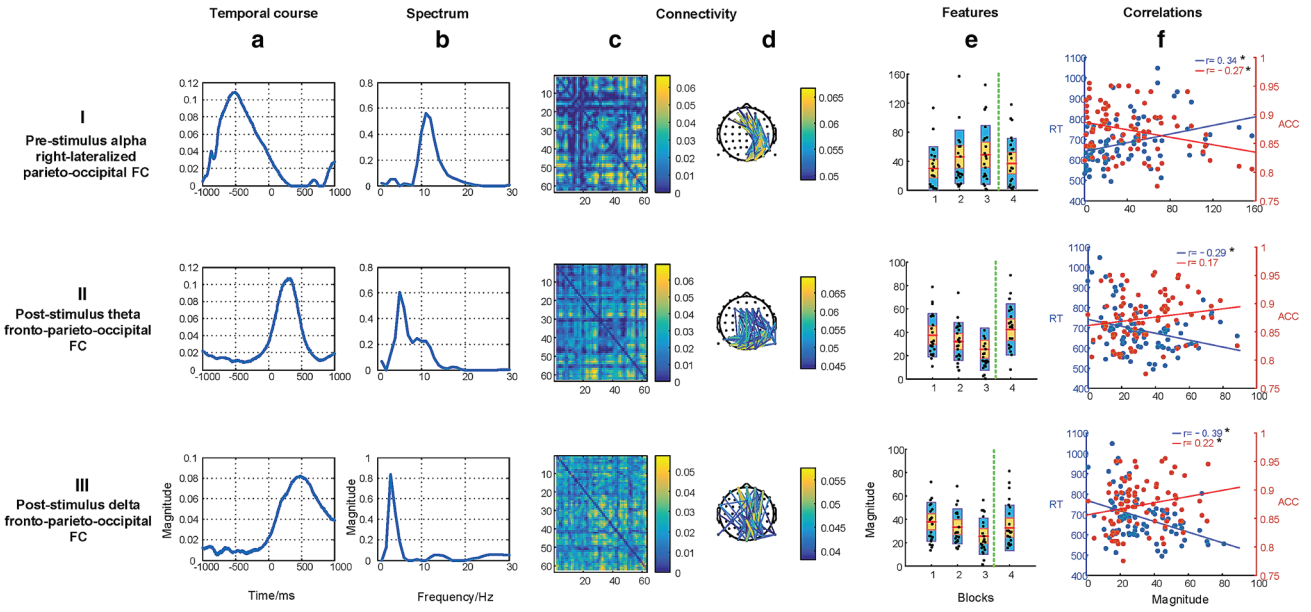

Fig. 5 The selected three TCA components in the hits condition. Each row represents one component, consisting of four dimensional information including the temporal factor showing time varies during sustained attention (**a**), the spectral factor showing the specific oscillatory activations in the corresponding FC (**b**), the connectivity factor representing the symmetrical weighted connectivity matrix (**c**) and the 2D weighted connectivity visualization (showing the top 2% of the links with highest values, and the thresholding was only used for visualization), with different colors related to different connectivity strengths (**d**), and features' changes affected by time-on-task (blocks 1–3, marked with the vertical dotted green line) and motivation (block 4), and the red line in the bar represents the mean value, the yellow bar represents the standard deviation (SD), and the blue bar corresponds to the 95% confidence interval (**e**). Correlations between behavioral measurements, namely the response time (RT), and accuracy (ACC), and features are presented, with significant relationships ($p < 0.05$) marked with * (**f**). Note that the insignificant correlations between the hit rate and features are not presented in scatters but in Fig. S2

strength of the fdFC increased during the sustained attention task over time ($F(1.91, 36.29) = 5.32, p_{corr} = 0.027$) and the strength was stronger in block 3 than in block 1 ($t(20) = -3.43, p_{corr} = 0.003$). After providing rewards, the strength in block 4 decreased compared to block 3 ($t(20) = 3.43, p_{corr} = 0.004$) and the strength in block 4 recovered to the initial level in block 1 ($t(20) = 0.58, p_{corr} = 0.284$).

Post-stimulus Theta Fronto-Parieto-Occipital FC

There was a close association between the component (row II of Fig. 5) and the response time ($r = -0.29, p = 0.01$). The temporal course of the fronto-parieto-occipital FC ranged from 0 to 500 ms and the spectrum of it peaked around 5 Hz. There was a decline of the strength of the fdFC during prolonged task engagement ($F(1.57, 31.35) = 3.26, p_{corr} = 0.049$). The strength was weaker in block 3 than in block 1 ($t(20) = 3.38, p_{corr} = 0.003$). The strength in block 4 was improved after providing incentives compared to block 3 ($t(20) = 2.61, p_{corr} = 0.013$). This improvement reached the strength of it in block 1, with no difference between blocks 1 and 4 ($t(20) = 0.95, p_{corr} = 0.285$).

Post-stimulus Delta Fronto-Parieto-Occipital FC

The component (Row III of Fig. 5) was significantly associated with the response time ($r = -0.39, p < 0.01$) and accuracy ($r = 0.22, p = 0.47$). The fronto-parieto-occipital FC that peaked around 490 ms in temporal course was dominated by the delta band. Results revealed a decline of the strength of the fdFC with time-on-task ($F(1.69, 33.75) = 3.65, p_{corr} = 0.049$). The strength was weaker in block 3 than in block 1 ($t(20) = 2.76, p_{corr} = 0.012$). A slight increase of the strength in block 4 was detected after providing incentives compared to block 3 ($t(20) = 1.70, p_{corr} = 0.053$). There was no significant difference between blocks 1 and 4 ($t(20) = 0.45, p_{corr} = 0.467$).

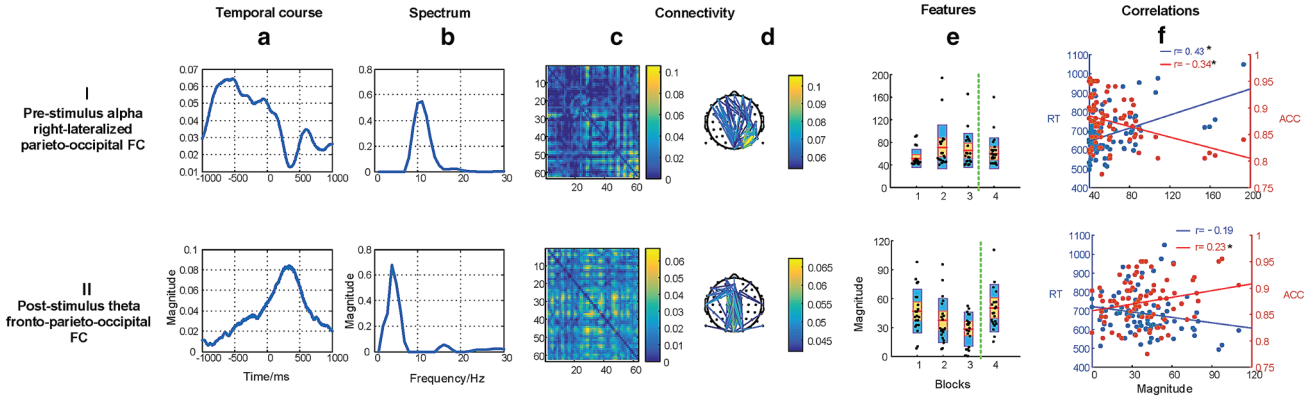

Fig. 6 Two selected TCA components in the misses condition. Each row represents one component, consisting of the temporal factor showing the time varies (**a**); the spectral factor showing the dominated frequency band (**b**); the connectivity factor representing the symmetrical weighted connectivity matrix (**c**) and the 2D weighted connectivity visualization (showing the top 2% of the links with highest values, and the thresholding was only used for visualization), with different colors related to different connectivity strengths (**d**); the features' factor affected by time-on-task (blocks 1–3, marked with the vertical dotted green line) and motivation (block 4), and the red line in the bar represents the mean value, the yellow bar represents the standard deviation (SD), and the blue bar corresponds to the 95% confidence interval (**e**). Correlations between behavioral measurements, namely the response time (RT, in blue line), and accuracy (ACC, in red line), and variations of blocks across all subjects are displayed, significant relationships ($p < 0.05$) marked with * (**f**). Note that the insignificant correlations between the hit rate and features are not presented in scatters but in Fig. S3

TCA Components in the Misses Condition

We extracted 25 TCA components based on the DIFFIT and finally selected two components modulated by the sustained attention task, representing (I) the pre-stimulus alpha right-lateralized parieto-occipital FC and (II) the post-stimulus theta fronto-parieto-occipital FC, as shown in Fig. 6. Similar to the hits condition, the beta right/left sensorimotor FCs were not detected in the misses condition, whereas different from the hits condition, the delta fronto-parieto-occipital FC was not observed in the misses condition.

Pre-stimulus Alpha Parieto-Occipital FC

The component in row I of Fig. 6 was positively correlated with the response time ($r = 0.43, p < 0.01$) and negatively correlated with the accuracy ($r = -0.34, p < 0.01$). The right-lateralized parieto-occipital FC emerged mainly around − 1000 to 0 ms stimulus-onset and was dominated by the alpha band. The strength of the fdFC increased slightly with time-on-task ($F(1.95, 39.04) = 3.38, p_{corr} = 0.068$) and the strength was stronger in block 3 than in block 1 ($t(20) = 2.46, p_{corr} = 0.023$). The impaired strength was not modulated by rewards, with no difference between blocks 4 and 3 ($t(20) = 1.26, p_{corr} = 0.112$).

Post-stimulus Theta Fronto-Parieto-Occipital FC

Row II of Fig. 6 shows a component that has a significant relationship with the accuracy ($r = 0.23, p = 0.039$). The fronto-parieto-occipital FC ranged in the time window of 0–500 ms and peaked around 5 Hz in the spectrum. There was a slight decline of the strength of the fdFC with time-on-task ($F(1.65, 32.89) = 2.83, p_{corr} = 0.068$). The strength was weaker in block 3 than in block 1 ($t(20) = 2.85, p_{corr} = 0.020$). The strength in block 4 increased relative to block 3 ($t(20) = 2.90, p_{cor} = 0.009$) after providing rewards and the increment of the strength reached the level of it in block 1 ($t(20) = -0.55, p_{corr} = 0.443$).

Discussion

By applying the analysis framework composed of wPLI and TCA to the high-temporal resolution EEG collected during a sustained attention task over 80 min, we examined how a cascade of fundamental functions was reflected by the fdFC and which stages or a combination of stages were affected by vigilance decrement and motivation. In tandem, we performed the analysis framework in the correct rejections, hits, and misses conditions to explore the distinctive involvement of functions in different conditions. Following the main steps of the framework (Fig. 2), we firstly calculated the time–frequency domain wPLI from whole-brain electrodes in each block and subject and then constructed a fourth-order tensor (Time × Frequency × Connectivity × (Subjects × Blocks)) by concatenating the data in blocks and subjects. Afterward, the TCA was applied to the fourth-order tensor to characterize the interacted, low dimensional, and representative components, suggesting the when (specific time windows), how (particular frequency band), and where (definite brain regions) of sustained attention were affected by vigilance

decrement. A total of four types of neuromarkers were identified, namely the pre-stimulus alpha right-lateralized parieto-occipital FC, the post-stimulus theta fronto-parieto-occipital FC, delta fronto-parieto-occipital FC, and beta right/left sensorimotor FCs. These fdFCs emerged in different time windows and conditions to support the implementation of a sustained attention task. Results demonstrated that all fdFCs were impaired by vigilance decrement, but they were differently modulated by motivation. The pre-stimulus alpha parieto-occipital FC and the post-stimulus theta and delta fronto-parieto-occipital FCs were restored by the motivation to the initial level, but the beta left sensorimotor FC was not modulated by motivation. Interestingly, the beta right sensorimotor FC increased only in the first 10 min but decreased in the last 10 min during the interval of motivation manipulation. Taken together, assisted with the tensor-based framework, we successfully derive a sequence of fdFCs involved in sustained attention and the discrepancies of these fdFCs among distinct conditions, as well as the organizations of them modulated by time-on-task and motivation.

Horizontal Analysis: Fundamental Functions in Sustained Attention

In the present study, the time window of the alpha right-lateralized parieto-occipital FC ranged from − 1000 to 0 ms. The theta fronto-parieto-occipital FC peaked around 280–320 ms and the delta fronto-parieto-occipital FC peaked around 460–490 ms across emerged conditions. The beta (peaked at approximately 20 Hz) right and left sensorimotor FCs peaked around 670 and 740 ms, respectively. These fdFCs emerged in the temporal order of the alpha parieto-occipital, theta fronto-parieto-occipital, delta fronto-parieto-occipital, and beta right/left FCs. When these results are interpreted in the context of the roles suggested for the fdFCs, a series of fundamental functions underlying sustained attention can be tracked.

A previous study has demonstrated that the event-related desynchronization within the alpha band in the occipital brain regions is associated with the anticipatory attention for a forthcoming stimulus (Bastiaansen et al. 2001). Moreover, the lateralization of alpha is a critical index of spatial attention (Thut et al. 2006). A large body of research has shown that the alpha band increases in the ipsilateral hemisphere while decreases in the contralateral hemisphere when humans deploy their attention to one location (Thut et al. 2006; Worden et al. 2000). The alpha right-lateralized parieto-occipital FC in our study might be an index of anticipatory attention, although the lateralization is opposite to that in earlier studies. These diverging results concerning the lateralization might result from the specific task design where the stimulus was presented only on the left of the fixation, as pointed out in an earlier publication based on the same dataset (Reteig et al. 2019). Secondly, the post-stimulus theta phase coherence in fronto-parieto-occipital topography has been linked to the attentional stability (Lutz et al. 2009) and the variability of brain responses (Reteig et al. 2019). In line with these previous studies, our results also observed the involvement of the frontal, parietal, and occipital brain regions in the theta band, suggesting that the attentional stability might be indexed by the theta fronto-parieto-occipital FC. Next, earlier work has suggested that the fronto-occipital brain network in delta band is closely related to the working memory (Gulbinaite et al. 2014; Harper et al. 2017). Consistent with these findings, the delta fronto-parieto-occipital FC extracted in our study is likely to relate to the working memory. Finally, the close relationship between the beta band and the response movement has been built in the literature (Pfurtscheller and Aranibar 1977). The 20 Hz mu rhythm is particularly associated with the motor cortical function, with the bilateral engagement of the somatomotor cortex even in unilateral movement (Hari and Salmelin 1997). In the present study, the beta (peaked around 20 Hz) right/left somatomotor FCs might provide evidence for response movement.

In sum, according to the timeline and the cognitive content, the four types of neuromarkers appear to correspond to a cascade of fundamental functions in sustained attention consisting of the attentional preparatory, attentional stability, working memory, and response movement.

Vertical Analysis: Functional Discrepancies in Different Conditions

Our study detected the pre-stimulus alpha parieto-occipital FC and the post-stimulus theta fronto-parieto-occipital FC in the correct rejections, hits, and misses conditions. The alpha and theta FCs continuously presented despite the different responses participants conducted. In line with our findings, a different set of results have reported that the pre-stimulus alpha power and the post-stimulus theta phase presented in these three conditions (Reteig et al. 2019). Integrating the fdFCs with the fundamental functions underlying sustained attention, these findings appear to indicate that people need to prepare attention for each upcoming stimulus and the attentional stability exists in all three conditions.

The delta fronto-parieto-occipital FC was derived only in correct responses, including correctly inhibiting non-target (the correct rejections condition) and detecting target (the hits condition), but not in error responses of detecting target (the misses condition). As referred above, the delta FC is related to working memory. It is likely that the inability to detect targets is owing to a failure of the target-related working memory process. The working memory encompasses subprocesses of information encoding, maintenance,

or retrieval (Düzel et al. 2010; Quentin et al. 2019), but our results cannot infer which subprocess or a combination of them are dysfunctional in the misses condition.

A substantial amount of studies have examined the role of beta band in the motor cortex during reaction responses, suggesting that the response execution is related to beta rhythmic desynchronization and the response inhibition is associated with beta synchronization (Pfurtscheller and Aranibar 1977; Pfurtscheller and Lopes Da Silva 1999; Zabielska-Mendyk et al. 2018). The increased beta band during response inhibition to distractors is also well known as the "beta rebound" phenomenon (Bola and Sabel 2015). In this work, the beta right/left sensorimotor FCs emerged only in the correct rejections condition. Our findings are agreement with previous studies showing the synchronization of beta band in response inhibition and desynchronization in response execution. Interestingly, we did not extract the beta FCs in the misses condition although no responses were conducted in this condition. It is plausible that the inability to detect target is not the failure of response execution, but the failure of other functions such as working memory, which is consistent with the results presented by the delta fronto-parieto-occipital FC.

Unlike the magnitude differences—alpha power, N1/P1 component, and theta phase—between hits and misses conditions reported in the previous study (Reteig et al. 2019), the present work successfully found the functional discrepancies in the hits, misses, and correct rejections conditions. The patterns of fdFC shift to subserve distinct responses (e.g., correct rejections, hits, misses) during sustained attention.

The fdFCs Affected by Vigilance Decrement and Motivation

The pre-stimulus alpha parieto-occipital FC was more right-lateralized with the decrease of vigilance and less right-lateralized after manipulating motivation in our study. Similar results have been reported in an earlier study that increased attentional load and time-on-task give rise to more right-lateralization in posterior alpha asymmetry (Newman et al. 2013), although the earlier study does not explore the changes of lateralization influenced by motivation. Our results reaffirm that the non-spatial factor of time-on-task modulates the biases of spatial attention and further verify that the motivation is another non-spatial factor influencing the attention biases. In contrast to most externally-cued attention orienting studies, our study and the earlier study (Newman et al. 2013) did not set up pre-target cues, but we demonstrated that the anticipatory pre-stimulus alpha was also apparent in no-cued attention orienting.

We found that the post-stimulus theta fronto-parieto-occipital FC decreased with time-on-task and increased after manipulating motivation. In line with previous studies (Lutz et al. 2009; Reteig et al. 2019), the theta FC could be interpreted as a reliable index indicating the changes of attentional stability or brain responses modulated by time-on-task and motivation. These results suggest that human attentional stability could be impaired by vigilance decrement and this ability could be restored after providing rewards.

The post-stimulus delta fronto-parieto-occipital FC decreased with time-on-task and increased after providing rewards, indicating that the function of working memory in sustained attention was impaired by vigilance decrement and recovered by rewards. The impairment by the decrement of vigilance is supported by a piece of indirect evidence that higher working memory capacity is related to weaker fronto-parietal FC (Gulbinaite et al. 2014). Consistent with our results, a previous study has demonstrated the enhancement effect of reward on the working memory capacity (Sanada et al. 2013). Our finding seems to show that the working memory, at least the function involved in sustained attention, is sensitive to both time-on-task and motivation.

The post-stimulus beta right/left sensorimotor FCs decreased after long durations of task performance. Akin to a previous study (Guo et al. 2018), we elucidated that time-on-task is one of the main factors leading to the degrading of response inhibition. We also found that the ipsilateral right sensorimotor FC, but not the contralateral left sensorimotor FC, was restored by motivation when participants inhibited with a right finger's response. This appears to illustrate that the right sensorimotor activation is more sensitive to motivation than the left sensorimotor, in the situation that bilateral somatomotor networks are engaged in the unilateral movement. Although we cannot make conclusions on the source of the reward restoration, the connections between the right hemisphere and response inhibition have also been built in an earlier research (Aron et al. 2003). Another theoretical work also suggests that successful versus unsuccessful inhibited differential responses are related to the right hemisphere during rewarded condition (Padmala and Pessoa 2010).

Transient and Partial Restoration of fdFCs After Manipulating Motivation

Prolonged performance (60 min) of a sustained attention task lead to vigilance decrement, impairing all types of fdFCs. Participants were motivated with an extra monetary reward in the last 20 min interval. Four types of fdFCs, except for the left sensorimotor FC, were restored by reward, although the recovery of the right sensorimotor FC was transient. The right sensorimotor FC increased only in the first 10 min and then fell down to the low vigilance level in the last 10 min. The restoration of fdFCs by motivation appears to inconsistent with the overload theories, which states that cognitive resources are limited and vigilance decrement

is determined only by resource depletion. The partial and transient improvement by motivation might agree with the motivational control and energetical costs theoretical model, where participants evaluate the costs and benefits and also assess their energetic resources to decide to expend or reserve their efforts.

There are still three caveats in explaining the results. First of all, the modulation effect of reward on the pre-stimulus alpha parieto-occipital FC is detected in the correct rejections and hits conditions, but not in the misses condition. It is possible that the differences are from the robustness of motivation itself or the instability of preparation of attention in the misses condition. Secondly, the number of trials cannot be equalized in the correction rejections and hits/miss conditions because of the experimental design. This imbalance might result in some differences in the TCA components. Finally, the task-related component selection is critical for the application of the tensor-based framework. Not only with the behavioral data association analyses but also more robustness and efficient methods should be developed for TCA component selection to provide comprehensive consideration.

Conclusion

We apply an analysis framework composed of wPLI and TCA to a long period of sustained attention EEG dataset and derive a cascade of fdFCs involved in a sustained attention task. The pre-stimulus alpha parieto-occipital FC, post-stimulus theta fronto-parieto-occipital FC, delta fronto-parieto-occipital FC, and beta right/left sensorimotor FCs are derived, corresponding to different functions in sustained attention. We successfully detect the modulations of fdFCs affected by vigilance decrement and motivation. All these fdFCs are impaired by vigilance decrement. Especially, the pre-stimulus alpha FC parieto-occipital drifts rightward with time-on-task. The impairments of fdFCs are partially restored by motivation. The post-stimulus beta left sensorimotor network is not modulated by rewards. The right sensorimotor FC is more associated with motivation than the left sensorimotor FC, although the effect of improvement by motivation on the right sensorimotor FC is transient. Our results lay the ground for the hybrid model that vigilance decrement is determined by motivational control and energetical costs. The analysis framework provides feasibility for identifying dynamic organizations of frequency-specific FC in cognitive tasks.

Acknowledgements This study is to memorize Prof. Tapani Ristaniemi for his great help to the author, Fengyu Cong and Jia Liu. This work is supported by the National Natural Science Foundation of China (No. 91748105 & 81471742), the Fundamental Research Funds for the Central Universities in Dalian University of Technology in China [DUT2019], the scholarships from China Scholarship Council [Nos. 201600090044; 201600090042], and the mobility grant to visit Macmaster University. The authors would like to express their thanks to Heleen A. Slagter and her research group for publishing the sustained attention data on the OSF platform.

Funding Open access funding provided by University of Jyvaskyla.

Compliance with Ethical Standards

Conflict of interest All authors declare that they have no conflict of interest.

References

Aron AR, Fletcher PC, Bullmore ET, Sahakian BJ, Robbins TW (2003) Stop-signal inhibition disrupted by damage to right inferior frontal gyrus in humans. Nat Neurosci 6:115–116. https://doi.org/10.1038/nn1003

Bastiaansen MCM, Böcker KBE, Brunia CHM, De Munck JC, Spekreijse H (2001) Event-related desynchronization during anticipatory attention for an upcoming stimulus: a comparative EEG/MEG study. Clin Neurophysiol 112:393–403. https://doi.org/10.1016/S1388-2457(00)00537-X

Benjamini Y, Hochberg Y (1995) Controlling the false discovery rate : a practical and powerful approach to multiple testing. J R Stat Soc Ser B 57:289–300. https://doi.org/10.1111/j.2517-6161.1995.tb02031.x

Benjamini Y, Yekutieli D (2001) The control of the false discovery rate under dependency. Ann Stat 29:1165–1188

Benjamini Y, Yekutieli D (2005) False discovery rate-adjusted multiple confidence intervals for selected parameters. J Am Stat Assoc 100:71–81. https://doi.org/10.1198/016214504000001907

Bernat EM, Williams WJ, Gehring WJ (2005) Decomposing ERP time-frequency energy using PCA. Clin Neurophysiol 116:1314–1334. https://doi.org/10.1016/j.clinph.2005.01.019

Boksem MAS, Tops M (2008) Mental fatigue: costs and benefits. Brain Res Rev 59:125–139. https://doi.org/10.1016/j.brainresrev.2008.07.001

Bola M, Sabel BA (2015) Dynamic reorganization of brain functional networks during cognition. Neuroimage 114:398–413. https://doi.org/10.1016/j.neuroimage.2015.03.057

Caggiano DM, Parasuraman R (2004) The role of memory representation in the vigilance decrement. Psychon Bull Rev 11:932–937. https://doi.org/10.3758/BF03196724

Cichocki A, Zdunek R, Phan AH, Amari S (2009) Nonnegative matrix and tensor factorizations: applications to exploratory multi-way data analysis and blind source separation. Br J Psychiatry. https://doi.org/10.1192/bjp.112.483.211-a

Cichocki A, Phan AH, Caiafa C, Brain R (2008) Flexible HALS algorithm for sparse non-negative matrix/tensor fatorization. In: IEEE workshop on machine learning for signal processing. IEEE, Cancun, Mexico, pp. 73–78. https://doi.org/10.1109/MLSP.2008.4685458

Cichocki A, Zdunek R, Amari SI (2007) Hierarchical ALS algorithms for nonnegative matrix and 3D tensor factorization. Lecture Notes Computing Science (including Subser. Lect. Notes Artif. Intell. Lect. Notes Bioinformatics) 4666 LNCS, pp 169–176

Clark K, Gregory Appelbaum L, van den Berg B, Mitroff SR, Woldorff MG (2015) Improvement in visual search with practice: Mapping learning-related changes in neurocognitive stages of processing. J Neurosci 35:5351–5359. https://doi.org/10.1523/JNEUROSCI.1152-14.2015

Cohen MX (2014) Analyzing neural time series data: theory and practice. MIT Press, Cambridge

Cole MW, Reynolds JR, Power JD, Repovs G, Anticevic A, Braver TS (2013) Multi-task connectivity reveals flexible hubs for adaptive task control. Nat Neurosci 16:1348–1355. https://doi.org/10.1038/nn.3470

Cong F, He Z, Hämäläinen J, Leppänen PHT, Lyytinen H, Cichocki A, Ristaniemi T (2013a) Validating rationale of group-level component analysis based on estimating number of sources in EEG through model order selection. J Neurosci Methods 212:165–172. https://doi.org/10.1016/j.jneumeth.2012.09.029

Cong F, Kalyakin I, Ahuttunen-Scott T, Li H, Lyytinen H, Ristaniemi T (2010) Single-trial based independent component analysis on mismatch negativity in children. Int J Neural Syst 20:279–292. https://doi.org/10.1142/S0129065710002413

Cong F, Lin QH, Kuang LD, Gong XF, Astikainen P, Ristaniemi T (2015) Tensor decomposition of EEG signals: a brief review. J Neurosci Methods 248:59–69. https://doi.org/10.1016/j.jneumeth.2015.03.018

Cong F, Phan AH, Astikainen P, Zhao Q, Wu Q, Hietanen JK, Ristaniemi T, Cichocki A (2013b) Multi-domain feature extraction for small event-related potentials through nonnegative multi-way array decomposition from low dense array eeg. Int J Neural Syst 23:1–18. https://doi.org/10.1142/S0129065713500068

Cong F, Zhou G, Astikainen P, Zhao Q, Wu Q, Nandi AK, Hietanen JK, Ristaniemi T, Cichocki A (2014) Low-rank approximation based non-negative multi-way array decomposition on event-related potentials. Int J Neural Syst. https://doi.org/10.1142/S012906571440005X

Davies DR, Parasurman R (1982) The psychology of vigilance. Academic Press, New York

Delorme A, Makeig S (2004) EEGLAB: an open source toolbox for analysis of single-trial EEG dynamics including independent component analysis. J Neurosci Methods 134:9–21. https://doi.org/10.1016/j.jneumeth.2003.10.009

Dien J (2010) Evaluating two-step PCA of ERP data with geomin, infomax, oblimin, promax, and varimax rotations. Psychophysiology 47:170–183. https://doi.org/10.1111/j.1469-8986.2009.00885.x

Düzel E, Penny WD, Burgess N (2010) Brain oscillations and memory. Curr Opin Neurobiol 20:143–149. https://doi.org/10.1016/j.conb.2010.01.004

Fries P, Str E (2015) Rhythms for cognition: communication through coherence. Neuron 88:220–235. https://doi.org/10.1016/j.neuron.2015.09.034

Gillberg M, Åkerstedt T (1998) Sleep loss and performance: no "safe" duration of a monotonous task. Physiol Behav 64:599–604. https://doi.org/10.1016/S0031-9384(98)00063-8

Gulbinaite R, van Rijn H, Cohen MX (2014) Fronto-parietal network oscillations reveal relationship between working memory capacity and cognitive control. Front Hum Neurosci 8:1–13. https://doi.org/10.3389/fnhum.2014.00761

Guo Z, Chen R, Liu X, Zhao G, Zheng Y, Gong M, Zhang J (2018) The impairing effects of mental fatigue on response inhibition: an ERP study. PLoS ONE 13:1–18. https://doi.org/10.1371/journal.pone.0198206

Hari R, Salmelin R (1997) Human cortical oscillations: a neuromagnetic view through the skull. Trends Neurosci 20:44–49. https://doi.org/10.1016/S0166-2236(96)10065-5

Harper J, Malone SM, Iacono WG (2017) Theta- and delta-band EEG network dynamics during a novelty oddball task. Psychophysiology 54:1590–1605. https://doi.org/10.1111/psyp.12906

Harshman AR (1970) Foundations of the PARAFAC procedure: models and conditions for an "explanatory" multimodal factor analysis. UCLA Work. Pap. Phonetics, pp 1–84

Hitchcock FL (1927) The expression of a tensor or a polyadic as a sum of products. J Math Phys 6:164–189. https://doi.org/10.1002/sapm192761164

Kurzban R, Duckworth A, Kable JW, Myers J (2013) An opportunity cost model of subjective effort and task performance. Behav Brain Sci 36:661–679. https://doi.org/10.1017/S0140525X12003196

Lim J, Dinges DF (2008) Sleep deprivation and vigilant attention. Ann N Y Acad Sci 1129:305–322. https://doi.org/10.1196/annals.1417.002

Lim J, Wu W, Wang J, Detre JA, Dinges DF, Hengyi R (2010) Imaging brain fatigue from sustained mental workload: an ASL perfusion study of the time-on-task effect. Neuroimage 49:3426–3435. https://doi.org/10.1016/j.neuroimage.2009.11.020

Liu J, Zhang C, Zhu Y, Liu Y (2020a) Dissociable effects of reward on P300 and EEG spectra under conditions of high vs. low vigilance during a selective visual attention task. Front Hum Neurosci. https://doi.org/10.3389/fnhum.2020.00207

Liu J, Zhang C, Zhu Y, Ristaniemi T, Parviainen T, Cong F (2020b) Automated detection and localization system of myocardial infarction in single-beat ECG using Dual-Q TQWT and wavelet packet tensor decomposition. Comput Methods Programs Biomed 184:105120. https://doi.org/10.1016/j.cmpb.2019.105120

Loftus GR, Masson MEJ (1994) Confidence Intervals in within-subject designs. Psychon Bull Rev 1:476–490. https://doi.org/10.3758/BF03210951

Lorist MM, Bezdan E, ten Caat M, Span MM, Roerdink JBTM, Maurits NM (2009) The influence of mental fatigue and motivation on neural network dynamics; an EEG coherence study. Brain Res 1270:95–106. https://doi.org/10.1016/j.brainres.2009.03.015

Lutz A, Slagter HA, Rawlings NB, Francis AD, Greischar LL, Davidson RJ (2009) Mental training enhances attentional stability: neural and behavioral evidence. J Neurosci 29:13418–13427. https://doi.org/10.1523/JNEUROSCI.1614-09.2009

Mackworth NH (1948) The breakdown of vigilance durning prolonged visual search. Q J Exp Psychol 1:6–21. https://doi.org/10.1080/17470214808416738

Maclean KA, Aichele SR, Bridwell DA, Mangun GR, Wojciulik E, Saron CD (2009) Interactions between endogenous and exogenous attention during vigilance. Atten Percept Psychophys 71:1042–1058. https://doi.org/10.3758/APP.71.5.1042

Manly T, Robertson IH, Galloway M, Hawkins K (1999) The absent mind: further investigations of sustained attention to response. Neuropsychologia 37:661–670. https://doi.org/10.1016/S0028-3932(98)00127-4

Mørupa M, Hansena LK (2009) Automatic relevance determination for multi-way models. J Chemom 23:352–363. https://doi.org/10.1002/cem.1223

Newman DP, O'Connell RG, Bellgrove MA (2013) Linking time-on-task, spatial bias and hemispheric activation asymmetry: a neural correlate of rightward attention drift. Neuropsychologia 51:1215–1223. https://doi.org/10.1016/j.neuropsychologia.2013.03.027

O'Neill GC, Tewarie PK, Colclough GL, Gascoyne LE, Hunt BAE, Morris PG, Woolrich MW, Brookes MJ (2017) Measurement

of dynamic task related functional networks using MEG. Neuroimage 146:667–678. https://doi.org/10.1016/j.neuroimage.2016.08.061

Padmala S, Pessoa L (2010) Interactions between cognition and motivation during response inhibition. Neuropsychologia 48:558. https://doi.org/10.1016/j.neuropsychologia.2009.10.017

Pfurtscheller G, Aranibar A (1977) Event-related cortical desynchronization detected by power measurements of scalp EEG. Electroencephalogr Clin Neurophysiol 42:817–826. https://doi.org/10.1016/0013-4694(77)90235-8

Pfurtscheller G, Lopes Da Silva FH (1999) Event-related EEG/MEG synchronization and desynchronization: basic principles. Clin Neurophysiol 110:1842–1857. https://doi.org/10.1016/S1388-2457(99)00141-8

Quentin R, King JR, Sallard E, Fishman N, Thompson R, Buch ER, Cohen LG (2019) Differential brain mechanisms of selection and maintenance of information during working memory. J Neurosci 39:3728–3740. https://doi.org/10.1523/JNEUROSCI.2764-18.2019

Reteig LC, van den Brink RL, Prinssen S, Cohen MX, Slagter HA (2019) Sustaining attention for a prolonged period of time increases temporal variability in cortical responses. Cortex 117:16–32. https://doi.org/10.1016/j.cortex.2019.02.016

Rosenberg MD, Finn ES, Scheinost D, Papademetris X, Shen X, Constable RT, Chun MM (2016) A neuromarker of sustained attention from whole-brain functional connectivity. Nat Neurosci 19:165–171. https://doi.org/10.1038/nn.4179

Sanada M, Ikeda K, Kimura K, Hasegawa T (2013) Motivation enhances visual working memory capacity through the modulation of central cognitive processes. Psychophysiology 50:864–871. https://doi.org/10.1111/psyp.12077

Sauseng P, Hoppe J, Klimesch W, Gerloff C, Hummel FC (2007) Dissociation of sustained attention from central executive functions: local activity and interregional connectivity in the theta range. Eur J Neurosci 25:587–593. https://doi.org/10.1111/j.1460-9568.2006.05286.x

See JE, Howe SR, Warm JS, Dember WN (1995) Meta-analysis of the sensitivity decrement in vigilance. Psychol Bull 117:230–249. https://doi.org/10.1037/0033-2909.117.2.230

Seli P, Cheyne JA, Xu M, Purdon C, Smilek D (2015) Motivation, intentionality, and mind wandering: implications for assessments of task-unrelated thought. J Exp Psychol Learn Mem Cogn 41:1417–1425. https://doi.org/10.1037/xlm0000116

Slagter HA, Prinssen S, Reteig LC, Mazaheri A (2016) Facilitation and inhibition in attention: functional dissociation of pre-stimulus alpha activity, P1, and N1 components. Neuroimage 125:25–35. https://doi.org/10.1016/j.neuroimage.2015.09.058

Stam CJ, Nolte G, Daffertshofer A (2007) Phase lag index: assessment of functional connectivity from multi channel EEG and MEG with diminished bias from common sources. Hum Brain Mapp 28:1178–1193. https://doi.org/10.1002/hbm.20346

Sun Y, Lim J, Kwok K, Bezerianos A (2014) Functional cortical connectivity analysis of mental fatigue unmasks hemispheric asymmetry and changes in small-world networks. Brain Cogn 85:220–230. https://doi.org/10.1016/j.bandc.2013.12.011

Taya F, Dimitriadis SI, Dragomir A, Lim J, Sun Y, Wong KF, Thakor NV, Bezerianos A (2018) Fronto-parietal subnetworks flexibility compensates for cognitive decline due to mental fatigue. Hum Brain Mapp 39:3528–3545. https://doi.org/10.1002/hbm.24192

Taylor MM, Creelman CD (1967) PEST: efficient estimates on probability functions. J Acoust Soc Am 41:782–787. https://doi.org/10.1121/1.1910407

Tenke CE, Kayser J (2005) Reference-free quantification of EEG spectra: combining current source density (CSD) and frequency principal components analysis (fPCA). Clin Neurophysiol 116:2826–2846. https://doi.org/10.1016/j.clinph.2005.08.007

Thomson DR, Besner D, Smilek D (2015) A resource-control account of sustained attention: evidence from mind-wandering and vigilance paradigms. Perspect Psychol Sci 10:82–96. https://doi.org/10.1177/1745691614556681

Thut G, Nietzel A, Brandt SA, Pascual-Leone A (2006) α-Band electroencephalographic activity over occipital cortex indexes visuospatial attention bias and predicts visual target detection. J Neurosci 26:9494–9502. https://doi.org/10.1523/JNEUROSCI.0875-06.2006

Vidaurre D, Hunt LT, Quinn AJ, Hunt BAE, Brookes MJ, Nobre AC, Woolrich MW (2018) Spontaneous cortical activity transiently organises into frequency specific phase-coupling networks. Nat Commun. https://doi.org/10.1038/s41467-018-05316-z

Vigário R, Oja E (2008) BSS and ICA in neuroinformatics: from current practices to open challenges. IEEE Rev Biomed Eng 1:50–61. https://doi.org/10.1109/RBME.2008.2008244

Vinck M, Oostenveld R, Van Wingerden M, Battaglia F, Pennartz CMA (2011) An improved index of phase-synchronization for electrophysiological data in the presence of volume-conduction, noise and sample-size bias. Neuroimage 55:1548–1565. https://doi.org/10.1016/j.neuroimage.2011.01.055

Worden MS, Foxe JJ, Wang N, Simpson GV (2000) Anticipatory biasing of visuospatial attention indexed by retinotopically specific alpha-band electroencephalography increases over occipital cortex. J Neurosci 20:1–6. https://doi.org/10.1523/jneurosci.20-06-j0002.2000

Zabielska-Mendyk E, Francuz P, Jaśkiewicz M, Augustynowicz P (2018) The effects of motor expertise on sensorimotor rhythm desynchronization during execution and imagery of sequential movements. Neuroscience 384:101–110. https://doi.org/10.1016/j.neuroscience.2018.05.028

Zhu Y, Liu J, Mathiak K, Ristaniemi T, Cong F (2019) Deriving electrophysiological brain network connectivity via tensor component analysis during freely listening to music. IEEE Trans. Neural Syst. Rehabil. Eng. https://doi.org/10.1109/TNSRE.2019.2953971

Zhu Y, Liu J, Ye C, Mathiak K, Astikainen P, Ristaniemi T, Cong F (2020a) Discovering dynamic task-modulated functional networks with specific spectral modes using MEG. Neuroimage. https://doi.org/10.1016/j.neuroimage.2020.116924

Zhu Y, Zhang C, Poikonen H, Toiviainen P, Huotilainen M, Mathiak K, Ristaniemi T, Cong F (2020b) Exploring frequency-dependent brain networks from ongoing EEG using spatial ICA during music listening. Brain Topogr 33:289–302. https://doi.org/10.1007/s10548-020-00758-5

III

AUTOMATED DETECTION AND LOCALIZATION SYSTEM OF MYOCARDIAL INFARCTION IN SINGLE-BEAT ECG USING DUAL-Q TQWT AND WAVELET PACKET TENSOR DECOMPOSITION

by

Jia Liu, Chi Zhang, Yongjie Zhu, Tapani Ristaniemi, Tiina Parviainen, Fengyu Cong, 2020

Computer methods and programs in biomedicine

DOI: 10.1016/j.cmpb.2019.105120

Computer Methods and Programs in Biomedicine 184 (2020) 105120

Contents lists available at ScienceDirect

Computer Methods and Programs in Biomedicine

journal homepage: www.elsevier.com/locate/cmpb

Automated detection and localization system of myocardial infarction in single-beat ECG using Dual-Q TQWT and wavelet packet tensor decomposition

Jia Liu[a,b], Chi Zhang[a], Yongjie Zhu[a,b], Tapani Ristaniemi[b], Tiina Parviainen[c], Fengyu Cong[a,b,*]

[a] School of Biomedical Engineering, Faculty of Electronic Information and Electrical Engineering, Dalian University of Technology, Dalian, China
[b] Faculty of Information Technology, University of Jyvaskyla, Jyvaskyla, 40014, Finland
[c] Centre for Interdisciplinary Brain Research, Department of Psychology, Faculty of Education and Psychology, University of Jyvaskyla, Jyvaskyla, 40014, Finland

ARTICLE INFO

Article history:
Received 13 August 2019
Revised 3 October 2019
Accepted 3 October 2019

Keywords:
Electrocardiogram (ECG)
Myocardial infarction (MI)
Dual-Q tunable Q-factor wavelet transformation (Dual-Q TQWT)
Discrete wavelet packet transform (DWPT)
Multilinear principal component analysis (MPCA)

ABSTRACT

Background and objective: It is challenging to conduct real-time identification of myocardial infarction (MI) due to artifact corruption and high dimensionality of multi-lead electrocardiogram (ECG). In the present study, we proposed an automated single-beat MI detection and localization system using dual-Q tunable Q-factor wavelet transformation (Dual-Q TQWT) denoising algorithm.

Methods: After denoising and segmentation of ECG, a fourth-order wavelet tensor (leads × subbands × samples × beats) was constructed based on the discrete wavelet packet transform (DWPT), to represent the features considering the information of inter-beat, intra-beat, inter-frequency, and inter-lead. To reduce the tensor dimension and preserve the intrinsic information, the multilinear principal component analysis (MPCA) was employed. Afterward, 84 discriminate features were fed into a classifier of bootstrap-aggregated decision trees (Treebagger). A total of 78 healthy and 328 MI (6 types) records including 57557 beats were chosen from PTB diagnostic ECG database for evaluation.

Results: The validation results demonstrated that our proposed MI detection and localization system embedded with Dual-Q TQWT and wavelet packet tensor decomposition outperformed commonly used discrete wavelet transform (DWT), empirical mode decomposition (EMD) denoising methods and vector-based PCA method. With the Treebagger classifier, we obtained an accuracy of 99.98% in beat level and an accuracy of 97.46% in record level training/testing for MI detection. We also achieved an accuracy of 99.87% in beat level and an accuracy of 90.39% in record level for MI localization.

Conclusion: Altogether, the automated system brings potential improvement in automated detection and localization of MI in clinical practice.

1. Introduction

Myocardial infarction (MI) is defined as myocardial cell death due to prolonged ischemia [1]. As one of the main causes of death and disability, MI is an intractable disease and can result in artery disease. In clinical practice, many techniques, including electrocardiographic (ECG), biochemical markers, imaging and so on, are used to assist in the diagnosis of MI. Among these techniques, the non-invasive ECG, an economic tool, is widely used in MI detection [2,3]. The ECG abnormalities of MI can be observed in the PR segment, the QRS complex, the ST segment or the T wave [1]. However, the diagnosis of MI usually requires multiple ECGs because the ECG signals are time-varying in nature with small amplitude. Manual inspection in clinical practice is not only time-consuming and strenuous but also leads to inter- and intra-evaluator variability [4,5]. Therefore, a computer-aided diagnosis system (CADS) of MI should be developed to realize time-saving and reliable analysis [6–11].

Good quality ECG is a guarantee of reliable CADS, while the ECG signals are often corrupted by noise [12]. The ECG signals are usually mixed with different kinds of artifacts, such as power line interference, muscle artifacts, and baseline drifts. Therefore, it is necessary to remove artifacts by implanting denoising method in CADS. In [13], Fatin and colleagues removed the low frequency 0–0.351 Hz and high frequency >45 Hz from ECG with 6-level

* Corresponding author at: School of Biomedical Engineering, Dalian University of Technology, Dalian, China.
E-mail addresses: jialiu15@foxmail.com (J. Liu), cong@dlut.edu.cn (F. Cong).

https://doi.org/10.1016/j.cmpb.2019.105120
0169-2607/

db6 discrete wavelet transform (DWT) decomposition in arrhythmia recognition. However, the DWT fails to separate the noise from ECG when two types of signals co-occur at the same frequency band. According to the nature of waveforms in ECG, the morphological-based algorithm should be considered in ECG denoising. Blanco-Velasco et al. [14] applied the empirical mode decomposition (EMD), in which partial intrinsic mode functions (IMFs) were reconstructed to remove noise mixed with ECG from the MIT-BIH database. Although EMD has been widely used in ECG denoising, it still leads to the mode-mixing problem [15]. Therefore, it is challenging to find an effective denoising method to obtain high signal-noise-ratio (SNR) ECG signal. Dual-Q tunable Q-factor wavelet transformation (Dual-Q TQWT), a morphological-based algorithm, was first introduced in [16–18]. Although Dual-Q TQWT is applied to speech analysis [16], limited attention has been focused on ECG denoising until now. Using the resonance-based morphological separation, the Dual-Q TQWT might provide new sight for ECG denoising. In our study, we applied the Dual-Q TQWT as a denoising method in MI detection and localization system.

Feature extraction plays an important role in CADS. Recent studies have developed effective feature extraction methods in automated MI detection and localization system, as shown in Table 5. In [10], a multiscale energy and eigenspace approach was proposed based on DWT. The approach obtained an accuracy of 99.58% in MI localization with 72 features from frame-based (4 beats) ECG. Sun et al. [7] presented a multiple instance learning for MI detection system based on time-domain features of ST segments and R-R intervals from ECG. Their method obtained a sensitivity of 92.6% in single-beat MI detection with 74 features. Similarly, 36 time-domain features of Q wave, T wave, and ST level elevation were extracted in [3]. They achieved an accuracy of 98.3% in single-beat MI detection. In addition to linear time-domain features, Acharya et al. [11] calculated 12 types of nonlinear features covering different types of entropy, fractal dimension, and Lyapunov exponent. They obtained an accuracy of 98.8% in MI detection with 47 features based on single-beat and single-lead ECG. However, it is still challenging to propose efficient and low complexity feature extraction approaches to extract discriminate and generalization features. The tensor decomposition, different from other state-of-art feature extraction methods, can directly exploit multi-mode information contained in the tensor structure. Using tensor decomposition, the information of inter-lead, inter-beat, intra-beat, and inter-frequency can be considered as parameters. Especially, considering the lead of ECG as a parameter instead of manual selection can avoid under-fitting (single-lead) or over-fitting (12-lead). Sibasankar et al. [8] developed a third-order tensor method (leads × beats × samples) for MI detection and localization, but they failed to achieve high performance in single-beat ECG based on DWT. In their study, they selected discriminant features from different tensor modes in different wavelet coefficients of DWT with visual observation, impeding the precise frequency and automated data-driven analysis. In contrast, the discrete wavelet packet transform (DWPT) has these advantages: each layer has an equal number of wavelet packet coefficients; the last layer can cover all the frequency subbands. These advantages provide the possibility of fourth-order tensor formation.

In our present study, we presented an automated MI detection and localization system equipped with Dual-Q TQWT denoising method and fourth-order wavelet packet tensor (leads × subbands × samples × beats). The tensor-based MPCA was applied to reduce the dimensionality of the wavelet packet tensor. The optimal features were classified by a classifier of bootstrap-aggregated decision trees (Treebagger). In our system, the MI detection, a two-class classifier, is used to distinguish MI patients from healthy volunteers for preliminary screening. The MI localization, a multi-class classifier, is a progressive diagnosis for different types of MI patients. The two-step MI classification is precise and resource efficient in practice. The PTB diagnostic ECG database was chosen for system evaluation.

Table 1
Numbers of records and beats from different groups.

Type	AMI	ALMI	IMI	ASMI	ILMI	IPLMI	H
Records	46	42	89	76	56	19	78
Beats	6306	6568	12,115	11,232	8280	2714	10,342

2. Database

The ECG signals were chosen from the Physikalisch-Technische Bundesanstalt (PTB) [19] diagnostic ECG database provided by PhysioBank [20]. A total of 549 records from 290 subjects (mean age = 57.2 years, 209 men) were collected in the Department of Cardiology of University Clinic Benjamin Franklin in Berlin, Germany. Each record contains 12 conventional leads (I, II, III, AVR, AVL, AVF, V1, V2, V3, V4, V5, V6) and 3 Frank leads (VX, VY, VZ) ECG, which were digitized at 1000 Hz with 16 bit resolution over a range of ±16.384 mV. According to the clinical statistics, 268 subjects' data, including eight different heart disease groups (216) and one healthy group (52), were provided in the database. Among these groups, the myocardial infarction group diagnosed as six different MIs (anterior: AMI, anterior-lateral: ALMI, inferior: IMI, anterior-septal: ASMI, inferior-lateral: ILMI, inferior-posterior-lateral: IPLMI) and the healthy group (H) were chosen for MI detection and localization evaluation in the present study. The numbers of records and beats from MI patients and healthy volunteers were listed in Table 1.

3. Methods

The present study presented a novel MI detection and localization system using Dual-Q TQWT denoising method and wavelet packet tensor decomposition. The diagram of detection and localization system is shown in Fig. 1. For the preprocessing stage, ECG data were down-sampled to 250 Hz and filtered with 1000-order 0.5 Hz high-pass and 40 Hz low-pass FIR filters implanted in EEGLAB [21]. Furthermore, a mean value was subtracted from each lead to eliminate the offset effect [22]. The Dual-Q TQWT, apart from the conventional methods, was applied to ECG denoising.

3.1. Denoising with Dual-Q TQWT

The Dual-Q TQWT is a resonance-based, rather than a frequency or scale based signal decomposition algorithm, which utilizes sparse signal representations and morphological component analysis (MCA) [18]. Using this method, a signal can be decomposed into the sum of a high-resonance component and a low-resonance component. Each component is represented sparsely by TQWT algorithm with high Q-factor and low Q-factor.

TQWT is a discrete wavelet transform with flexible Q-factor [17]. Three parameters: Q-factor (Q), the redundancy (r), and decomposition level (J) should be set during TWQT decomposition. The frequency responses and wavelets of different parameters are displayed in Fig. 2. The parameter Q is related to oscillation numbers of wavelet, and the parameter r is an index of the overlapping between adjacent frequency responses. All three parameters are closely related. TQWT is developed as J level of two-channel filter banks attaching to low-pass filter output, resulting in $J+1$ subbands. The low- pass ($H_0^{(j)}(w)$) and high-pass ($H_1^{(j)}(w)$) filters

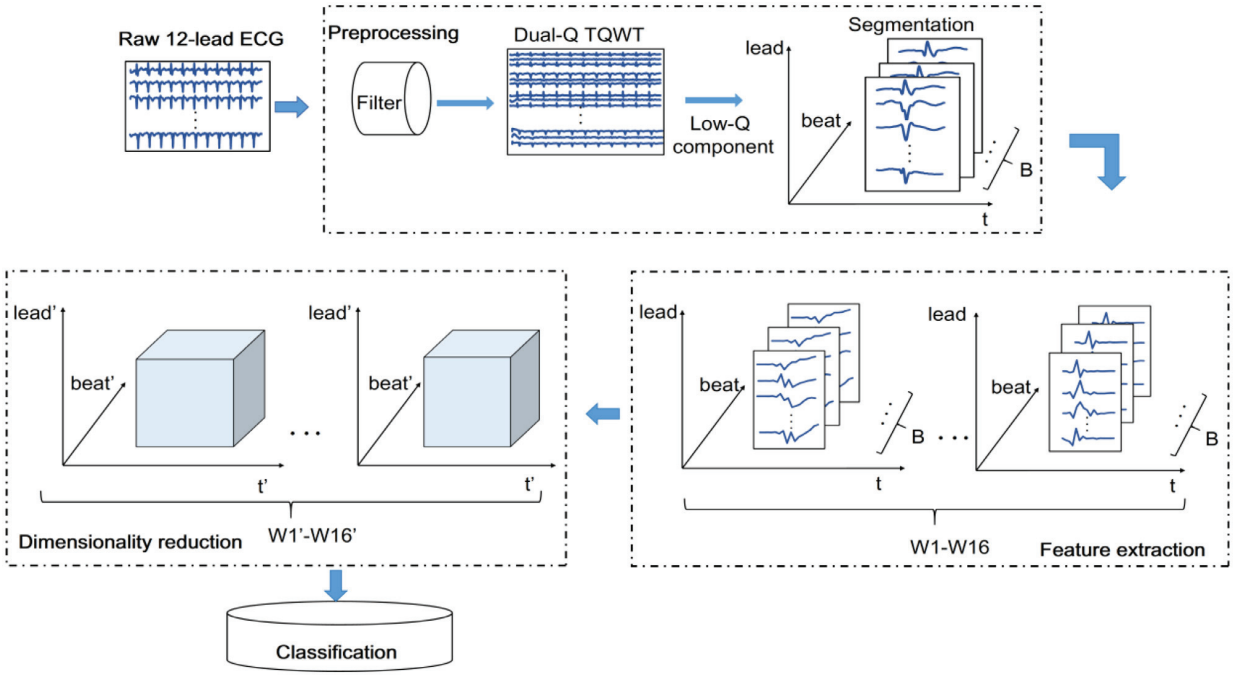

Fig. 1. Schematic diagram of MI detection and localization system.

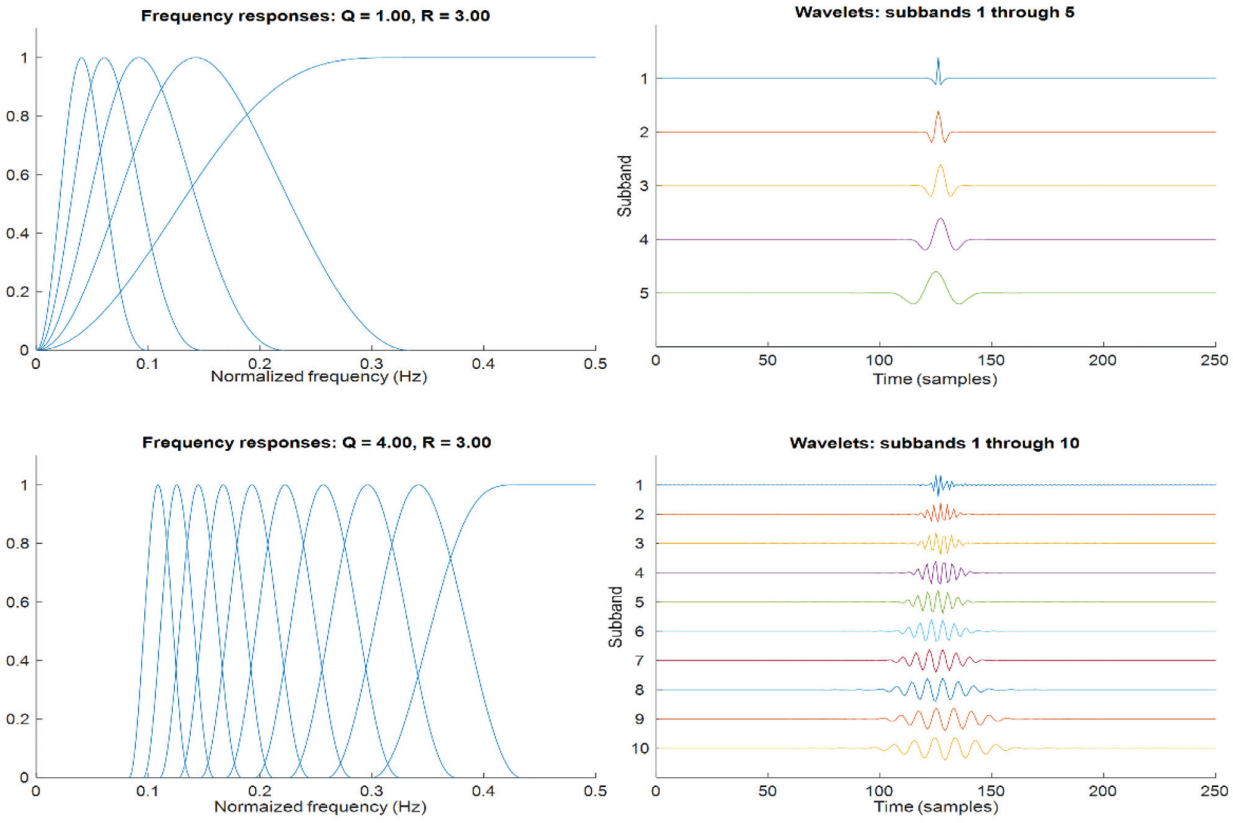

Fig. 2. Frequency responses and wavelets of TQWT with $Q=1$, $J=4$ (top) and $Q=4$, $J=9$ (down).

are defined as:

$$H_0^{(j)}(w) = \begin{cases} \prod_{m=0}^{j-1} H_0\left(\frac{w}{\alpha^m}\right), & |w| \le \alpha^j \pi \\ 0, & \alpha^j \pi < |w| \le \pi \end{cases} \quad (1)$$

$$H_1^{(j)}(w) = \begin{cases} H_1\left(\frac{w}{\alpha^{j-1}}\right) \prod_{m=0}^{j-2} H_o^j\left(\frac{w}{\alpha^m}\right), & (1-\beta)\alpha^{j-1}\pi \le |w| \le \alpha^{j-1}\pi \\ 0, & for\ others\ w \in [-\pi\ \pi] \end{cases} \quad (2)$$

where low-pass scaling $\alpha \le 1$, and high-pass scaling $\beta \le 1$. The parameters Q and r are given by:

$$r = \frac{\beta}{1-\alpha} \quad (3)$$

$$Q = \frac{f_c}{BW} = \frac{2-\beta}{\beta} \quad (4)$$

where BW and f_c are the bandwidth and center frequency, respectively.

Given a signal $\mathbf{x}$, Dual-Q TQWT decomposes $\mathbf{x}$ into $\mathbf{x_1}$ and $\mathbf{x_2}$ components, where $\mathbf{x_1}$ consists largely of oscillations and $\mathbf{x_2}$ consists largely of transients. The $\mathbf{x}$ is the sum of $\mathbf{x_1}$ and $\mathbf{x_2}$. Using TQWT, x can be denoted as $TQWT_1$ and $TQWT_2$ with high and low Q-factors. The constrained optimization problem can be represented as [16]:

$$argmin_{\boldsymbol{w}_1, \boldsymbol{w}_2} \sum_{j=1}^{J1+1} \lambda_{1,j} \left\| \boldsymbol{w}_{1,j} \right\|_1 + \sum_{j=1}^{J2+1} \lambda_{2,j} \left\| \boldsymbol{w}_{2,j} \right\|_1 \quad (5)$$

$$\mathbf{x} = \mathbf{x}_1 + \mathbf{x}_2 = \mathrm{TQWT}_1{}^{-1}(\boldsymbol{w}_1) + \mathrm{TQWT}_2{}^{-1}(\boldsymbol{w}_2) \quad (6)$$

where $\boldsymbol{w}_{i,j}$ denotes subband j of TQWT_i for $i = 1,2$. The λ_1 and λ_2, computed from the norms of wavelets based on the mentioned three parameters in TQWT, are the regularization parameters for high and low Q-factor TQWT. The MCA [23] based on split augmented Lagrangian shrinkage algorithm (SALSA) [24] is applied to estimate the solution of the optimization problem. The six parameters, Q_1, r_1, J_1 for high Q-factor TQWT and Q_2, r_2, J_2 for low Q-factor TQWT, should be preset considering the mathematical theory of TQWT, ECG morphology, running time, and goodness-of-fit. To prevent an excessive ringing of wavelets, the parameter r should be set as greater than or equal to 3 [9,25]. In our study, the parameters r_1 and r_2 are equal to 3, consistent with literature studies [25,26]. The low factor Q_2 is usually set to 1 [16], while the high factor Q_1 is set to 4 in our work. The parameters J is set as half of the maximum of $J_{\max}$ with $J_1 = 10$, $J_2 = 25$ because low J cannot cover the signal and high J leads to high dimension computations [27–29].

$$J_{max} = \left\lceil \frac{\log(\beta N - 8)}{log(1-\alpha)} \right\rceil \quad (7)$$

where N is the number of samples of ECG signal.

After filtering and denoising, the ECG signals were segmented into beats based on R-peak, detected by the Pan-Tompkins algorithm [30]. Each beat has 162 samples including 250 ms before and 400 ms after R-peak detection. A total of 57,557 ECG beats were obtained from 6 types of MI groups and 1 healthy group, as shown in Table 1.

3.2. Feature extraction by DWPT

The discrete wavelet packet transform (DWPT) has been successfully used in ECG feature extraction [31]. Compared with the DWT, the DWPT provides more spectral information in detail. Let $\mathbf{S} = [\mathbf{s}_1, \mathbf{s}_2, \ldots, \mathbf{s}_v]$ be a 12-lead ECG beat of one subject, where $v = 12$ leads, $Ls = 162$ samples, $S \in R^{Ls \times v}$. In the DWPT, both the approximation and detail coefficients are decomposed in each level, resulting in 2^j subbands at J^{th} level decomposition. The sample length of the sub-band at j level is ls, where $ls \cong Ls/2^j$. In our study, the preprocessed ECG beats were subjected to 4 levels of DWPT using db4 mother wavelet to extract concise and distinctive features. We chose 16 subbands at the 4th decomposition level covering all the frequency bands, each of which contained specific characteristics. The 16 subbands have the same number of coefficients (16 samples), which provides good feasibility for wavelet packet tensor decomposition analysis. The wavelet packet coefficient matrix extracted from 12-lead m^{th} beat is converted into wavelet packet tensor $\mathcal{W}_m \in \boldsymbol{R}^{I_1 \times I_2 \times I_3}$, where the modes of I_1, I_2, I_3 are the 12-lead of ECG, the 16 subbands of DWPT at 4th level, and the 16 samples of each subband. Hence, a total of B wavelet packet tensors from all subjects are represented as $\mathcal{W} = [\mathcal{W}_1, \mathcal{W}_2, \ldots, \mathcal{W}_m, \ldots, \mathcal{W}_B]$, where $m = 1, 2, \ldots, B$.

3.3. Dimensionality reduction by MPCA

In the view of the high dimensionality of wavelet packet tensor, it is necessary to reduce the dimensionality of discriminate features to obtain a good performance of pattern recognition and to improve processing speed with less memory capacity. Compared with vector-based dimensionality reduction algorithm of principal component analysis (PCA), the multilinear principal component analysis (MPCA) can be applied to a tensor object for feature extraction and dimensionality reduction [32,33]. Although MPCA is widely used in other fields, such as gait recognition [32] and face recognition [34], the application in multivariate time series has not been promoted [31,35].

The MPCA is realized following 4 steps [32]. First, the data are preprocessd by centralizing the input samples. Second, data are initialized by calculating the eigen-decomposition of the eigenvectors corresponding to the most significant eigenvalues. The input of MPCA are wavelet packet tensors of B beats, $\in \boldsymbol{R}^{I_1 \times I_2 \times I_3 \times B}$. Using a multilinear transformation $\{\tilde{\mathbf{U}}^{(n)} \in \mathrm{R}^{I_n \times I_n'},\ I_n' \le I_n,\ n = 1, 2, \ldots, N,\ N = 3\}$, where the $\tilde{\mathbf{U}}^{(n)}$ is the n^{th} projection matrix, the input tensor $\boldsymbol{R}^{I_1 \times I_2 \times I_3}$ of each beat $\mathcal{W}_m$ can be mapped onto a low dimensionality tensor space $\boldsymbol{R}^{I_1' \times I_2' \times I_3'}$ to extract optimal features. The low dimensionality output of MPCA with maximum captured variation is represented as:

$$\mathcal{Y}_m = \mathcal{W}_m \times \tilde{\mathbf{U}}^{(1)^T} \times_2 \tilde{\mathbf{U}}^{(2)^T} \times_3 \tilde{\mathbf{U}}^{(3)^T} \quad (8)$$

where $\mathcal{Y}_m \in \boldsymbol{R}^{I_1' \times I_2' \times I_3'}$, B beats of outputs are $\mathcal{Y} = [\mathcal{Y}_1, \mathcal{Y}_2, \ldots, \mathcal{Y}_m, \ldots, \mathcal{Y}_B]$, $\mathcal{Y} \in \boldsymbol{R}^{I_1' \times I_2' \times I_3' \times B}$. The realization of dimension reduction can be simplified as an optimal problem:

$$\left\{\tilde{\mathbf{U}}^{(n)^T},\ n = 1,\ 2,\ 3\right\} = argmax_{\tilde{\mathbf{U}}^{(1)},\ \tilde{\mathbf{U}}^{(2)},\ \tilde{\mathbf{U}}^{(3)}}\ \psi_{\mathcal{Y}} \quad (9)$$

where $\psi_{\mathcal{Y}}$ is the total of B transformed tensor scatters, and $\psi_{\mathcal{Y}} = \sum_{m=1}^{B} \|\mathcal{Y}_m - \tilde{\mathcal{Y}}\|_F^2$, where the $\tilde{\mathcal{Y}} = (\sum_{m=1}^{B} \mathcal{Y}_m)/B$. Based on the solution of Eq. (8), the scatter of n-mode unfolding matrix is given by:

$$\boldsymbol{\Phi}^{(n)} = \sum\nolimits_{m=1}^{B} \left(\mathbf{W}_m^{(n)} - \tilde{\mathbf{W}}_m^{(n)}\right) \cdot \tilde{\mathbf{U}}_{\boldsymbol{\Phi}(n)} \cdot \tilde{\mathbf{U}}^T{}_{\boldsymbol{\Phi}(n)} \left(\mathbf{W}_m^{(n)} - \tilde{\mathbf{W}}_m^{(n)}\right)^T \quad (10)$$

Where $\mathbf{W}_m^{(n)}$ is the n-mode unfolding matrix of the tensor $\mathcal{W}_m$, and $\tilde{\mathbf{U}}_{\Phi(n)}$ can be evaluated as:

$$\tilde{\mathbf{U}}_{\Phi(n)} = \tilde{\mathbf{U}}^{(n+1)} \otimes \tilde{\mathbf{U}}^{(n+2)} \otimes \ldots \otimes \tilde{\mathbf{U}}^{(N)} \otimes \tilde{\mathbf{U}}^{(1)} \otimes \tilde{\mathbf{U}}^{(2)} \ldots \otimes \tilde{\mathbf{U}}^{(n-1)} \quad (11)$$

where $\otimes$ is the Kronecker product. The optimization step is solved using the Eqs. (10) and (8) in the iteration. Finally, the high-dimensional data are projected into low-dimensionality tensor space.

3.4. Classification

The optimal features extracted from MPCA were fed into a classifier. As a decision support tool, the decision tree (DT) utilizes a tree-like model of decisions and possible consequences. It is a directed graph, with three sets of decision, chance, and terminal nodes (also known as leaves) [36]. A DT, equipped with two functions of denoting payoffs and probabilities, can be learned in a recursive partitioning manner based on an attribute value test. Although DT has an advantage of simplicity, it is unstable and easily affected by noise. The Bootstrap-aggregated, one of the most popular techniques for constructing ensembles to improve the robustness, takes base DT learner and invokes it many times with replacement samples [37]. As an important parameter of Treebagger, the number of trees can reach several hundreds or thousands depending on the nature of the training sets. By taking the majority votes or averaging predictions of different DTs, the Treebagger leads to better performance than a DT.

In our study, the performance of classifiers was measured by sensitivity (SE), specificity (SP), and accuracy (ACC) [38]. Based on the confusion matrix obtained from predicted class and actual class, the SE, SP, and ACC are evaluated as:

$$\mathrm{SE} = \frac{\mathrm{TP}}{\mathrm{TP} + \mathrm{FN}} \tag{12}$$

$$\mathrm{SP} = \frac{\mathrm{TN}}{\mathrm{TN} + \mathrm{FP}} \tag{13}$$

$$\mathrm{ACC} = \frac{\mathrm{TP} + \mathrm{TN}}{\mathrm{TP} + \mathrm{TN} + \mathrm{FP} + \mathrm{FN}} \tag{14}$$

where TP, TN, FP, and FN correspond to true positive, true negative, false positive, and false negative. The ROC (receiver operating characteristics) was also adopted to visualize the performance of classifiers [39].

4. Results and discussion

Using 78 healthy and 328 MI records chosen from the PTB ECG database, the novel detection and localization system of MI with Dual-Q TQWT and wavelet packet tensor decomposition proposed in our work were evaluated. First, we evaluated the performance of these algorithms in our system. According to the good performance of the algorithms, we distinguished the MI patients from healthy volunteers with single-beat ECG. Furthermore, each specific MI patient was localized at one of 6 different MI types. Finally, our automated MI detection and localization system was compared with earlier published studies.

4.1. ECG denoising and MPCA evaluation

Based on high and low Q-factors wavelets and frequency responses, as shown in Fig. 2, Dual-Q TQWT decomposes the filtered ECG signal into the sum of a high Q-factor component and a low Q-factor component. Fig. 3 displays the decomposition results consisting of original and resonance waveforms. From this figure, we found that the high Q-factor component corresponded to sustained oscillations, consisting of low- and high-frequency bands unrelated to typical morphology of ECG (e.g. PR segment, QRS waveform, et al.). In contrast, the low Q-factor component corresponded to the transients following the morphology of the original waveform, with high signal-noise-ratio (SNR). Due to the characteristics of morphological segments and high SNR, the low Q-factor component was chosen for further processing. The denoised data were segmented into beats and decomposed into 4-level DWPT to extract features. Using 16 subbands in the fourth level, a wavelet packet tensor (leads × subbands × samples × beats) was formed. In our work, the MPCA was applied to wavelet packet tensor for dimensionality reduction. Compared with the vector-based PCA, the tensor-based MPCA could reserve inherent properties of features.

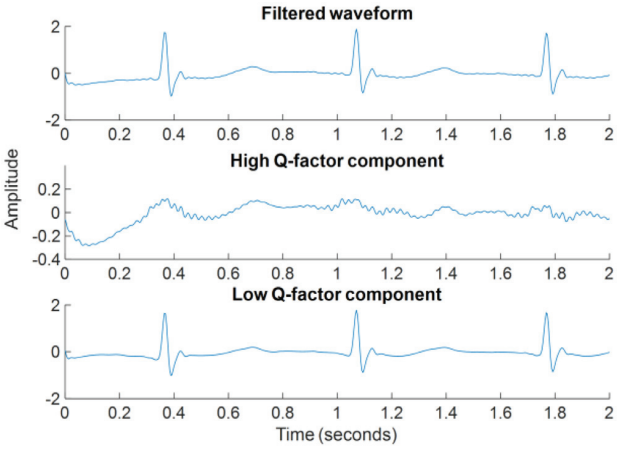

Fig. 3. Resonance decomposition with Dual-Q TQWT.

Table 2
Comparisons among denoising methods.

	Filtered	Dual-Q TQWT	DWT	EMD
ACC	83.64%	91.36%	89.89%	91.28%
SEN	96.73%	98.27%	97.98%	98.26%
SPE	83.74%	91.36%	89.89%	91.27%
Time(s)	-	45.63	2.98	225.89

To illustrate the performance of the denoising algorithm, we compared the Dual-Q TQWT with commonly used denoising methods discrete wavelet transform (DWT) [13] and empirical mode decomposition (EMD) [13]. Based on the data from healthy volunteers and 5 groups of MI (without IPLMI), the performance of a multi-class classifier of Treebagger in the record level was chosen as criteria of these comparisons. The comparison results are illustrated in Table 2. The results demonstrate that the performance of denoising methods outperforms filter processing. Compared with the state-of-art denoising methods (DWT and EMD), our proposed Dual-Q TQWT is comparable considering the running time (s/record) and performance. The good results validate the utility of Dual-Q TQWT denoising in MI detection and localization system.

For wavelet packet coefficients, we compared the results of WPT-Tensor and WPT-Vector (by reshaping wavelet packet tensor to vector). WPT-Vector achieved an accuracy, a sensitivity, and a specificity of 88.73%, 97.75%, and 88.75%, respectively. We also computed the performance of Dual-Q TQWT time-domain features without DWPT and obtained an accuracy, a sensitivity, and a specificity of 81.24%, 91.56%, and 80.95%, respectively. Altogether, the combination of Dual-Q TQWT + DWPT + MPCA yielded the highest performance compared with Dual-Q TQWT + DWPT + PCA and Dual-Q TQWT + MPCA.

4.2. Physiological ECG features from DWPT and MPCA

By applying DWPT, we extracted spatial, spectral, and temporal features from leads, frequency bands (subbands), and samples. Fig. 4 displays the physiological ECG waveforms in subbands 1–4 (significant variation of features) from 12 leads. We found that the waveforms in different subbands and leads were different in 6 types of MI patients and healthy volunteers. The abnormalities of MI could be displayed in the PR segment, the QRS complex, the ST segment, and the T wave in different subbands.

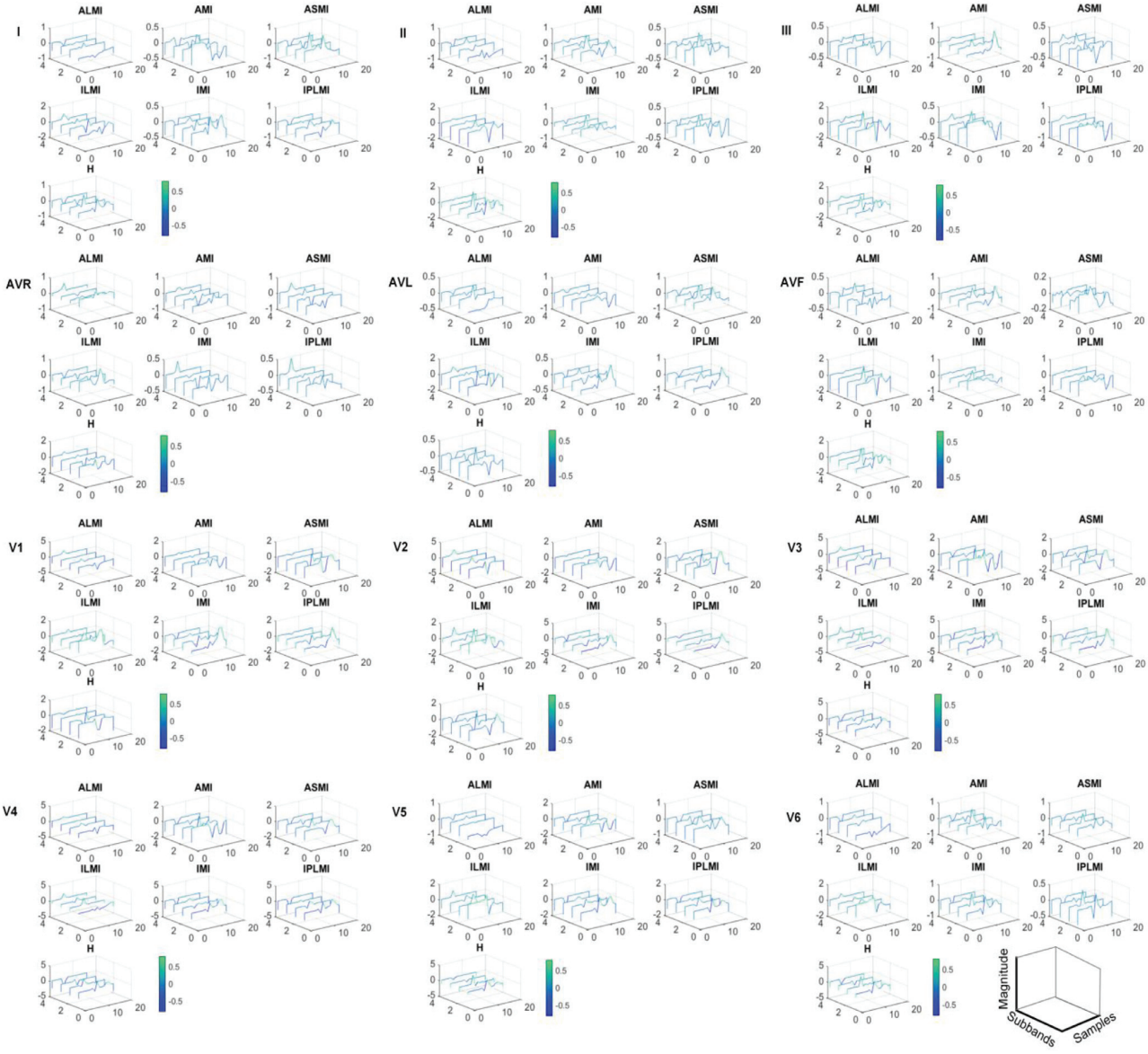

Fig. 4. DWPT features extracted from leads, sunbands, and samples of MI patients and healthy volunteers.

Although DWPT features are significantly different in different types of MI and healthy volunteers, as shown in Fig. 4, there is too much redundancy information in the fourth-order wavelet packet tensor. The wavelet packet tensor was subjected to MPCA and was reduced to low-dimensional tensor using matrices of multilinear projection. Fig. 5 displays three projection matrices in three modes. According to multilinear projection, we found four components in the spatial factor, which illustrated the multilinear combination of 12 leads. For the spectral factor, we found three components, especially subbands 1, 2, and 4, which were most important in MI identification. Each subband covers about 8 Hz from 0.5–125 Hz. Seven waveforms in the temporal factor were the representations of the PR segment, the QRS complex, the ST segment, and the T wave. The discriminant features of different types of MI patients and healthy volunteers are located in 4 components of spatial factor, 3 components of spectral factor, and 7 components of temporal factor.

4.3. MI detection

The MI detection was treated as a two-class classification, distinguishing the MI patients from healthy volunteers. There were 47,215 instances (heart beats) from 328 MI records and 10,342 instances from 78 healthy records. The dimensions (12 leads $\times$ 16 subbands $\times$ 16 samples $\times$ 57,557 beats) of wavelet packet tensor were reduced to low-dimension space of $4 \times 3 \times 7 \times 57{,}557$ beats by MPCA, where 90% energy was kept and the maximum number of interaction was set as 1. A total of 84 maximum optimal features were selected for MI detection. A Treebagger embedded with 200 trees was applied to classification. Fig. 6 shows the ROC curves corresponding to different sets of features (according to the ordering index of projected features in decreasing variance) with 90% instances for training and 10% for testing, which demonstrates the 84 features are not overfitting or underfitting.

We conducted training processes in both beat level (randomly selected instances from records) with 10-fold cross validation and

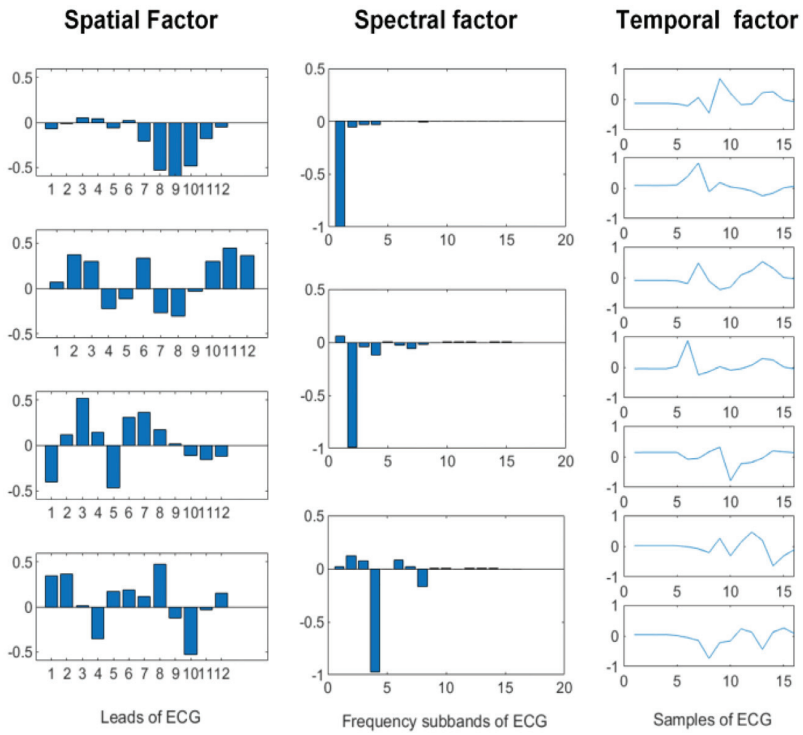

Fig. 5. MPCA matrices of multilinear projection.

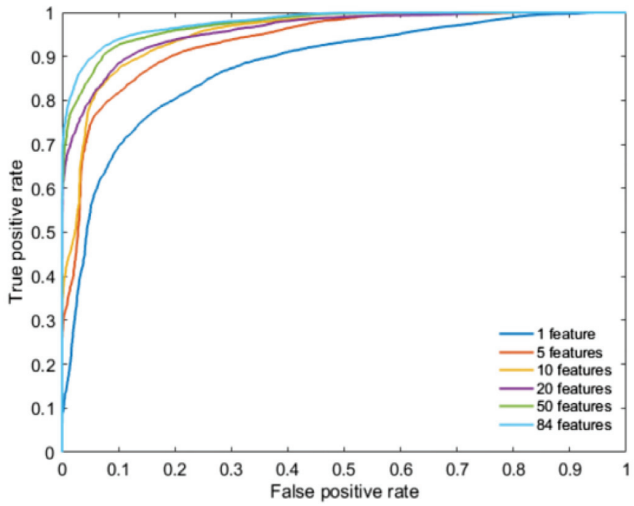

Fig. 6. ROC for MI detection with different features.

record level (considered instances from a set of MI and healthy records to avoid the same instance during training and testing) with handout method. For the training in beat level, we achieved an accuracy of 99.98%, a sensitivity of 100%, and a specificity of 99.90%, respectively. The confusion matrix of MI detection is shown in Table 3. As shown in the table, all 18,852 MI beats could be correctly classified, while 8 healthy beats of ECG among 4106 beats were misclassified to MI patients. Using only 10 features, we could achieve an accuracy of 99.41% for MI detection. For the training in record level, we selected randomly 90% records for training and the left 10% records for testing. We achieved an accuracy of 97.46%, a sensitivity of 99.09%, and a specificity of 90.26%, respectively. Compared with beat level classification results, the record level results reveal the inter-record and inter-subject variations.

Table 3
Confusion matrix of Treebagger for MI detection.

	H	MI
H	4162	8
MI	0	18,852

4.4. MI localization

In this section, the MI localization was seen as multi-class classification, localizing each specific group from 6 different types of MI. The 47,215 MI instances came from 46 AMI (6306), 42 ALMI (6568), 89 IMI (12,115), 76 ASMI (11,232), 56 ILMI (8280), and 19 IPLMI (2714) records. The dimensions (12 leads $\times$ 16 subbands $\times$ 16 samples $\times$ 47,215 beats) of wavelet packet tensor were reduced to low-dimension $4 \times 3 \times 7 \times 47{,}215$ beats by MPCA with the same settings in MI detection. The same classifier and beat- and record-level training processes were chosen for MI localization. Fig. 7 displays the changes in average accuracy, sensitivity, and specificity following the number of features with 10-fold cross validation, which demonstrates the necessity of 84 features in MI localization. For the beat level, the average accuracy, sensitivity, and specificity were 99.87% ($\pm$ 0.05%), 99.97% ($\pm$ 0.01%), and 99.88% ($\pm$ 0.05%), respectively. The confusion matrix of 6 types of MI is presented in Table 4. From the confusion matrix, we found that all the ILMI beats could be classified correctly. Other types of MI were easily misclassified into IPLMI, with 5 AMI beats, 2 ALMI beats, 3 IMI beats, and 3 ASMI beats. The beats of ASMI were easily mixed with other types of MI. By using only 10 features, we could achieve an accuracy of 99.35% for MI localization. For the record level, we presented the performance with 90% records for training and the left 10% records for testing. We achieved an accuracy of 90.39%, a sensitivity of 98.03%, and a specificity of 90.76%, respectively.

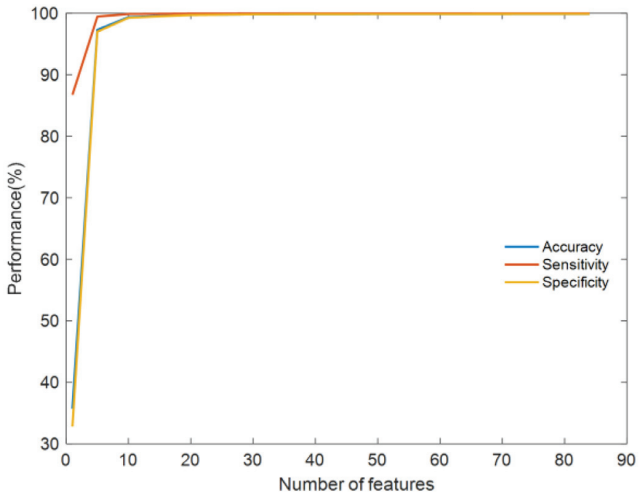

Fig. 7. Performance of MI localization with different features using 10-fold cross validation.

Table 4
Confusion matrix of Treebagger for MI localization.

	AMI	ALMI	IMI	ASMI	ILMI	IPLMI
AMI	2576	2	0	1	0	5
ALMI	2	2502	2	2	0	2
IMI	1	1	4563	3	0	3
ASMI	2	0	2	4798	0	3
ILMI	0	0	0	0	1115	0
IPLMI	0	0	2	1	0	3298

4.5. Comparison performance

Table 5 summarizes the studies employing different techniques in MI detection and localization with the same PTB ECG dataset. In our study, we down-sampled the ECG signal from 1000 Hz to 250 Hz, resulting in 162 samples in each beat. The samples in each beat are fewer than 650 samples in previous research [6,9,31]. Furthermore, a denoising method was applied differently from previous conventional filtering preprocessing. In comparison to filtered data and commonly used denoising methods, the advent of Dual-Q TQWT makes it possible to obtain better performance with fewer samples in each beat. To enhance real-time MI diagnosis, our work, as well as some earlier studies [8,10], was focused on single-beat rather than frame-based (4 beats) exploration. Furthermore, the number of ECG leads is another factor correlated with diagnosis efficiency and computer capacity. Instead of considering all 12 leads, some researchers explored the possibility of using fewer leads or just one single lead [6,9,11,40]. However, they only illustrated the single lead or 12 leads, ignoring the combination of different leads. Wavelet packet tensor is an efficient tool, which can take the ECG leads as one part of features. Using dimensionality reduction, optimal leads are selected, avoiding a manual operation of over-fitting or under-fitting. Different from third-order tensor used in [8], our work applied a fourth-order tensor consisting of frequency (taking advantage of an equal number of wavelet packet coefficients), leads, samples, and beats. The fourth-order wavelet packet tensor was dimensionality reduced in the tensor structure with MPCA, whose classification performance outperformed the commonly used vector-based PCA. Although feature extraction and selection were eliminated in these studies with convention neural network (CNN) [6,40–43], big data, long training time, and high quality service were other problems introduced in their studies. Previous studies achieved good performance without considering inter-subjects variations. Our study presented good results in both beat level and record level training/testing. The MI detection and localization system for single-beat containing fewer samples in our

Table 5
Comparison of studies using PTB ECG database.

Ref	Beat	Lead	Database	Over-fitting	Methods	Features	Results
[6]	1	12	MI: 369 RE H: 79 RE	No	Multiple instance learning + KNN, SVM	74	SE = 92.6%; SP = 88.1%
[3]	1	12	MI: 16,960 BE H: 3200 BE	Yes	Time domain features with DWT + KNN	36 (D,L)	SE = 99.97%; SP = 99.9% (D) SE = 98.67%; SP = 98.71% (L)
[9]	4	12	MI: 847 BE H: unknown	Yes	DWT multiscale energy eigenspace + SVM	72 (D,L)	ACC = 96%; SE = 93%; SP = 99% (D) ACC = 99.58% (L)
[10]	1	1	MI: 485,753 BE H: 125,652 BE	Yes	12 nonlinear features + KNN	47 (D) 25 (L)	ACC = 98.8%; SE = 99.45%; SP = 96.27% (D) ACC = 98.74%; SE = 99.55%; SP = 96.16% (L)
[5]	1	1	MI: 40,182 BE H: 10,546 BE	Yes	Deep convolutional neural network	_	ACC = 95.22%; SE = 95.49%; SP = 94.19%
[37]	1	1,12	MI: 485,752 BE H: 10,564 BE	Yes	Deep convolutional neural network	_	ACC = 99.78%
[7]	4	12	MI: 41,726 BE H: 9966 BE	No	DWT + High order singular value decomposition (HOSVD) + SVM	35 (D) 51 (L)	ACC = 95.3%; SE = 94.6%; SP = 96.0% (D) ACC = 98.1% (L)
Ourwork	1	12	MI: 47,215 BE H: 10,342 BE	No	Dual-Q TQWT + DWPT + MPCA + Treebagger	Record-level 84 (D,L) Beat-level 84 (D,L) 10 (D,L)	ACC = 97.46%; SE = 99.09%;SP = 90.26% (D) ACC = 90.39%; SE = 98.03%; SP = 90.76% (L) ACC = 99.98%; SE = 100%; SP = 99.9% (D) ACC = 99.87%; SE = 99.97%; SP = 99.88% (L) ACC = 99.41% (D); ACC = 99.35% (L)

D is MI detection, L is MI localization.

work is comparable to the earlier studies in the literature. We obtained an accuracy of 99.98% in MI detection and an accuracy of 99.87% in MI localization in beat level with 84 features. By using only 10 features in beat level, we obtained an accuracy of 99.41% in MI detection and an accuracy of 99.35% in MI localization. For the record level, we achieved an accuracy of 97.46% in MI detection and an accuracy of 90.39% in MI localization.

4.6. Computational complexity of methods

The proposed methods are implanted in MATLAB 2018b software in the Windows platform on a desk computer with Intel i5-7500 CPU (@ 3.4 GHz) and 8-GB RAM. For one record of ECG, the running time of Dual-Q TQWT (45.63 s) is shorter than the commonly used denoising algorithm EMD (225.89 s). The running time of DWPT feature extraction is 11.39 s, which is easier and more time-saving than features combination of linear, nonlinear, and entropy. Compared with the time spending on PCA (1795.21 s) used for dimensionality reduction, the tensor-based MPCA requires 123.84 s on 408 ECG records. The training and testing processes of Treebagger classifier spend 223.13 s and 0.67 s, respectively.

5. Conclusion

The power of machine learning and advanced signal processing provides an opportunity for intelligent medical assistance in clinical practice. However, automated, reliable, and real-time MI detection and localization is still a challenging problem because of artifacts corruption, high dimensionality, and inter-individual variations. In our present study, we introduced an automated MI detection and localization system using Dual-Q TQWT and wavelet packet tensor decomposition. By applying the Dual-Q TQWT denoising method, we achieved comparable good performance compared with the filtered data and commonly used denoising methods. Based on the low Q-factor component after denoising, a wavelet packet tensor was formed and then dimensionality reduced by tensor-based MPCA, which showed a better result than vector-based PCA. A total of 84 features chosen from MPCA dimensionality reduction were fed into a Treebagger classifier, reaching an accuracy of 97.46% in MI detection and an accuracy of 90.39% in MI localization considering the record variations. The high performance of our automated detection and localization system might be helpful in providing MI diagnosis care with minimal resources.

In future work, we will test the robustness of Dual-Q TQWT with different types of artifacts mixed with ECG data. Moreover, the automated MI detection and localization system will be applied to other heart disease diagnosis.

Declaration of Competing Interest

The authors have declared that no competing interests exist.

Acknowledgments

This work was supported by Fundamental Research Funds for the Central Universities in Dalian University of Technology in China (DUT2019, DUT16RC(3)021), the scholarships from China Scholarship Council (no. 201600090044, no. 201600090042), and the National Science Foundation of China (no. 91748105, no. 81471742, no. 61703069).

References

[1] K. Thygesen, J.S. Alpert, A.S. Jaffe, M.L. Simoons, B.R. Chaitman, H.D. White, Third universal definition of myocardial infarction, Circulation 126 (2012) 2020–2035, doi:10.1016/j.gheart.2012.08.001.

[2] B. Liu, J. Liu, G. Wang, K. Huang, F. Li, Y. Zheng, Y. Luo, F. Zhou, A novel electrocardiogram parameterization algorithm and its application in myocardial infarction detection, Comput. Biol. Med 61 (2015) 178–184, doi:10.1016/j.compbiomed.2014.08.010.

[3] M. Arif, I.A. Malagore, F.A. Afsar, Detection and localization of myocardial infarction using K-nearest neighbor classifier, J. Med. Syst. 36 (2012) 279–289, doi:10.1007/s10916-010-9474-3.

[4] R.J. Martis, U.R. Acharya, H. Adeli, Current methods in electrocardiogram characterization, Comput. Biol. Med. 48 (2014) 133–149, doi:10.1016/j.compbiomed.2014.02.012.

[5] Z. Chen, Emery N. Brown, R. Barbieri, Characterizing nonlinear heartbeat dynamics within a point process framework, IEEE Trans. Biomed. Eng 57 (2011) 1335–1347, doi:10.1109/TBME.2010.2041002.

[6] Y. Hagiwara, M. Adam, H. Fujita, J.H. Tan, S.L. Oh, U.R. Acharya, Application of deep convolutional neural network for automated detection of myocardial infarction using ECG signals, Inf. Sci. (Ny) 415–416 (2017) 190–198, doi:10.1016/j.ins.2017.06.027.

[7] L. Sun, Y. Lu, K. Yang, S. Li, ECG analysis using multiple instance learning for myocardial infarction detection, IEEE Trans. Biomed. Eng 59 (2012) 3348–3356, doi:10.1109/TBME.2012.2213597.

[8] S. Padhy, S. Dandapat, Third-order tensor based analysis of multilead ECG for classification of myocardial infarction, Biomed. Signal Process. Control 31 (2017) 71–78, doi:10.1016/j.bspc.2016.07.007.

[9] M. Kumar, R.B. Pachori, U.R. Acharya, Automated diagnosis of myocardial infarction ECG signals using sample entropy in flexible analytic wavelet transform framework, Entropy (2017) 19, doi:10.3390/e19090488.

[10] L.N. Sharma, R.K. Tripathy, S. Dandapat, Multiscale energy and eigenspace approach to detection and localization of myocardial infarction, IEEE Trans. Biomed. Eng. 62 (2015) 1827–1837, doi:10.1109/TBME.2015.2405134.

[11] U.R. Acharya, H. Fujita, V.K. Sudarshan, S.L. Oh, M. Adam, J.E.W. Koh, J.H. Tan, D.N. Ghista, R.J. Martis, C.K. Chua, C.K. Poo, R.S. Tan, Automated detection and localization of myocardial infarction using electrocardiogram: a comparative study of different leads, Knowledge-Based Syst. 99 (2016) 146–156, doi:10.1016/j.knosys.2016.01.040.

[12] Riccardo Barbieri, E.N. Brown, Analysis of heartbeat dynamics by point process adaptive filtering, IEEE Trans. Biomed. Eng. 53 (2006) 4–12, doi:10.1109/TBME.2005.859779.

[13] F.A. Elhaj, N. Salim, A.R. Harris, T.T. Swee, T. Ahmed, Arrhythmia recognition and classification using combined linear and nonlinear features of ECG signals, Comput. Methods Programs. Biomed. 127 (2016) 52–63, doi:10.1016/j.cmpb.2015.12.024.

[14] M. Blanco-Velasco, B. Weng, K.E. Barner, ECG signal denoising and baseline wander correction based on the empirical mode decomposition, Comput. Biol. Med. 38 (2008) 1–13, doi:10.1016/j.compbiomed.2007.06.003.

[15] R. Agarwal, J. Gotman, Computer-assisted sleep staging, IEEE Trans. Biomed. Eng. 48 (2001) 1412–1423, doi:10.1109/10.966600.

[16] I. Selesnick, in: TQWT, Toolbox Guide, NewYork, 2011, pp. 1–25.

[17] I.W. Selesnick, Wavelet transform with tunable Q-factor, IEEE Trans. Signal Process 59 (2011) 3560–3575, doi:10.1109/TSP.2011.2143711.

[18] I.W. Selesnick, Resonance-based signal decomposition: a new sparsity-enabled signal analysis method, Signal Processing 91 (2011) 2793–2809.

[19] R. Bousseljot, D. Kreiseler, A. Schnabel, Nutzung der EKG-Signaldatenbank Cardiodat der PTB über das internet, Biomed. Tech. 40 (1995) 317–318, doi:10.1515/bmte.1995.40.s1.317.

[20] S.H.Goldberger AL, L.A.N. Amaral, L. Glass, J.M. Hausdorff, Ivanov PCh, R.G. Mark, J.E. Mietus, G.B. Moody, C.-.K. Peng, PhysioBank, PhysioToolkit, and PhysioNet components of a new research resource for complex physiologic signals, Circulation 101 (2000) 215–220, doi:10.1161/01.CIR.101.23.e215.

[21] A. Delorme, S. Makeig, EEGLAB: an open source toolbox for analysis of single-trial EEG dynamics including independent component analysis, J. Neurosci. Methods 134 (2004) 9–21, doi:10.1016/j.jneumeth.2003.10.009.

[22] S.N. Yu, K.T. Chou, Integration of independent component analysis and neural networks for ECG beat classification, Expert Syst. Appl. 34 (2008) 2841–2846, doi:10.1016/j.eswa.2007.05.006.

[23] J.L. Starck, M. Elad, D.L. Donoho, Image decomposition via the combination of sparse representations and a variational approach, IEEE Trans. Image. Process. 14 (2005) 1570–1582, doi:10.1109/TIP.2005.852206.

[24] M.V. Afonso, J.M. Bioucas-Dias, M.A.T Figueiredo, Fast image recovery using variable splitting and constrained optimization, IEEE Trans. Image. Process. 19 (2010) 2345–2356, doi:10.1109/TIP.2010.2047910.

[25] A.R. Hassan, M.I.H. Bhuiyan, A decision support system for automatic sleep staging from EEG signals using tunable Q-factor wavelet transform and spectral features, J. Neurosci. Methods 271 (2016) 107–118, doi:10.1016/j.jneumeth.2016.07.012.

[26] S. Chaibi, T. Lajnef, Z. Sakka, M. Samet, A. Kachouri, A reliable approach to distinguish between transient with and without HFOs using TQWT and MCA, J. Neurosci. Methods 232 (2014) 36–46, doi:10.1016/j.jneumeth.2014.04.025.

[27] S. Patidar, R.B. Pachori, N. Garg, Automatic diagnosis of septal defects based on tunable-Q wavelet transform of cardiac sound signals, Expert Syst. Appl. 42 (2015) 3315–3326, doi:10.1016/j.eswa.2014.11.046.

[28] S. Patidar, R.B. Pachori, Classification of cardiac sound signals using constrained tunable-Q wavelet transform, Expert Syst. Appl. 41 (2014) 7161–7170, doi:10.1016/j.eswa.2014.05.052.

[29] S. Patidar, T. Panigrahi, Detection of epileptic seizure using Kraskov entropy applied on tunable-Q wavelet transform of EEG signals, Biomed. Signal Process. Control 34 (2017) 74–80, doi:10.1016/j.bspc.2017.01.001.

[30] J. Pan, W.J Tompkins, A real-time QRS detection algorithm, IEEE Trans. Biomed. Eng. BME-32 (1985) 230–236, doi:10.1109/TBME.1985.325532.
[31] H. He, Y. Tan, J. Xing, Unsupervised classification of 12-lead ECG signals using wavelet tensor decomposition and two-dimensional Gaussian spectral clustering, Knowledge-Based Syst. 163 (2019) 392–403, doi:10.1016/j.knosys.2018.09.001.
[32] H. Lu, K.N. Plataniotis, A.N. Venetsanopoulos, MPCA: multilinear principal component analysis of tensor objects, IEEE Trans. Neural Netw. 19 (2008) 18–39, doi:10.1109/TNN.2007.901277.
[33] H. Lu, K.N. Plataniotis, A.N. Venetsanopoulos, A survey of multilinear subspace learning, Pattern Recognit. 44 (2011) 1540–1551, doi:10.1016/j.physb.2011.12.087.
[34] J. Wang, A. Barreto, L. Wang, Y. Chen, N. Rishe, J. Andrian, M. Adjouadi, Multilinear principal component analysis for face recognition with fewer features, Neurocomputing 73 (2010) 1550–1555, doi:10.1016/j.neucom.2009.08.022.
[35] H. He, Y. Tan, Pattern clustering of hysteresis time series with multivalued mapping using tensor decomposition, IEEE Trans. Syst. Man Cybern. Syst. 48 (2018) 993–1004, doi:10.1109/TSMC.2017.2737578.
[36] B. Kamiński, M. Jakubczyk, P. Szufel, A framework for sensitivity analysis of decision trees, Cent. Eur. J. Oper. Res. 26 (2018) 135–159, doi:10.1007/s10100-017-0479-6.
[37] T.G. Dietterich, An experimental comparison of three methods for constructing ensembles of decision trees, Mach. Learn. 40 (2000) 139–157, doi:10.1023/A:1007607513941.
[38] D.G. Altman, J.M Bland, Diagnostic tests 1 - sensitivity and specificity, Med. Stat. Lab. Imp. Canser Res. Fund London 308 (1994) 1552, doi:10.1258/phleb.2012.012J05.
[39] D.M.W. Powers, Evaluation: from precision, recall and F-measure to ROC, informedness, markedness and corrrelation, J. Mach. Learn. Technol. 2 (2011) 37–63.
[40] U.B. Baloglu, M. Talo, O. Yildirim, R.S. Tan, U.R. Acharya, Classification of myocardial infarction with multi-lead ECG signals and deep CNN, Pattern Recognit. Lett. 122 (2019) 23–30, doi:10.1016/j.patrec.2019.02.016.
[41] H. Fujita, D. Cimr, Decision support system for arrhythmia prediction using convolutional neural network structure without preprocessing, Appl. Intell. (2019), doi:10.1007/s10489-019-01461-0.
[42] U.R. Acharya, H. Fujita, S.L. Oh, U. Raghavendra, J.H. Tan, M. Adam, A. Gertych, Y. Hagiwara, Automated identification of shockable and non-shockable life-threatening ventricular arrhythmias using convolutional neural network, Futur. Gener. Comput. Syst. 79 (2018) 952–959, doi:10.1016/j.future.2017.08.039.
[43] H. Fujita, D. Cimr, Computer aided detection for fibrillations and flutters using deep convolutional neural network, Inf. Sci. (Ny). 486 (2019) 231–239, doi:10.1016/j.ins.2019.02.065.

IV

CONGRUENCY AND VIGILANCE PRODUCE SEPARABLE CHANGES IN THE LATE POSITIVE COMPLEX DURING A FLANKER TASK

by

Jia Liu, Yongjie Zhu, Zheng Chang, Timo Hämäläinen, Fengyu Cong, 2020

Submitted

Request a copy from author.